WADC TECHNICAL REPORT 55-56

PART 3

ASTIA Document Nr. AD 130704

PROTECTIVE SHOT PEENING OF PROPELLERS
PART 3 - FATIGUE AND DISTORTION

RONALD F. BRODIUCK

LESSELLS AND ASSOCIATES, INC.

JUNE 1957

WRIGHT AIR DEVELOPMENT CENTER

PROTECTIVE SHOT PEENING OF PROPELLERS
PART 3 -- FATIGUE AND DISTORTION

Ronald F. Brodrick

Lessells and Associates, Inc.
Boston, Massachusetts

June 1957

Wright Air Development Center
Air Research and Development Command
United States Air Force
Wright-Patterson Air Force Base, Ohio

FOREWORD

ABSTRACT

This report is the third in a series covering work performed under Contract No. AF33(616)-2324 during the period from 1 February 1954 to 30 November 1956. The current report covers the period from 1 September 1955 through 30 November 1956. The object of the investigation was to determine any benefits of shot peening as a means of protecting aircraft propeller blades against the reduction of fatigue strength arising from service damage. This report covers additional fatigue tests supplementing those reported in Part 2 and including more severe damage than previously tested. It also covers tests conducted for the purpose of enabling estimates to be made of the limitations imposed by distortion in the peening of actual parts.

The results further substantiate the benefits of shot peening as a barrier to the detrimental effects of service damage. Tests on SAE 4340 steel specimens indicate that the benefits increase with increasing hardness of steel. Empirical relations derived from the distortion tests are also included. These relations allow prediction of the curvature to be expected from the peening of flat plates under any practical peening conditions.

TABLE OF CONTENTS

LIST OF TABLES

LIST OF ILLUSTRATIONS

I. INTRODUCTION

The work reported in this paper is directed at increased knowledge of the beneficial effects of shot peening in the prevention of fatigue failure in aircraft propeller blades. It has been hypothesized that the introduction of surface layer of compressive residual stress might impede the formation and growth of cracks at points subjected to damage in service. Experiments supporting this hypothesis were carried out and are reported in WADC TR 55—56, Parts 1 and 2. These reports cover the background material as well as the complete details of procedures involved in shot peening, measurement of residual peening stresses, fatigue tests, etc. These details will not be repeated in this report except in cases where they may have been altered in the more recent work. Material properties of the SAE 4340 steel and 76S-T6 aluminum are identical to those previously reported.

The current phase of the investigation involves 1) fatigue tests supplementing those previously reported and 2) a study directed at the prediction of the distortion which would accompany the shot peening of propeller blades. The latter phase is of interest because of the obvious limitations arising with maximum shot size and / or intensity and minimum blade thicknesses, especially as regards hollow blades. The studies of distortion discussed here are limited to flat plates of various thicknesses peened on one side only in order that the basic responses and parameters may be established.

II. FATIGUE TESTS

LIGHT DAMAGE

Additional tests covering the case of light damage on 4340 steel were conducted in order to provide supplementary data. It will be recalled that the light damage, as described in WADC TR 55-56, Part 2, is produced by fragments of broken glass striking the specimen. The supplementary data were desired in order to provide more tests for more accurate statistical analysis and to provide a check on the Prot slope, which previously was taken as the value reported in WADC TR 52-234. Table 1 is an outline of the test program involving the light damage. A few S-N tests were included for the purpose of checking the endurance limit indicated by the Prot method. Table 2 outlines the S-N test conditions. Complete data on all fatigue test specimens are given in Appendix I. The failure stresses indicated have been corrected for gouge depth.

TABLE 1

PROT TEST CONDITIONS -
LIGHT DAMAGE

Specimen Nos.	Ultimate Strength (psi)	Shot Size (in.)	Air Pressure (psi)	Stress Rate $\sqrt{psi}$/cycle
301-314	130,000	No Peening		0.2
315-328	130,000	.039	50	0.2
377-388	180,000	No Peening		0.07
389-400	180,000	No Peening		0.14
425-436	180,000	.066	50	0.07
437-448	180,000	.066	50	0.14
521-534	260,000	No Peening		0.2
559-572	260,000	.039	50	0.2

TABLE 2

CONDITIONS FOR S-N TESTS

Specimen Nos.	Ultimate Strength (psi)	Shot Size (in.)	Air Pressure (psi)	Damage
645-656	180,000	No Peening		None
657-668	180,000	.066	50	Light
669-680	260,000	No Peening		None
681-692	260,000	.039	50	Light

This correction is based on the reduction in nominal stress in a bending specimen by virtue of the depth from the original surface at which the failure originates. This depth is determined by breaking open the specimen and examining microscopically to discover the origin of failure. In the case of the light damage the correction is usually quite small, such that any errors in this principle of reducing the stress by the ratio of failure depth to half the thickness is quite small. In the case of very deep gouges, as discussed later, errors in this correction may be greater.

Figures 1 through 3 give the results of tests run for the purpose of checking the Prot slope. Previous data reported in WADC TR 55-56, Part 2 are included in these curves as well as in all the other applicable curves of light damage. Applicable values of the S-N results are also included in the figures. Two Prot slopes are drawn where the data permit. One slope is that reported in WADC TR 52-234, used in previous reports under this contract. The second is that derived from data obtained during the phase reported here. The second slope is greater, indicating lower endurance limits than the first. Some question arises as to the proper value of rate of stress increase to be used in the case of notched or damaged specimens. The rates plotted here are the nominal rate at the surface. It can be argued that the rate should be reduced to that determined by the nominal stress at the depth of failure. This would in general indicate higher endurance limits, although the change would be slight for shallow notches. On the other hand, it can be argued that the actual failure stress at the root of a notch is the product of the nominal stress and a stress concentration factor. If this were also applied to the stress rate, higher rates would be indicated. Which of these effects is the more realistic is unknown at the present time. It would thus appear that a basic deficiency exists in the Prot method when applied to notched specimens, except in cases wherein a nominal stress used for comparative purposes is adequate. Fortunately, the current investigation is satisfactorily covered by the latter situation in that comparative results are adequate, even though precise knowledge of the actual endurance limits is not obtained. With this in mind and in order to compare previous results with current results, the original slope as reported in WADC TR 52-234 has been used in calculating endurance limits. All conclusions are based on this Prot slope. It should be noted in passing that when the data are plotted using both the nominal surface stress and the nominal surface rate of stress increase, the slope agrees almost exactly with that reported in WADC TR 52-234.

Figures 4 through 6 give the results of all other Prot tests involving either no damage or light damage. These tests were run at the nominal rate of increase of .04 psi per cycle and endurance limits were determined by resorting to the slope, as described above. Figures 7 through 10 show the results of S-N tests. An overall summary of the average endurance limits indicated by the Prot and S-N tests for the cases of either no damage or light damage

FIGURE 1. FATIGUE TEST RESULTS, Rc 42, .000 in.
PEEN DEPTH, LIGHT DAMAGE

FIGURE 2. FATIGUE TEST RESULTS, Rc 42, .017in.
PEEN DEPTH, LIGHT DAMAGE
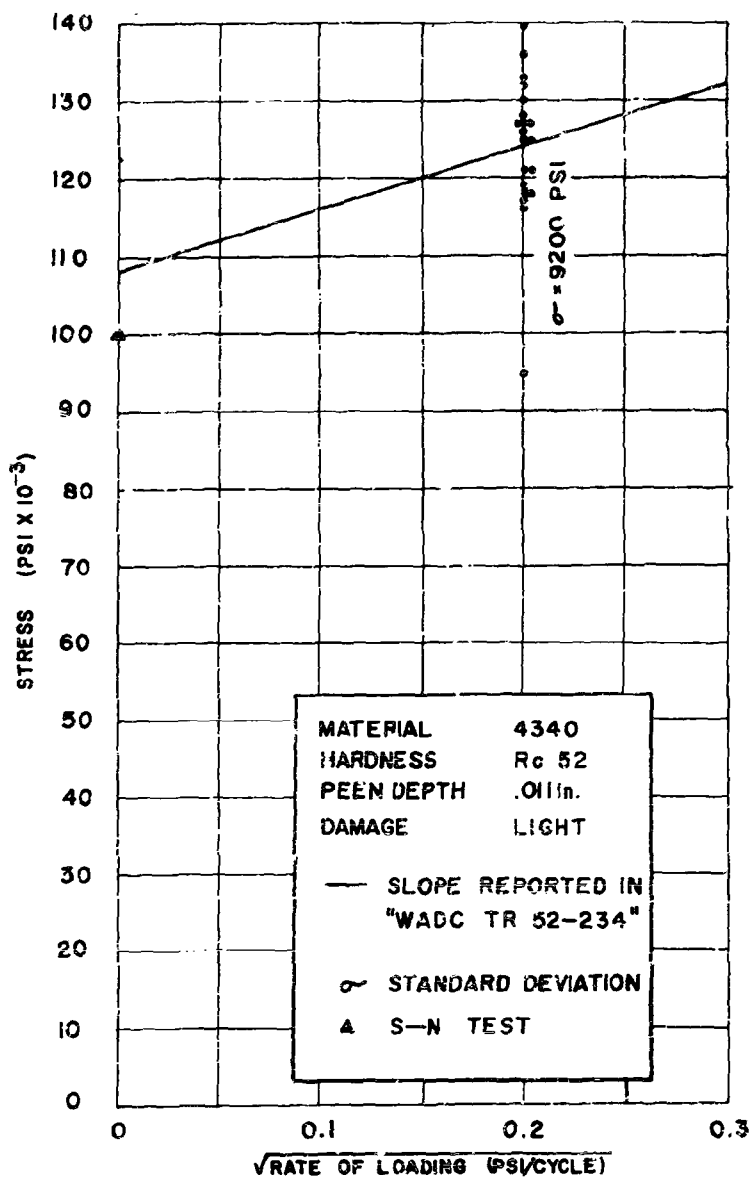
FIGURE 3. FATIGUE TEST RESULTS Rc 52, .011 in.
PEEN DEPTH, LIGHT DAMAGE
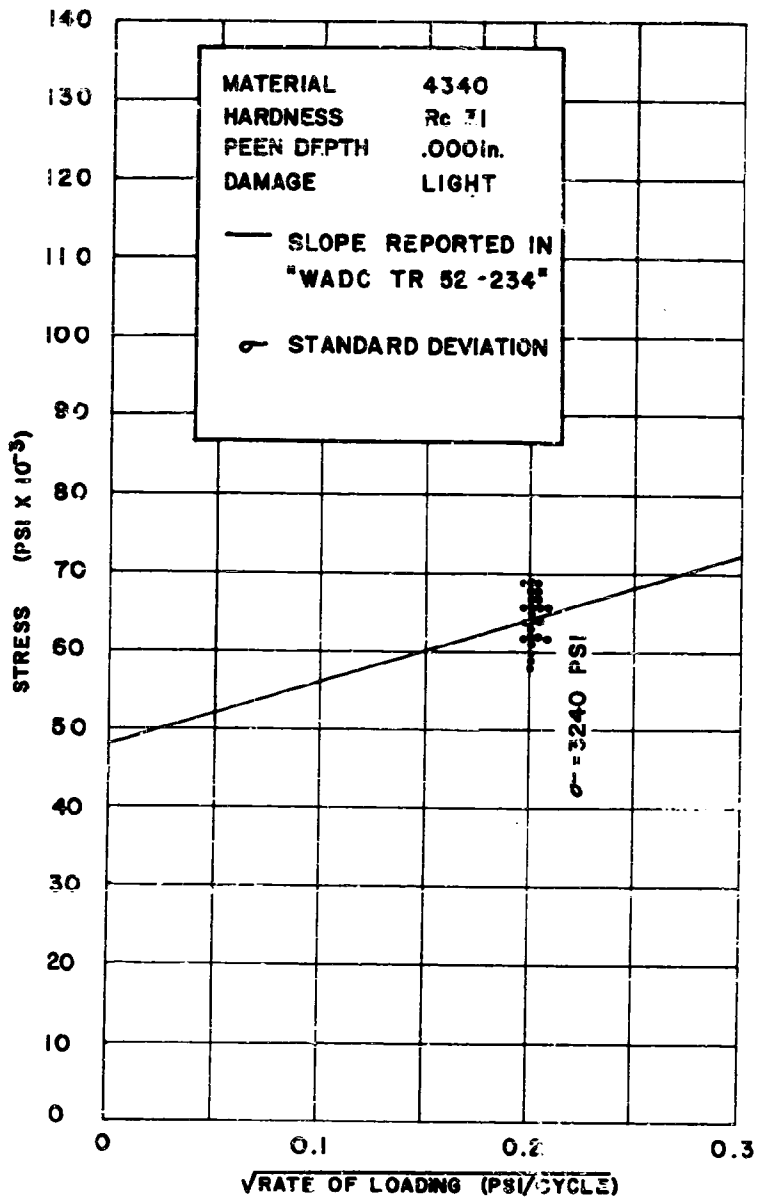
FIGURE 4. FATIGUE TEST   RESULTS Rc 31, .000 in.
PEEN DEPTH,   LIGHT DAMAGE
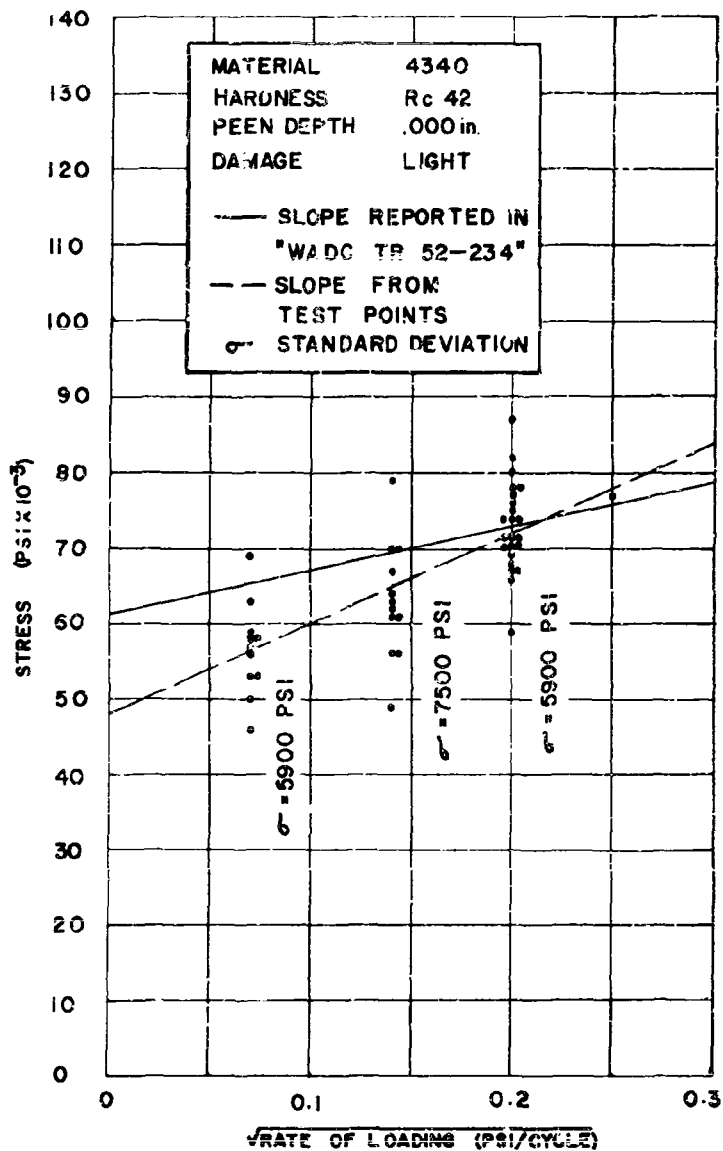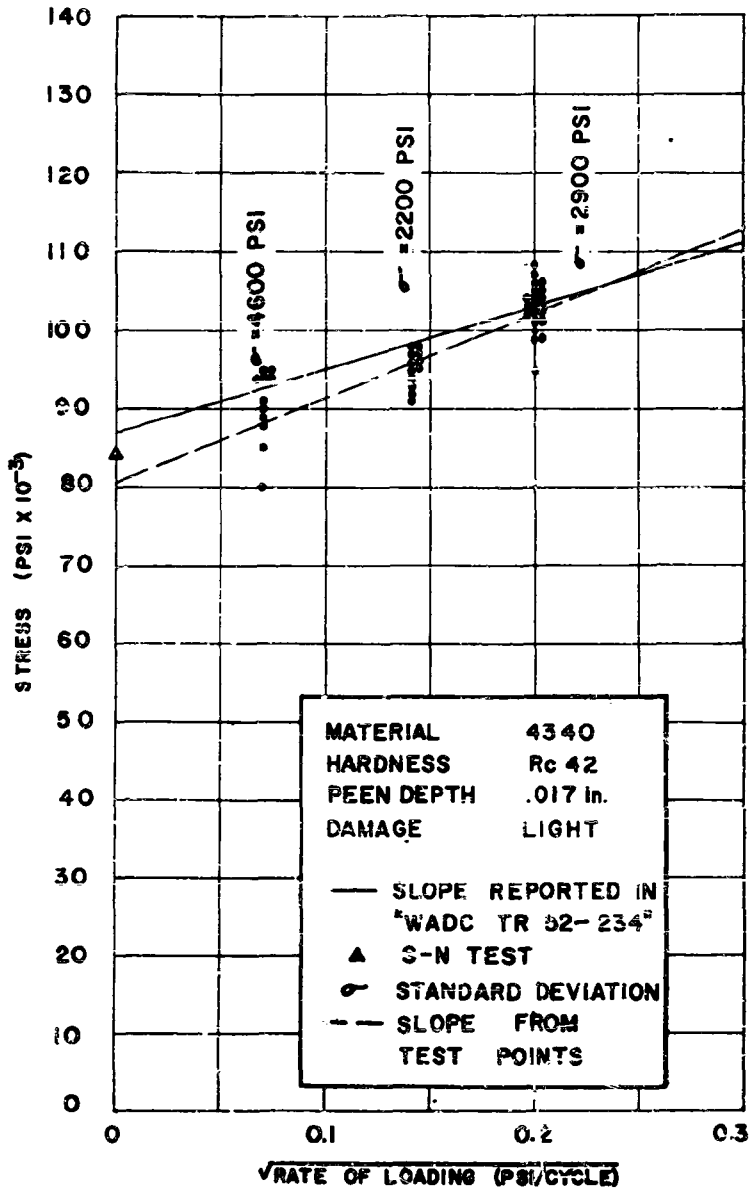
FIGURE 5. FATIGUE TEST   RESULTS Rc 31, .017 in.
PEEN DEPTH, LIGHT DAMAGE
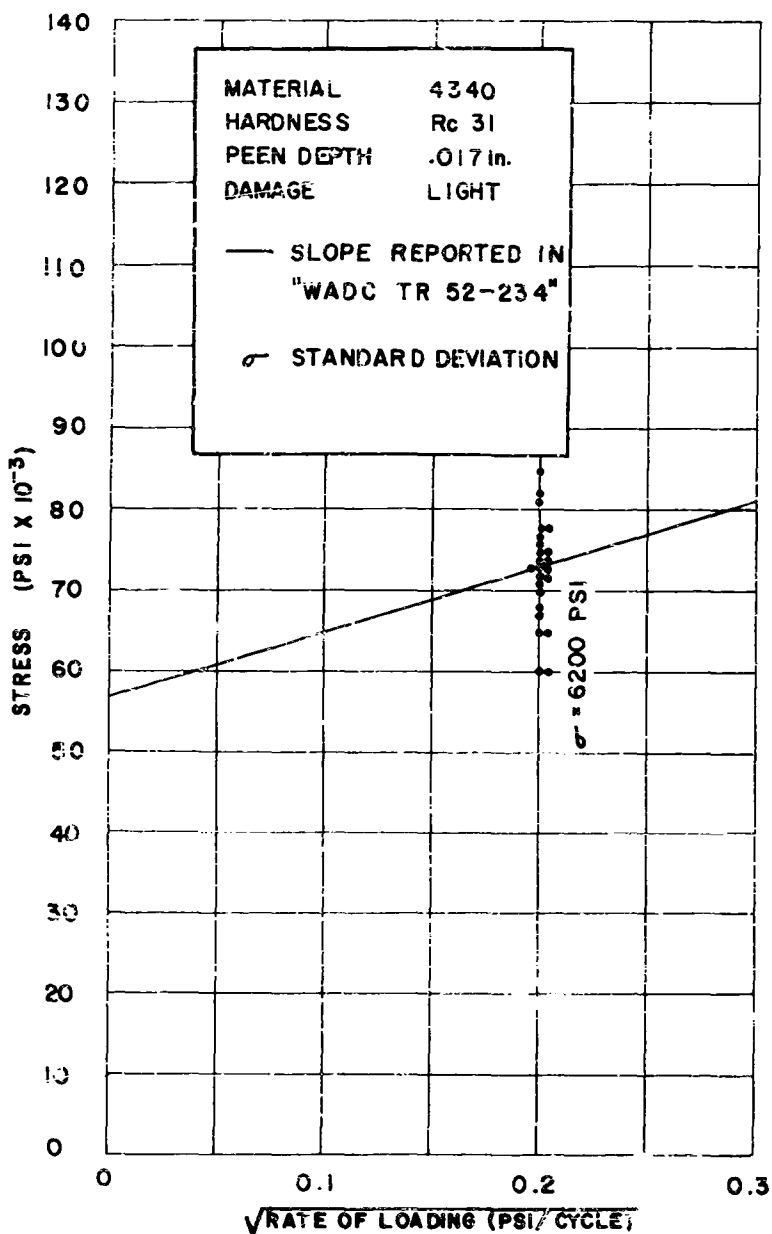
FIGURE 6. FATIGUE TEST RESULTS Rc 52, .000 in. PEEN DEPTH, LIGHT DAMAGE

FIGURE 7. S — N TEST RESULTS
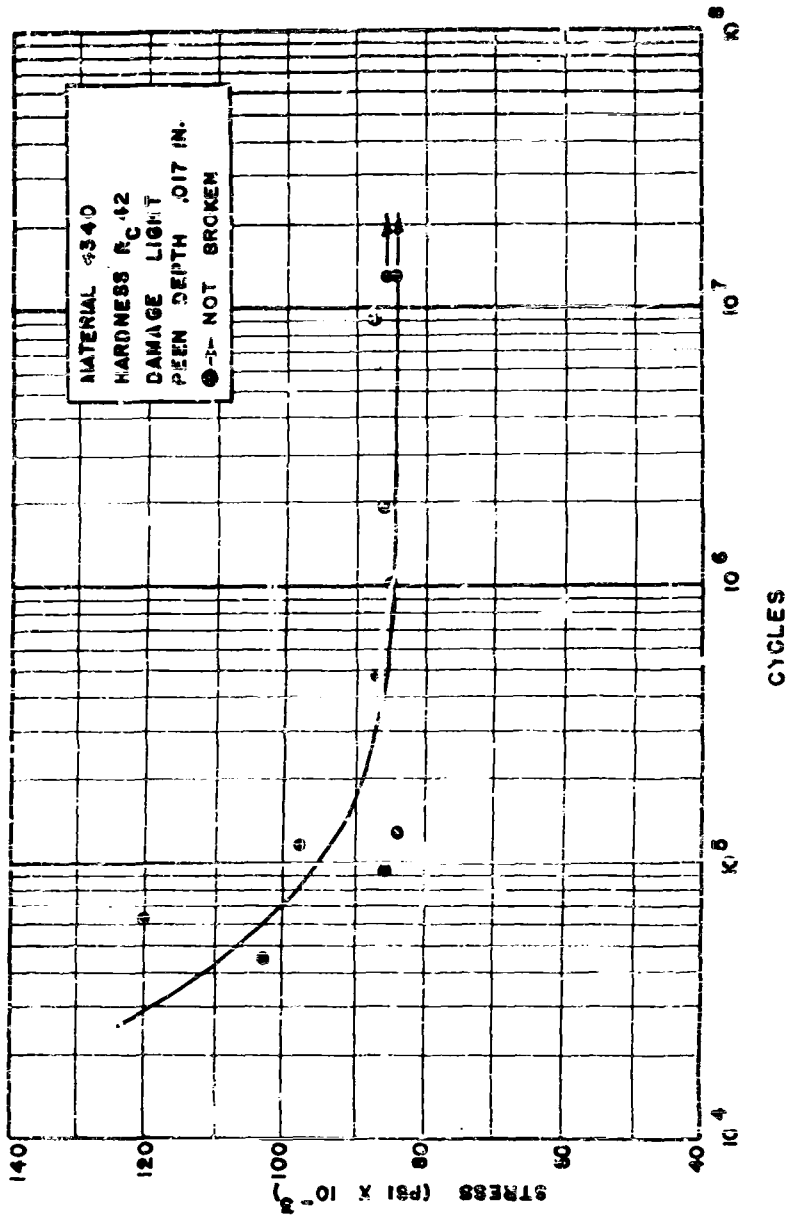
FIGURE 8. S—N TEST RESULTS

FIGURE 9. S—N TEST RESULTS

CYCLES

FIGURE 10. S—N TEST RESULTS

Chart labels (rotated):

STRESS (PSI × 10⁻³)

MATERIAL 4340
HARDNESS R$_c$ 52
DAMAGE LIGHT
PEEN DEPTH .01° IN.
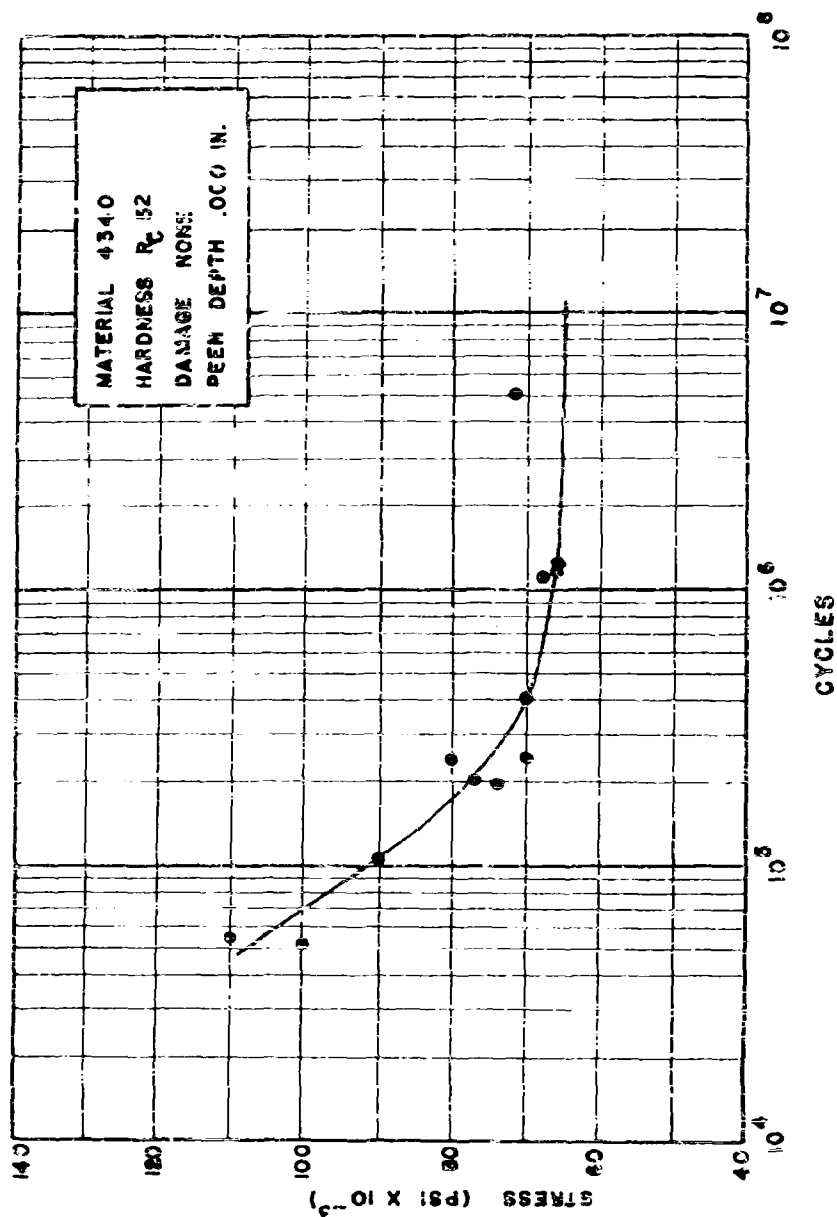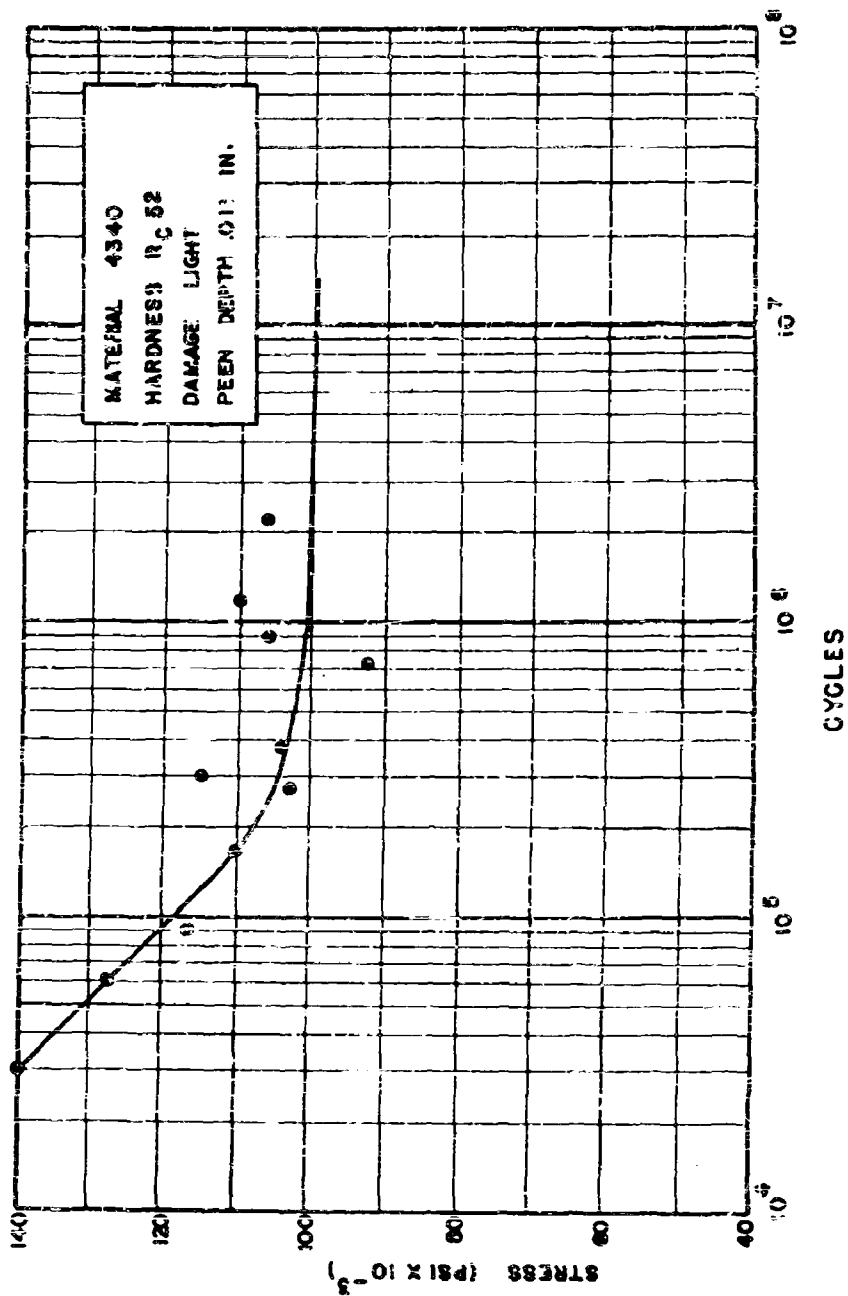
Prot and S-N tests for the cases of either no damage or light damage is given in Figure 11. As stated before, the results are averages which include the previous applicable data reported in WADC TR 55-56, Part 2.

Figure 12 shows the percent variation in failure stress vs. the ratio of depth of compression to depth of damage for the case of light damage.

Figure 13 is a photograph of the two surfaces of a failure which originated at a glass—like inclusion of spherical form. Figure 14 shows a typical sub-surface failure in which the presence of foreign matter was not definitely established. The "fish eye" which is typical of sub-surface fatigue failure is evident in the photographs.

HEAVY DAMAGE

Tests were also included in the current phase of the program in which heavier damage than used previously was imposed on the test specimens. This damage was produced by the same glass missile as described previously except that the glass was not fractured prior to contact with the specimen. Each specimen was subjected to a single gouge. In some cases the glass missile fractured very shortly after initial contact with the specimen producing a spray pattern of relatively light damage over the surface but with fre-quently a moderately deep groove over a distance of about 1/2 in. across the specimen. In other cases the glass missile did not frac-ture until it had traversed approximately 1/2 in. of the specimen. This resulted in a very sharp clean single groove varying in depth from zero at the point of contact to a maximum at the point of even-tual fracture. Attempts were made to measure the radius of curva-ture at the bottom of the groove. This radius could not be precisely determined but it is less than .0001 in. Considerable cold work was evident along the sides of the grooves. The groove usually ended rather abruptly at the point of eventual fracture of the glass, this end being filled with remaining fragments of glass. These deep gouges were obtained with all three hardnesses of the 4340 steel although the percentage of deep gouges decreased with increasing specimen hardness. An occasional deep gouge was found even at the highest hardness of R 52.

For purposes of analysis this heavy damage was divided into two categories according to whether or not the excessively deep gouges were formed. In all cases the failure stresses were cor-rected for depth by reducing the stress from the surface in a linear fashion by the ratio of depth of failure origin to semi—thickness of the bar. With the excessively deep gouges this procedure may be subject to some error. The nominal stress at the bottom of one of these deep gouges, as calculated in this fashion, is as little as one-

PROT TESTS ON 4340 STEEL EXCEPT AS NOTED

AVERAGE ENDURANCE LIMIT (PSI X 10^{-3})

120   100   80   60   40   20   0

Rc 31
- NO PEENING
- .017 PEEN DEPTH

Rc 42
- PARENT MATERIAL
- PARENT MATERIAL S-N
- NO PEENING
- .004 PEEN DEPTH
- .009 PEEN DEPTH
- .017 PEEN DEPTH
- .017 PEEN DEPTH S-N
- .027 PEEN DEPTH

Rc 52
- PARENT MATERIAL
- PARENT MATERIAL S-N
- NO PEENING
- .011 PEEN DEPTH
- .011 PEEN DEPTH S-N
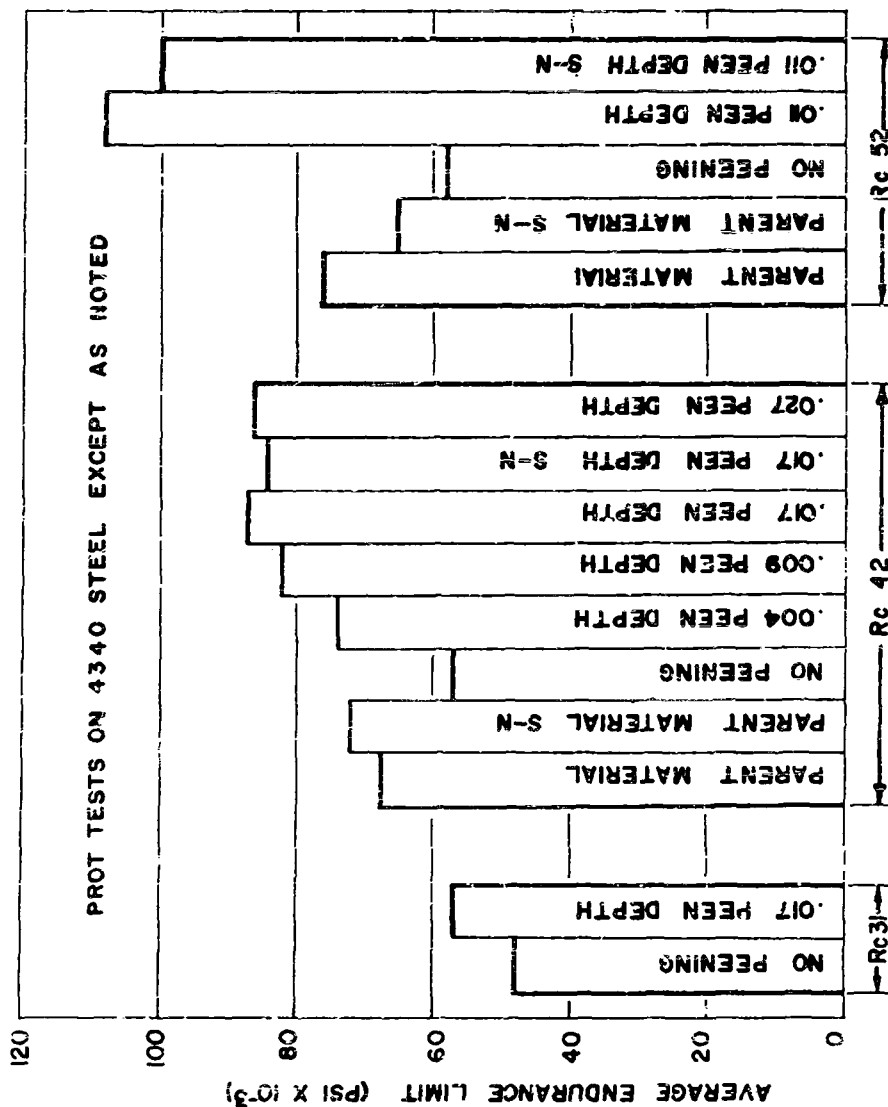
FIGURE 11. SUMMARY OF RESULTS — LIGHT DAMAGE
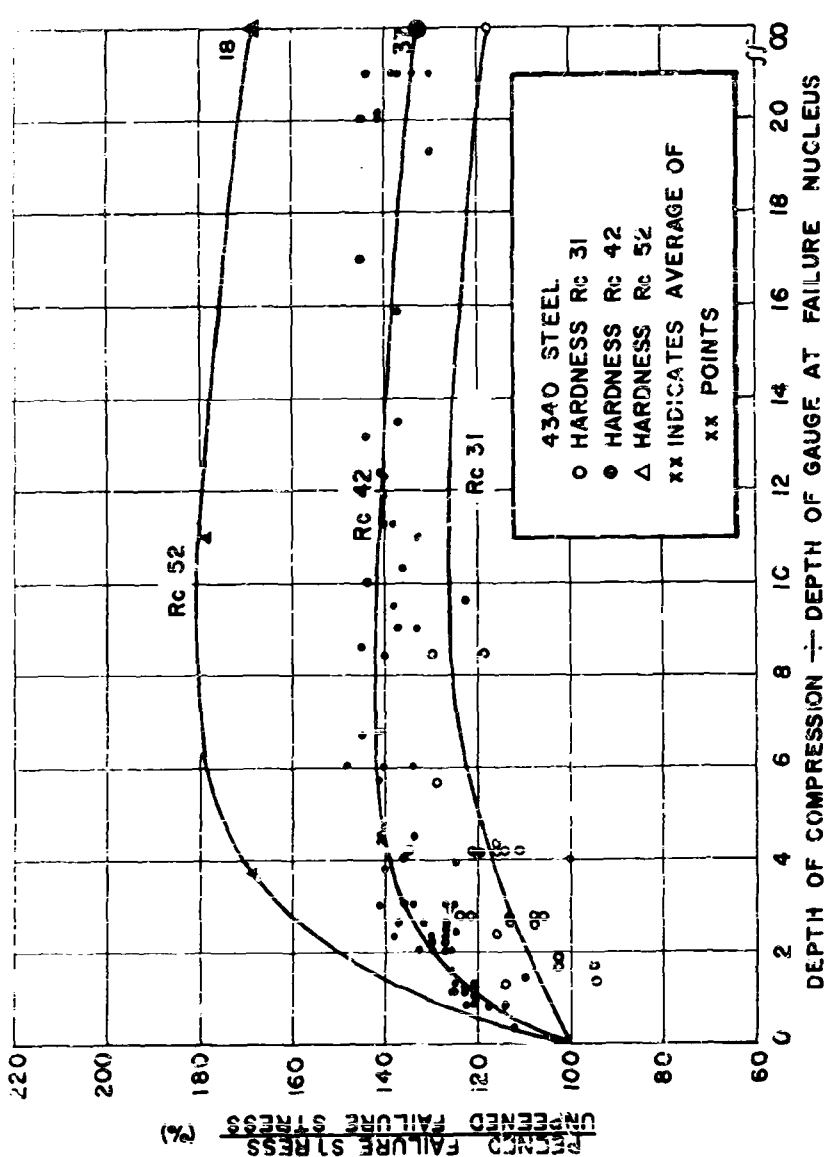
FIGURE 12. RELATIVE IMPROVEMENT OF FATIGUE PROPERTIES — LIGHT DAMAGE

B. INCLUSION IN PLACE—30X

A. PIT LEFT BY INCLUSION—30X
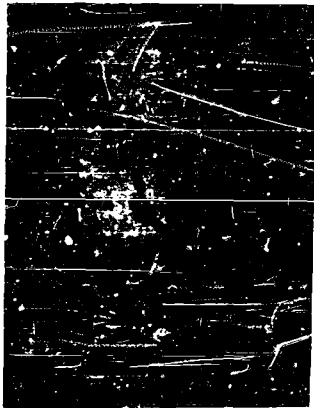
FIGURE 13. FAILURE AT INCLUSION
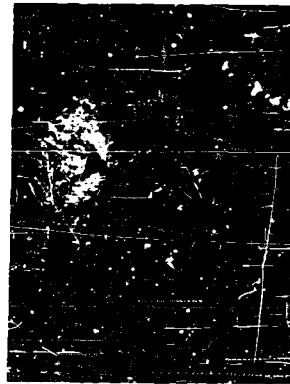
FIGURE 14. SUB-SURFACE FAILURE—30X

half the nominal stress at the surface of the bar. No correction was made for the reduction in section modulus due to the existence of the gouge. The inaccuracy is not considered serious however, inasmuch as the value of tests on the excessively deep gouges is very small. These gouges are such that rejection of a propeller blade containing such gouge would be unquestioned. Further, they are of depths far greater than could be benefited by any reasonable peening treatment. Consequently, value is placed only on these heavy gouges which are not of excessive depth, that is of depth exceeding approximately .016 in. Thus, specimens containing these heavy gouges of .016 in. depth or greater are not included in the analysis of results, although the failure data are given and the points are plotted.

Table 3 is an outline of the test program involving the heavy damage. Appendix I includes data on the specimens containing damage as well as those specimens previously mentioned.

TABLE 3

PROT TEST CONDITIONS - HEAVY DAMAGE

Specimen Nos.	Ultimate Strength (psi)	Shot Size (in.)	Air Pressure (psi)	Stress Rate $\sqrt{psi}$/cycle
329-352	130,000	.039	50	0.2
353-376	130,000	.125	90	0.2
401-424	180,000	No Peening		0.2
449-472	180,000	.066	50	0.2
473-496	180,000	.078	90	0.2
497-520	180,000	.125	90	0.2
535-558	260,000	No Peening		0.2
573-596	260,000	.039	50	0.2
597-620	260,000	.078	90	0.2
621-644	260,000	.125	90	0.2

Figures 15 through 24 give the results of Prot tests on the heavily damaged specimens of various hardnesses and peening treatments. Figure 25 gives the average results of these tests for the heavily damaged specimens. It can be seen that the benefits of peening are apparent even with the moderately heavy damage. Figure 26 shows the percent variation in failure stress vs. the ratio of depth of compression to depth of damage for the case of heavy damage.
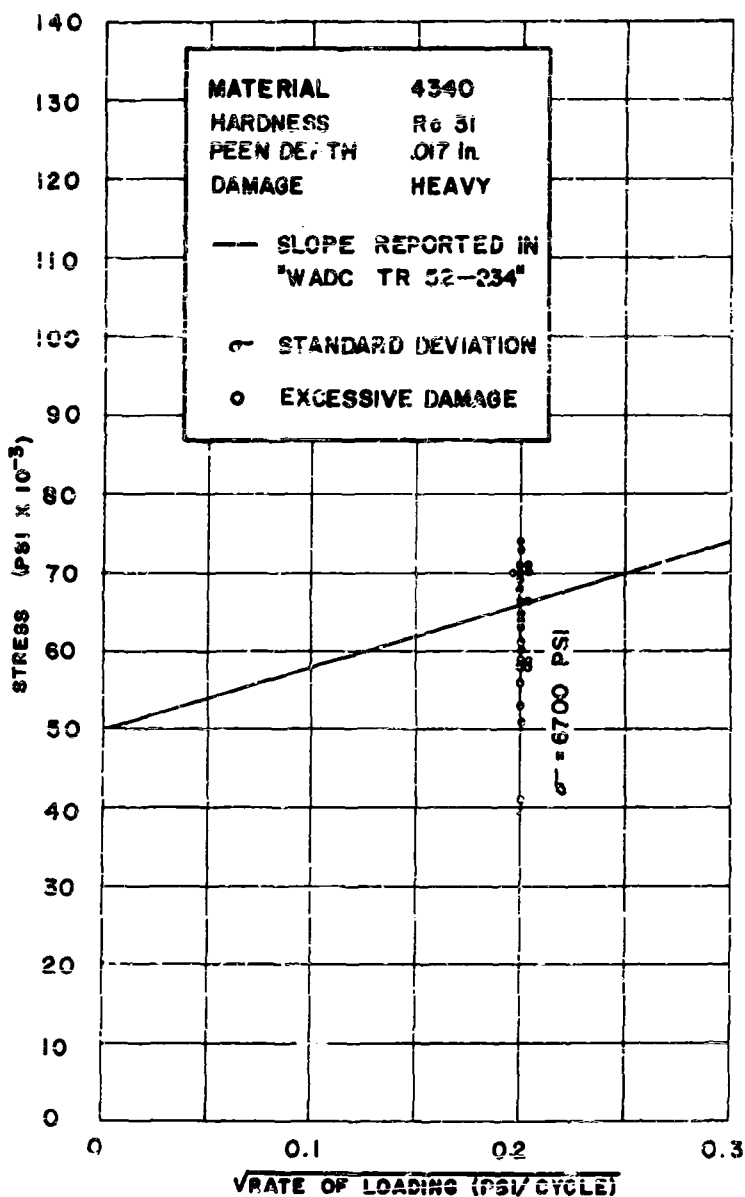
FIGURE 15. FATIGUE TEST RESULTS Rc 31, .017 in.
PEEN DEPTH, HEAVY DAMAGE

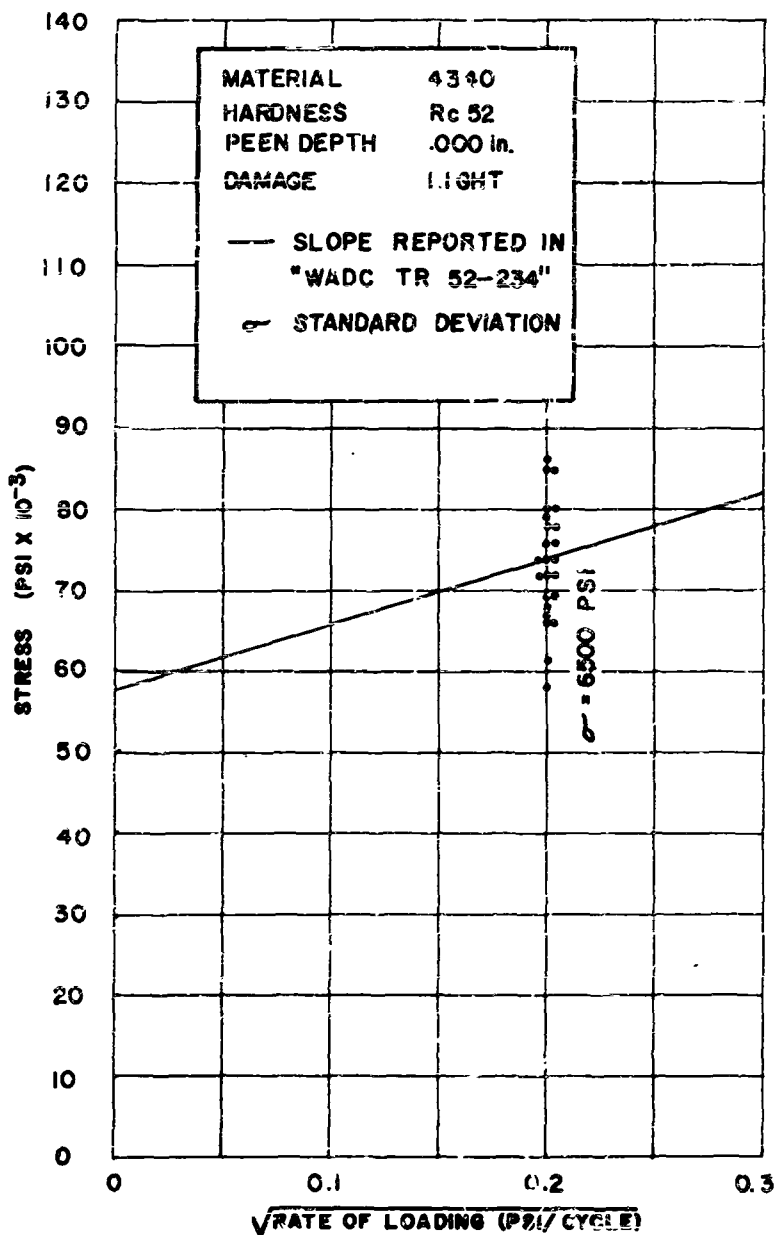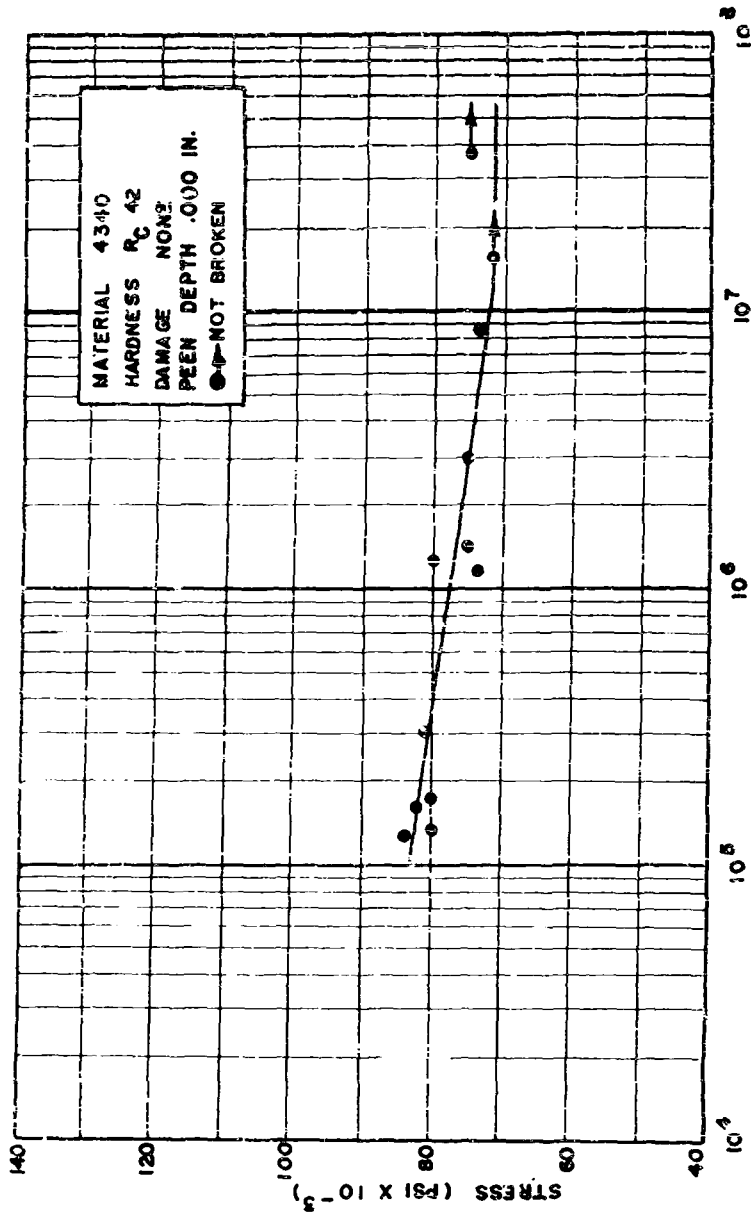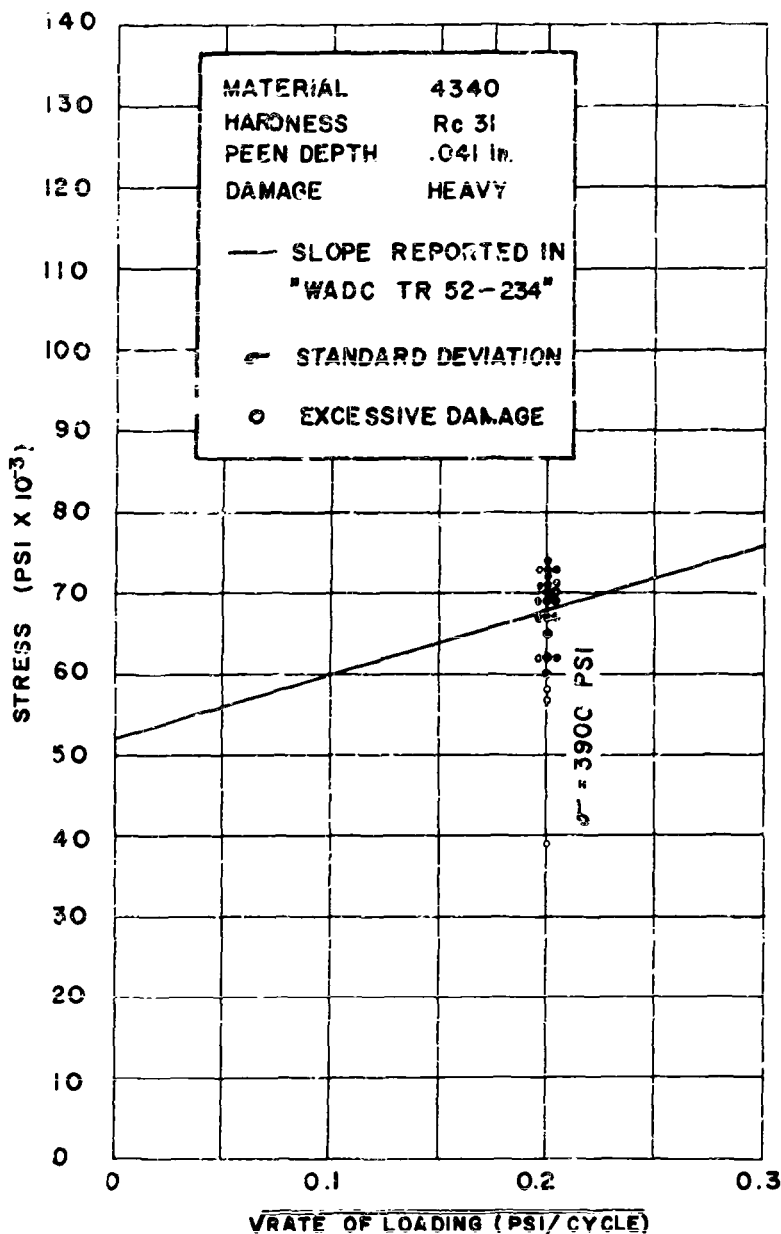FIGURE 16. FATIGUE TEST RESULTS Rc 31, .041 in.
PEEN DEPTH, HEAVY DAMAGE

The chart contains the following labels:

Y-axis: STRESS (PSI X 10⁻³)

X-axis: √RATE OF LOADING (PSI/ CYCLE)

Legend box:
MATERIAL   4340
HARDNESS   Rc 31
PEEN DEPTH   .041 in.
DAMAGE   HEAVY

— SLOPE REPORTED IN "WADC TR 52-234"
↵ STANDARD DEVIATION
○ EXCESSIVE DAMAGE

σ = 3900 PSI
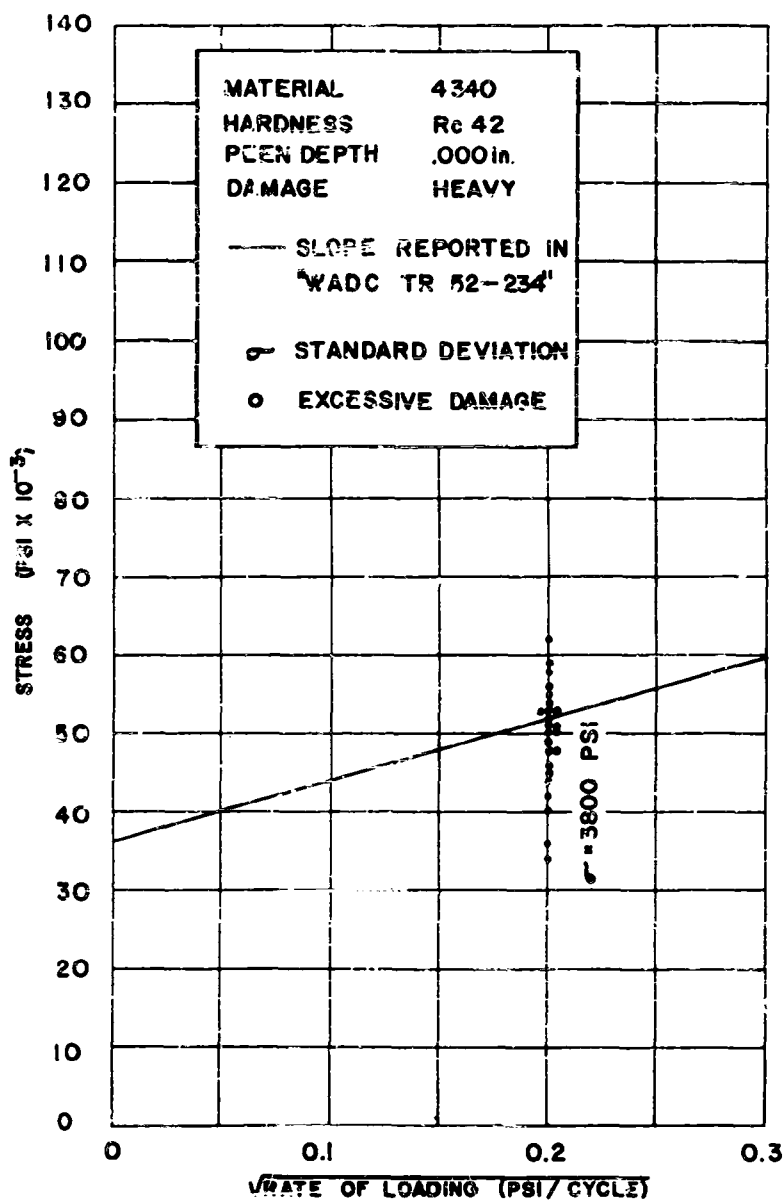
FIGURE 17. FATIGUE TEST RESULTS Rc 42, .000 in.
PEEN DEPTH, HEAVY DAMAGE
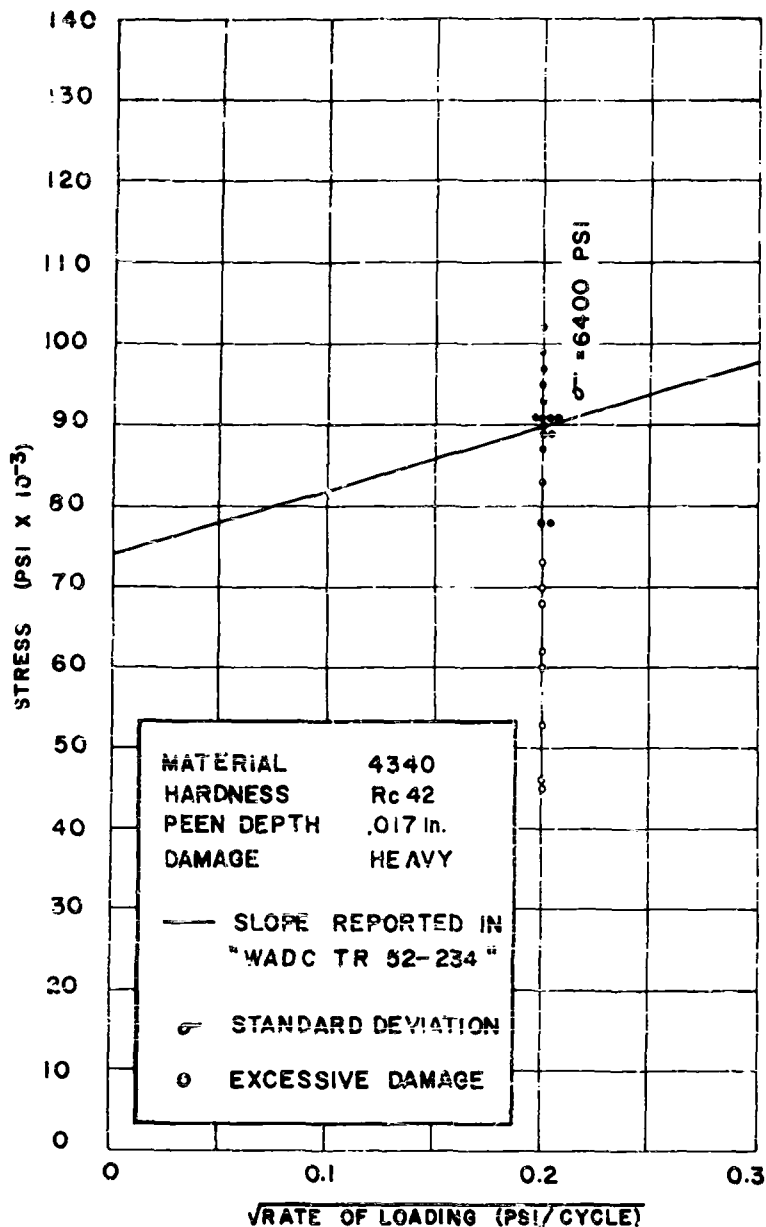
FIGURE 18. FATIGUE TEST RESULTS Rc 42, .017 in. PEEN DEPTH, HEAVY DAMAGE
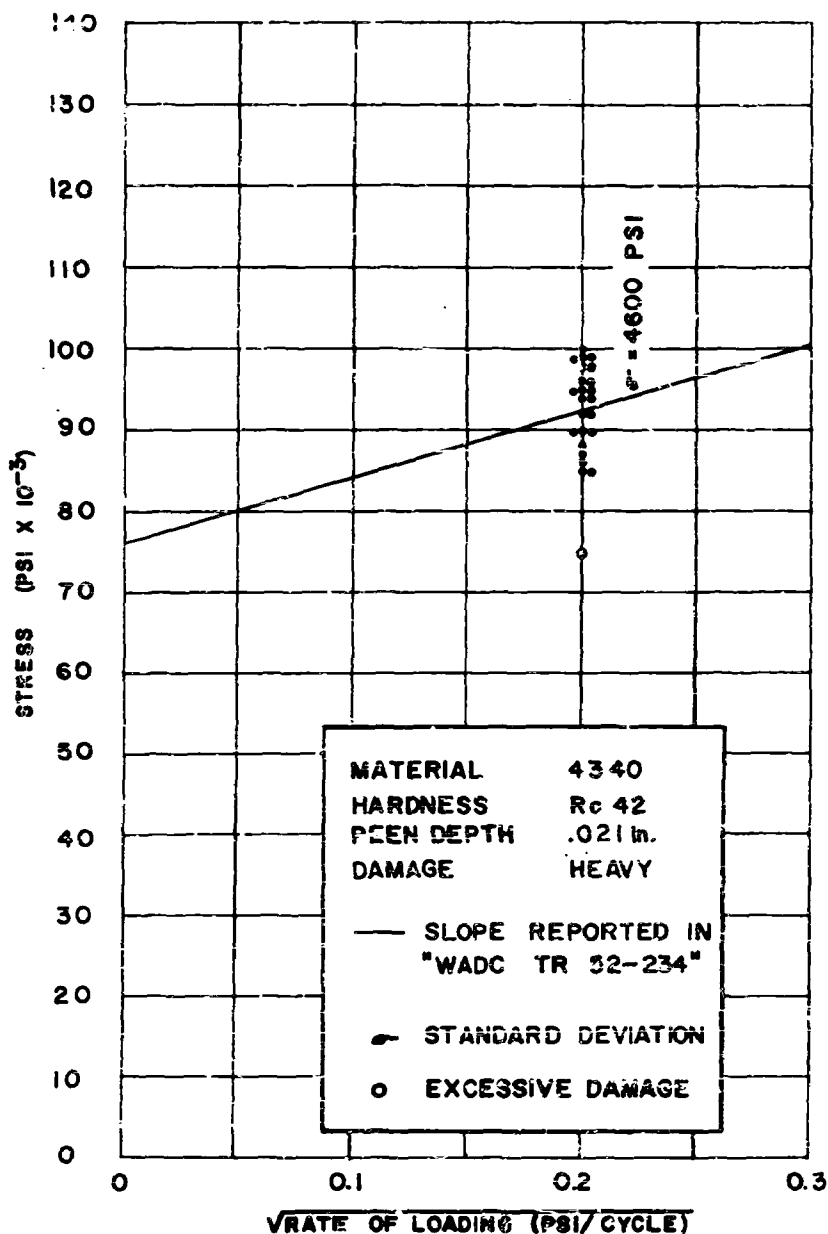
FIGURE 19. FATIGUE TEST RESULTS Rc 42, .021 in. PEEN DEPTH, HEAVY DAMAGE
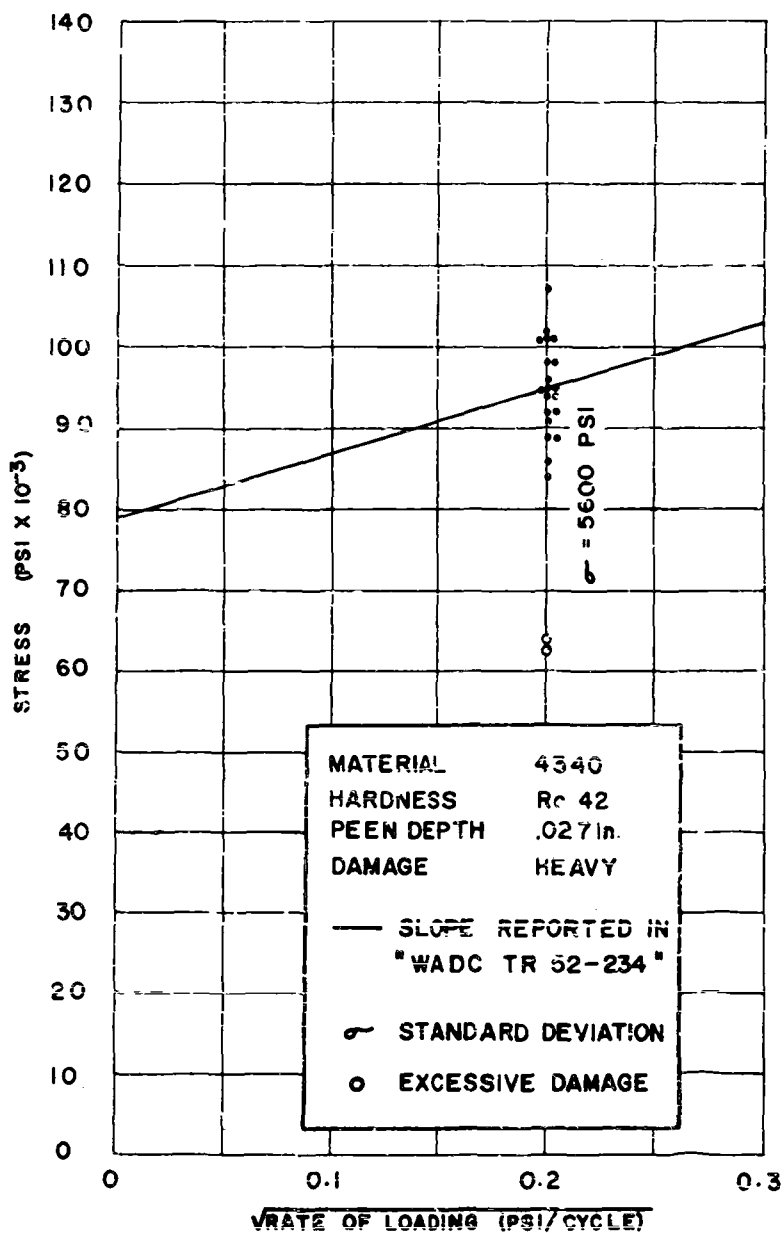
FIGURE 20. FATIGUE TEST RESULTS Rc 42, .027 in.
PEEN DEPTH, HEAVY DAMAGE
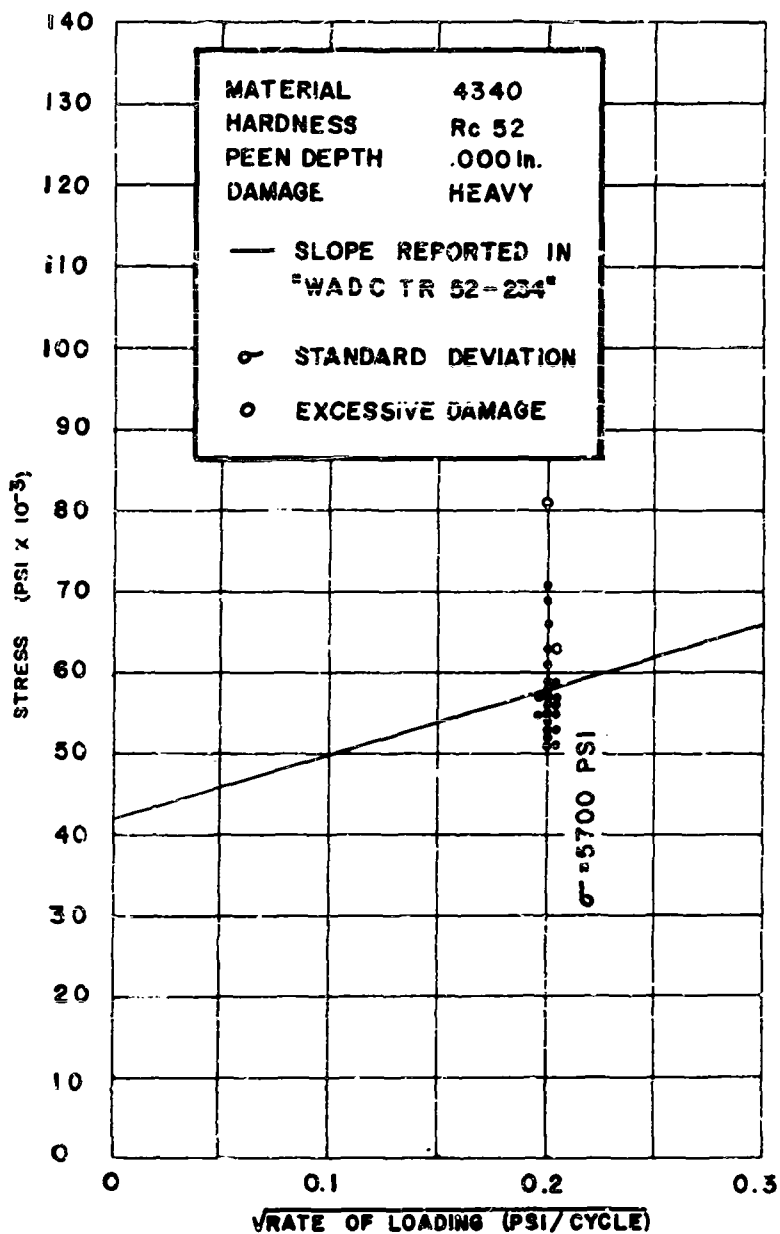
FIGURE 21. FATIGUE TEST RESULTS Rc 52, .000 in.
PEEN DEPTH, HEAVY DAMAGE
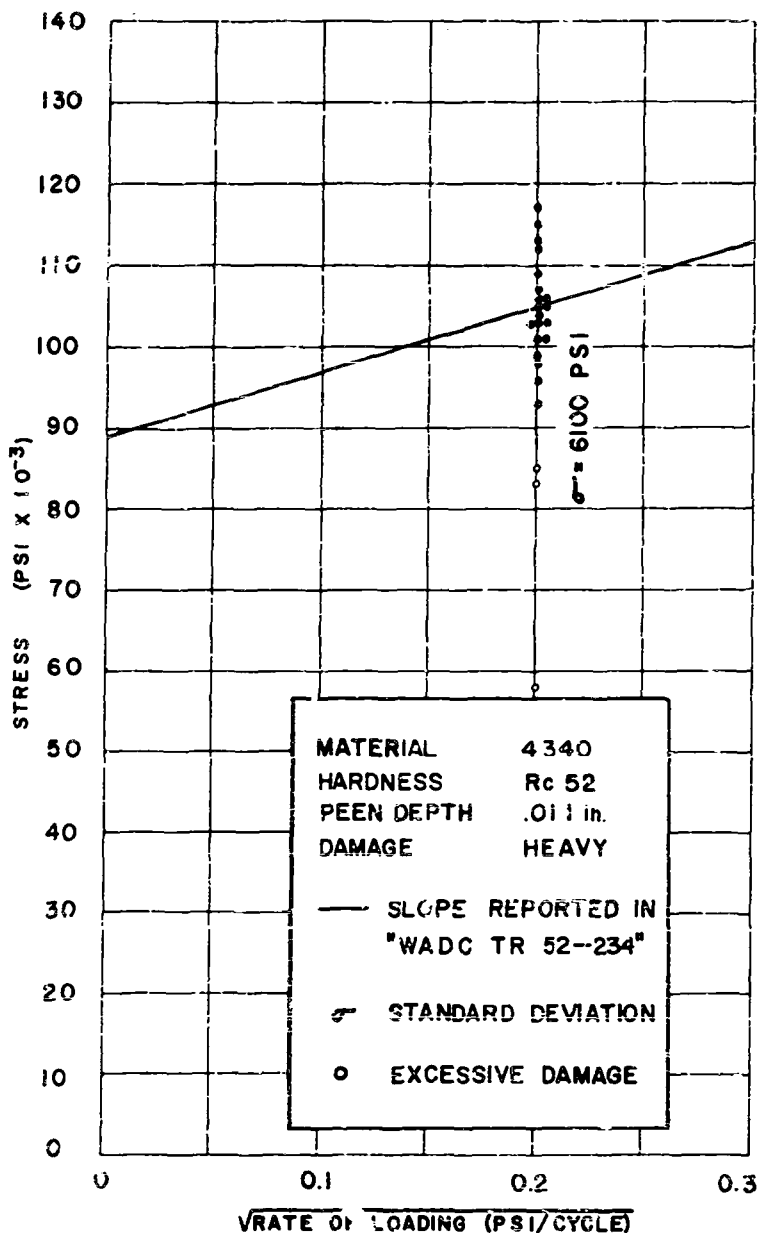
FIGURE 22. FATIGUE TEST RESULTS Rc 52, .011 in.
PEEN DEPTH, HEAVY DAMAGE
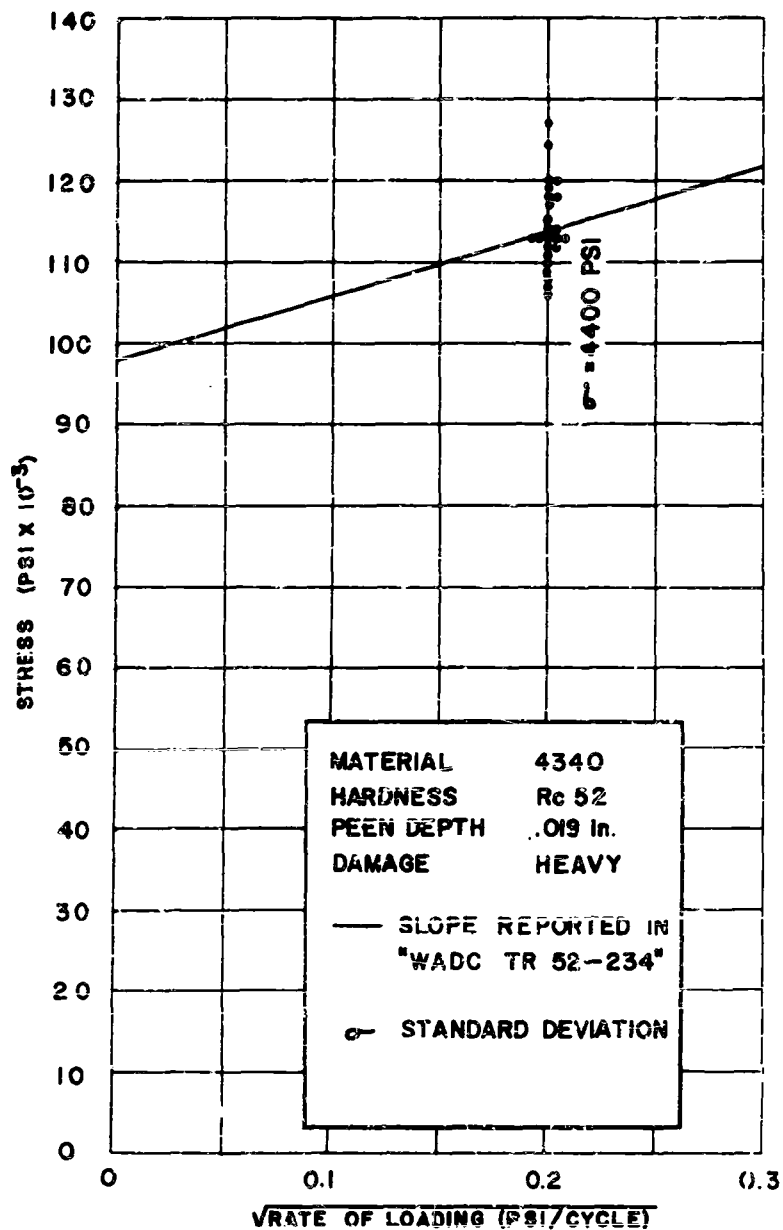
FIGURE 23. FATIGUE TEST RESULTS Rc 52, .018 in.
PEEN DEPTH, HEAVY DAMAGE
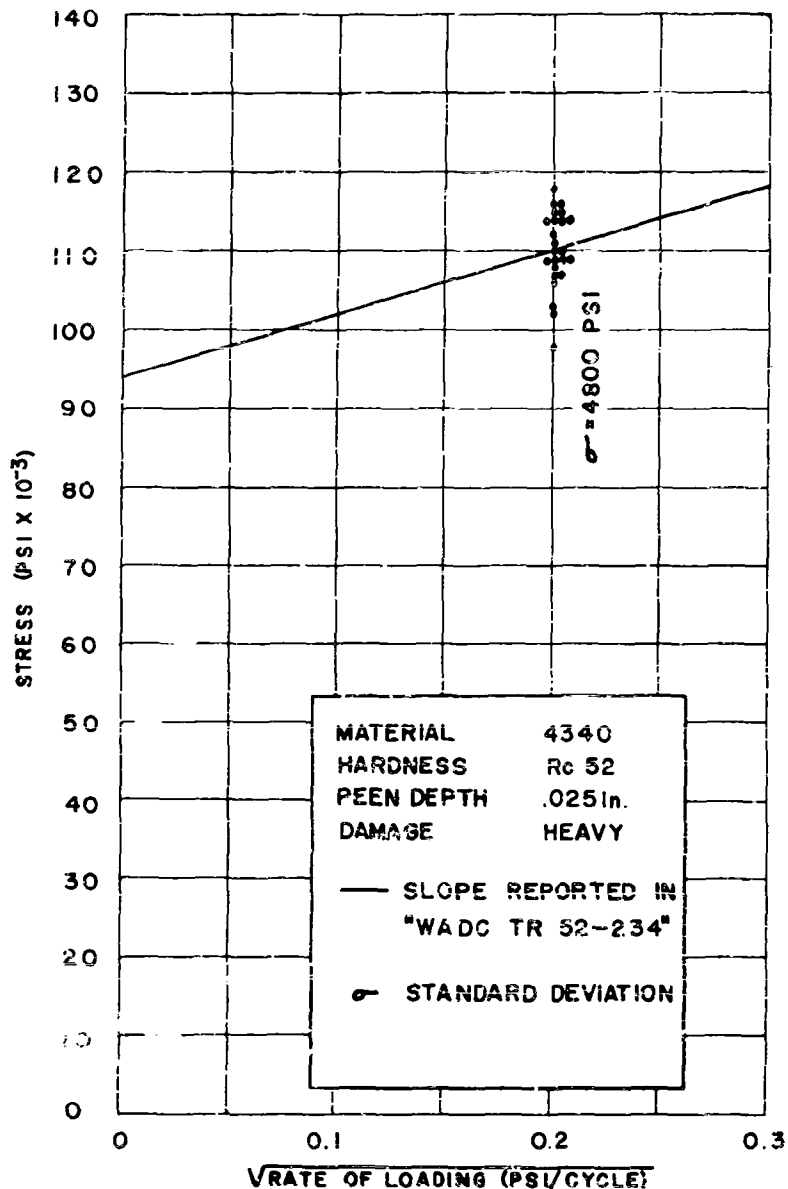
FIGURE 24. FATIGUE TEST RESULTS Rc 52, .025 in.
PEEN DEPTH, HEAVY DAMAGE
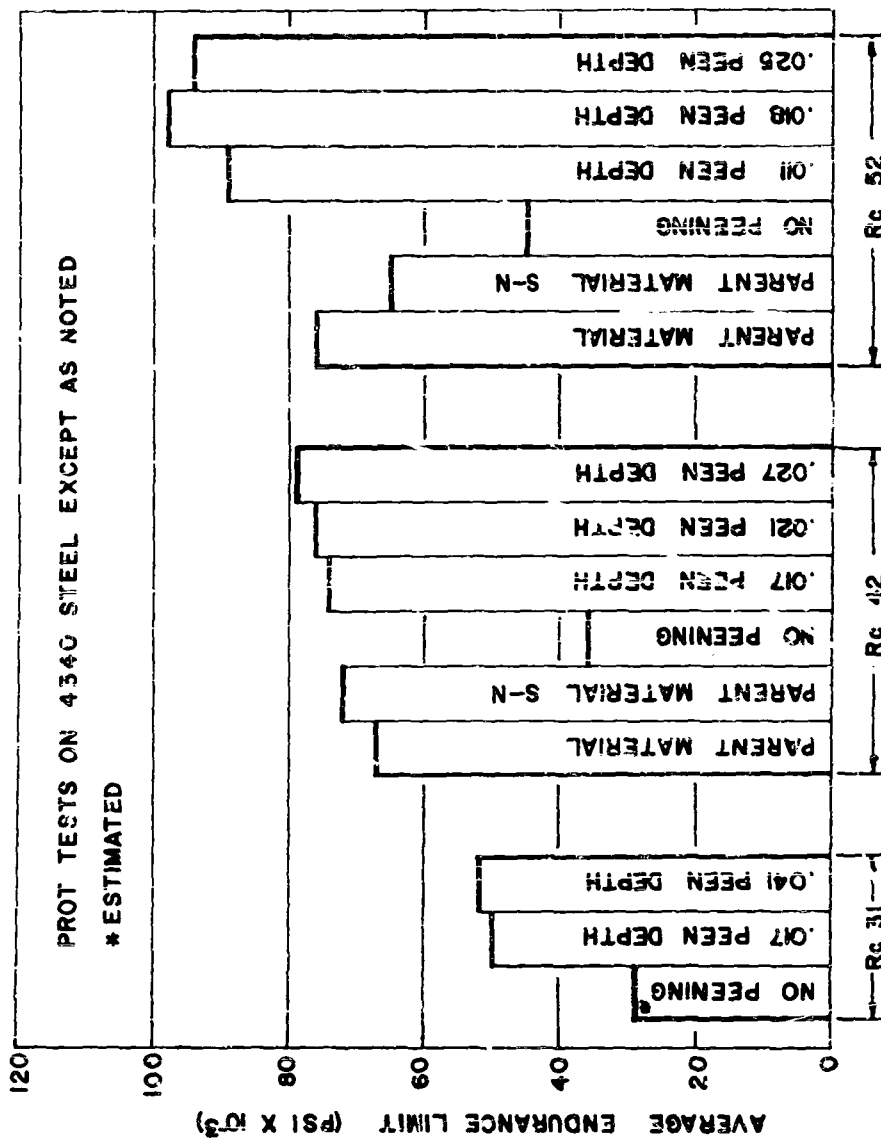
FIGURE 25. SUMMARY OF RESULTS— HEAVY DAMAGE
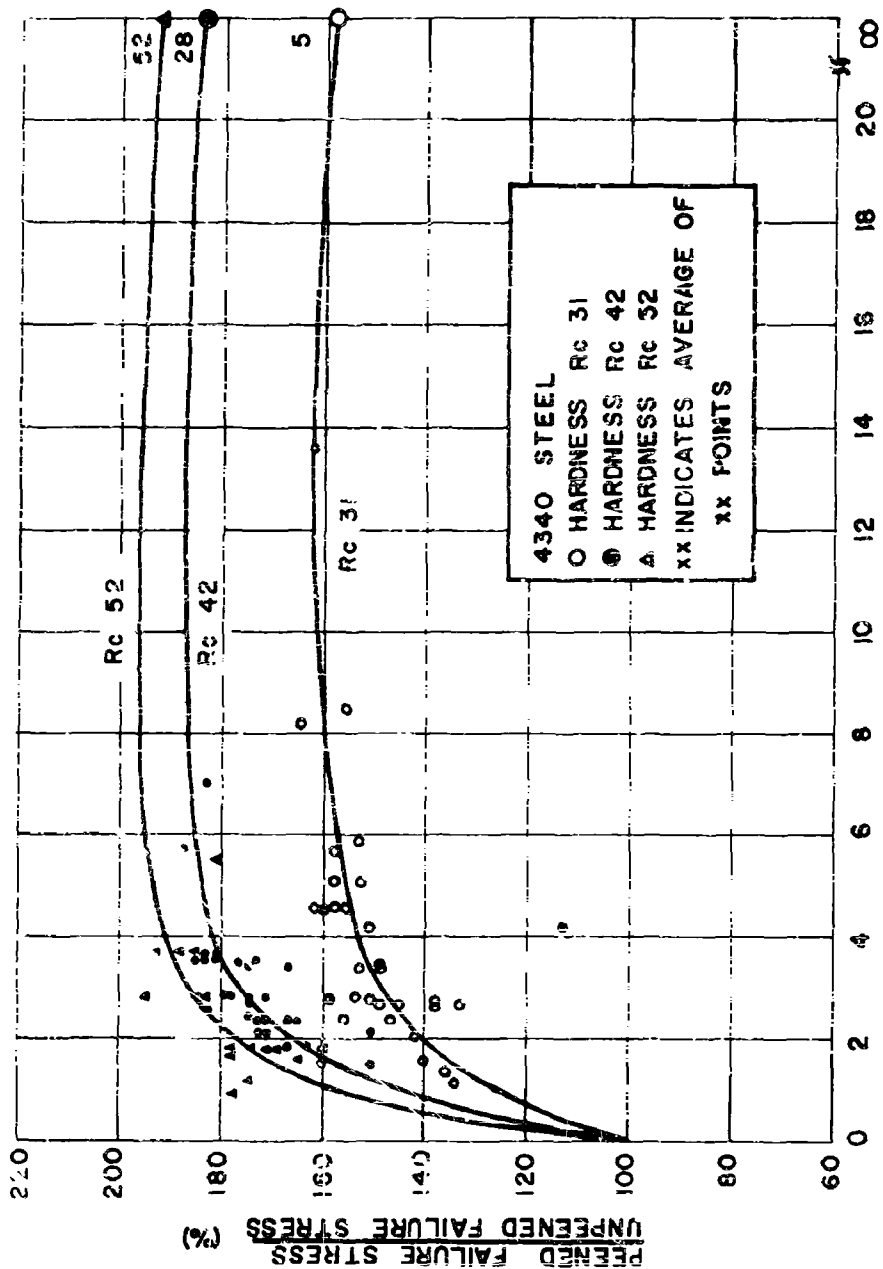
FIGURE 26. RELATIVE IMPROVEMENT OF FATIGUE PROPERTIES—HEAVY DAMAGE

III. DISTORTION

RESIDUAL STRESS AND CURVATURE

Because of the fact that the residual stresses produced by peening are a result of plastic and elastic strain, it is apparent that some dimensional change must necessarily accompany this treatment. The degree of this dimensional change is of course affected by the geometry of the part and the severity of peening. The propeller blade, being essentially a thin plate with some superimposed twist, might therefore be distorted to a sizeable degree by a heavy peening operation. It is essential that some knowledge of the distortion as a function of peening condition be obtained. This knowledge would enable prediction of the limits of peening in an actual case.

The study of distortion has been confined to flat plates peened on one side only. This case allows study of the fundamentals involved in distortion and permits expression of some of the factors affecting the distortion such as hardness, thickness, etc. The extension of data obtained from these simple tests would involve consideration of the particular geometry of interest.

In studying distortion, SAE 1040 steel specimens of varying thickness were peened under a variety of conditions. The resulting curvatures and residual stresses were evaluated. These data were then assembled in order to determine empirically the behaviour in distortion of the various thicknesses. This knowledge was then extended analytically to include the various hardnesses of steel as well as the single aluminum alloy under consideration. A listing of the residual stress specimens tested and the peening conditions involved is given in Table 4. All tests were undertaken at high shot coverage and using steel of hardness R_c 44. A constant shot flow rate (10 lb/min) and a fixed air pressure (50 psi) were used throughout the tests. Specimen size and shape were identical to those reported in Part 1 of WADC TR 55-56.

Since the distortion is produced primarily by the compressive stress from the peening operation, it seems apparent that the magnitude and depth of this compressive stress would be the most important factors in analyzing distortion. The maximum value of the stress, the depth, and the shape of the stress curve are involved in the force producing the distortion. These factors can be lumped together in terms of the compressive residual stress area which is the integral of stress times depth. This residual stress area then represents the force per unit width of flat specimen which is acting to produce extension and bending. Bending is the more predominant factor in the case of a flat specimen peened on one side only. If it is assumed that similar peening treatments produce the same compressive residual stress area on different thicknesses of identical

TABLE 4

RESIDUAL STRESS SPECIMENS

Specimen No.	Material	Hardness R_c	Shot Size	Air Pressure (psi)	Coverage	Thickness (in.)
1	4340 Steel	45	110	50	High	0.499
2	4340 Steel	44	110	50	High	0.498
3	4340 Steel	45	230	50	High	0.497
4	4340 Steel	43	230	50	High	0.496
5	4340 Steel	44	390	50	High	0.497
6	4340 Steel	44	390	50	High	0.498
7	4340 Steel	45	660	50	High	0.495
8	4340 Steel	45	660	50	High	0.499
9	4340 Steel	45	0.125 in.	50	High	0.498
10	4340 Steel	45	0.125 in.	50	High	0.499
11	4340 Steel	41	110	50	High	0.129
12	4340 Steel	41	110	50	High	0.129
13	4340 Steel	41	230	50	High	0.129
14	4340 Steel	41	230	50	High	0.129
15	4340 Steel	41	390	50	High	0.129
16	4340 Steel	41	390	50	High	0.129
17	4340 Steel	41	660	50	High	0.129
18	4340 Steel	41	660	50	High	0.129
19	4340 Steel	41	0.125 in.	50	High	0.129
20	4340 Steel	41	0.125 in.	50	High	0.129
21	4340 Steel	41	110	50	High	0.069
22	4340 Steel	41	110	50	High	0.067
23	4340 Steel	41	230	50	High	0.066
24	4340 Steel	41	230	50	High	0.067
25	4340 Steel	41	390	50	High	0.068
26	4340 Steel	41	390	50	High	0.066
27	4340 Steel	41	660	50	High	0.067
28	4340 Steel	41	660	50	High	0.069
29	4340 Steel	41	0.125 in.	50	High	0.067
30	4340 Steel	41	0.125 in.	50	High	0.069
31	4340 Steel	44	0.125 in.	50	High	0.714
32	4340 Steel	44	0.125 in.	50	High	0.714
33	4340 Steel	44	0.125 in.	50	High	0.998
34	4340 Steel	44	0.125 in.	50	High	0.998

materia'. . . . should be possible to calculate the curvature which would be . . . . d on each of these thicknesses. The energy of compressive st . . must be offset by equal amounts of energy in the remainder of specimen. Further, for equilibrium the compressive and tensile forces and moments must balance. Therefore, it should be possible to calculate approximately the entire residual stress distribution and the resulting specimen curvature knowing the characteristics of the compressive residual stress.

The test program was designed to study these affects as well as to detect relations between the potential energy of the specimen, the potential energy of an Almen strip peened simultaneously with the specimen, and the kinetic energy of the shot stream.

DISTORTION TEST RESULTS

The residual stress results for the various distortion test specimens are plotted in Figures 41 through 74 in Appendix II. The data from which these results are calculated are presented in Appendix III. As stated previously, the various tests involved only a single hardness of steel. These data are combined in the succeeding discussion with previous data on $1/4-$in. thick specimens of varying hardnesses of steel and of aluminum 76S-T6.

Figure 27 indicates that the compressive residual stress area is unaffected by specimen thickness above a thickness of $1/8$ in. for the peening conditions tested. Since for a given hardness of steel the maximum value of compressive stress is nearly constant and is at or near the surface, then a variation in compressive residual stress area is essentially directly proportional to the depth of compression. Thus, the depth of compression becomes a measure of distortion for specimens of constant hardness. Figure 28 shows the curvature vs. the depth of compressive layer for the various thicknesses of R_c42 material tested. Observation of this figure reveals a definite relation of curvature to thickness of specimen. It develops that the square of the thickness is the proportionality constant. Figure 29 is a plot of Ct^2 (curvature times the thickness squared) vs. depth of compression. It can be seen that, when plotted with this parameter, all thicknesses are represented on the same curve. Figure 29 also includes the average values of Ct^2 for each of the other hardnesses of steel and of aluminum. It should be noted that the latter values are based on only one thickness, it being assumed here that the same relations will apply that apply to the R_c42. Figures 30 through 32 show the curvature parameter Ct^2 plotted against the compressive residual stress areas for all hardnesses and shot conditions of steel. These three curves are essentially identical to each other. Figure 33 is the corresponding
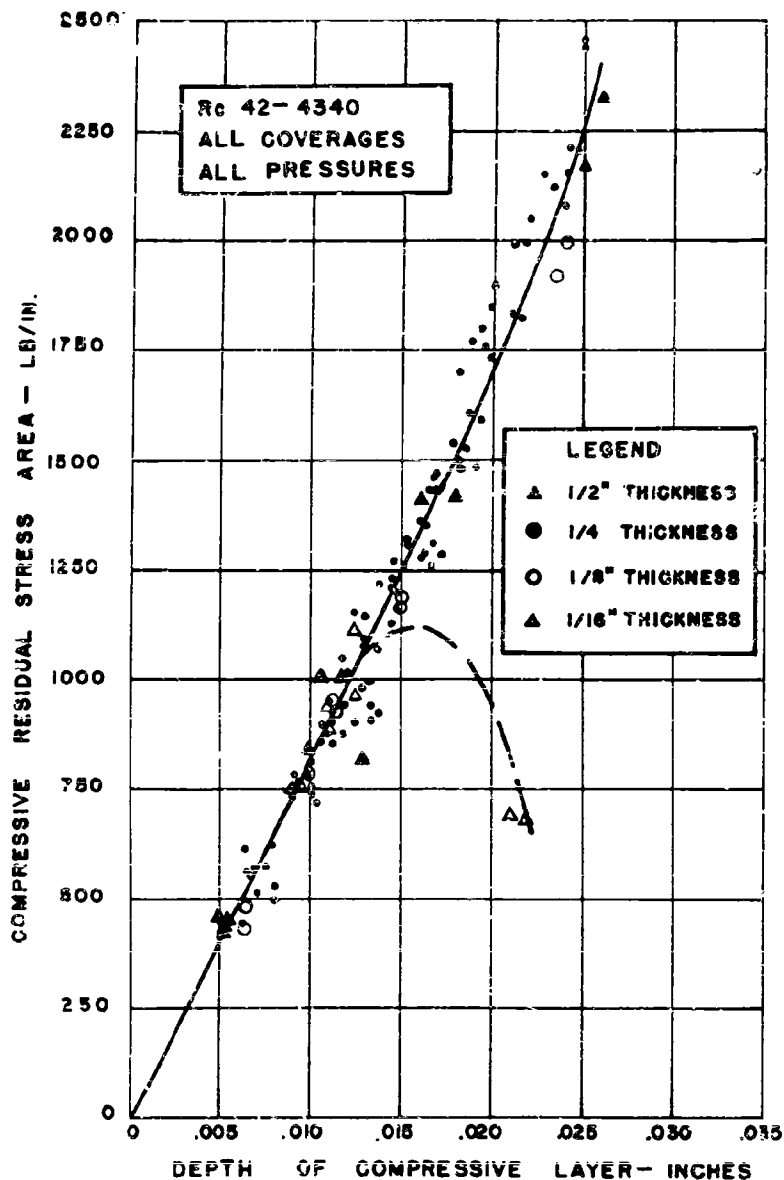
FIGURE 27. EFFECT OF THICKNESS ON COMPRESSIVE RESIDUAL STRESS AREA
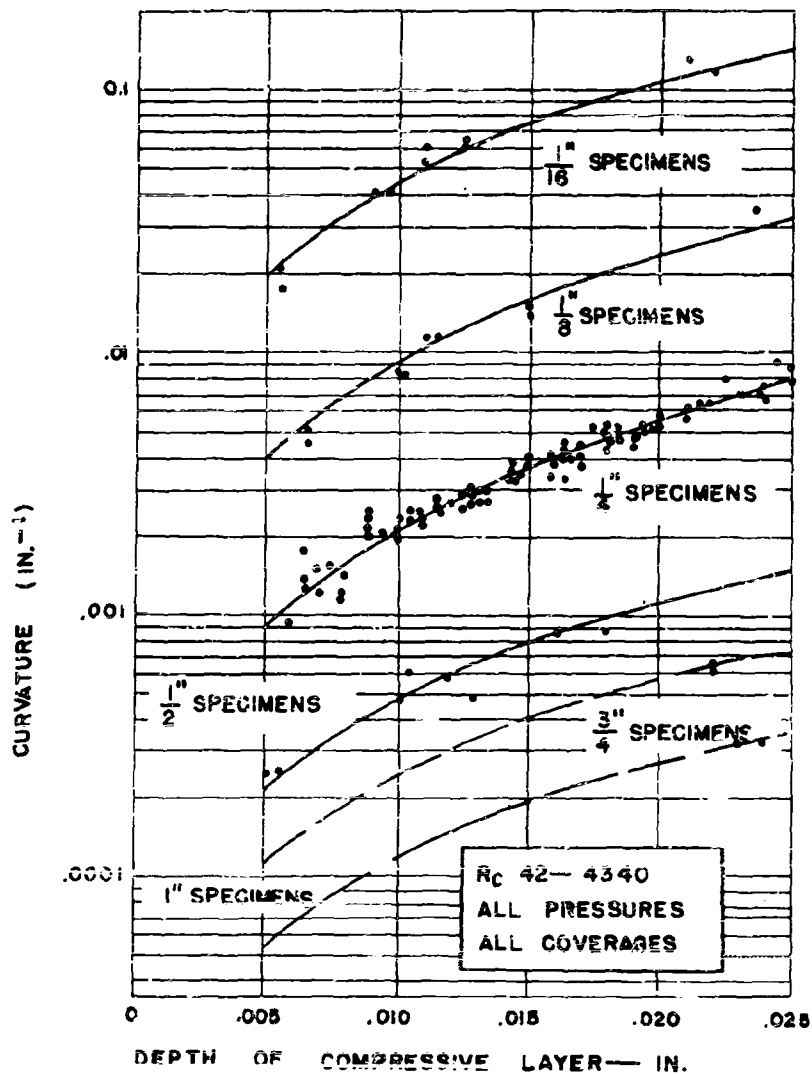
FIGURE 28. CURVATURE Vs. DEPTH OF COMPRESSIVE
LAYER

FIGURE 29. DISTORTION PARAMETER Vs. DEPTH OF COMPRESSION

The figure shows curves labeled Rc 31, Rc 42, and Rc 52 plotted with Ct^2 (in. x 10^4) on the vertical axis (0 to 5) and DEPTH OF COMPRESSIVE LAYER—IN. on the horizontal axis (0 to .030).

INCLUDES ALL THICKNESSES OF Rc 42. Rc 31 and Rc 52 TESTED FOR 1/4" THICKNESS
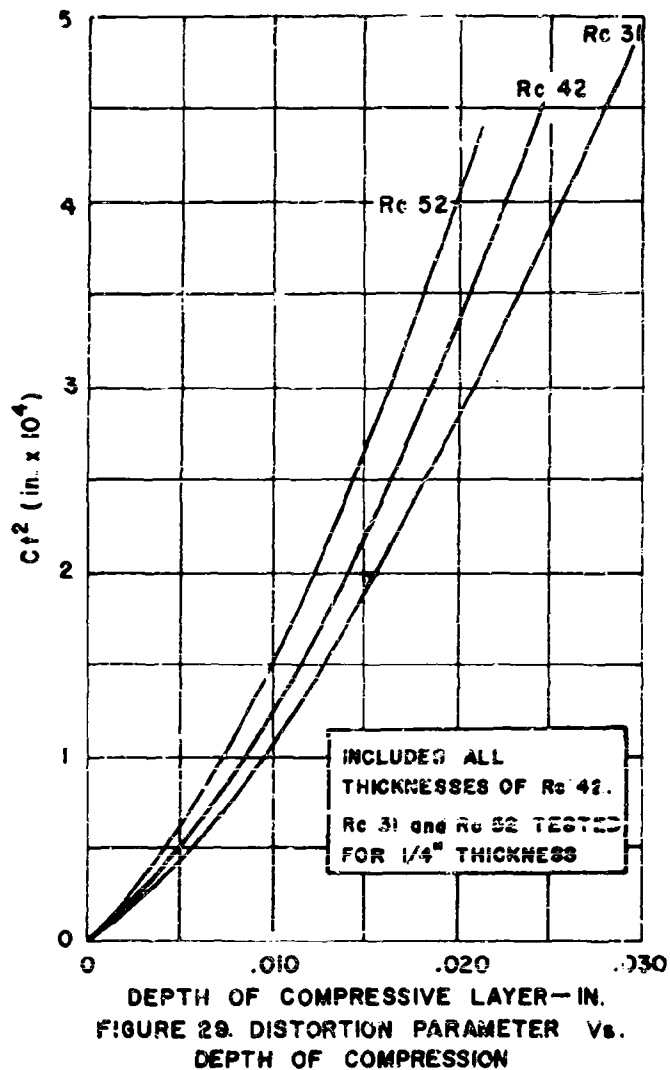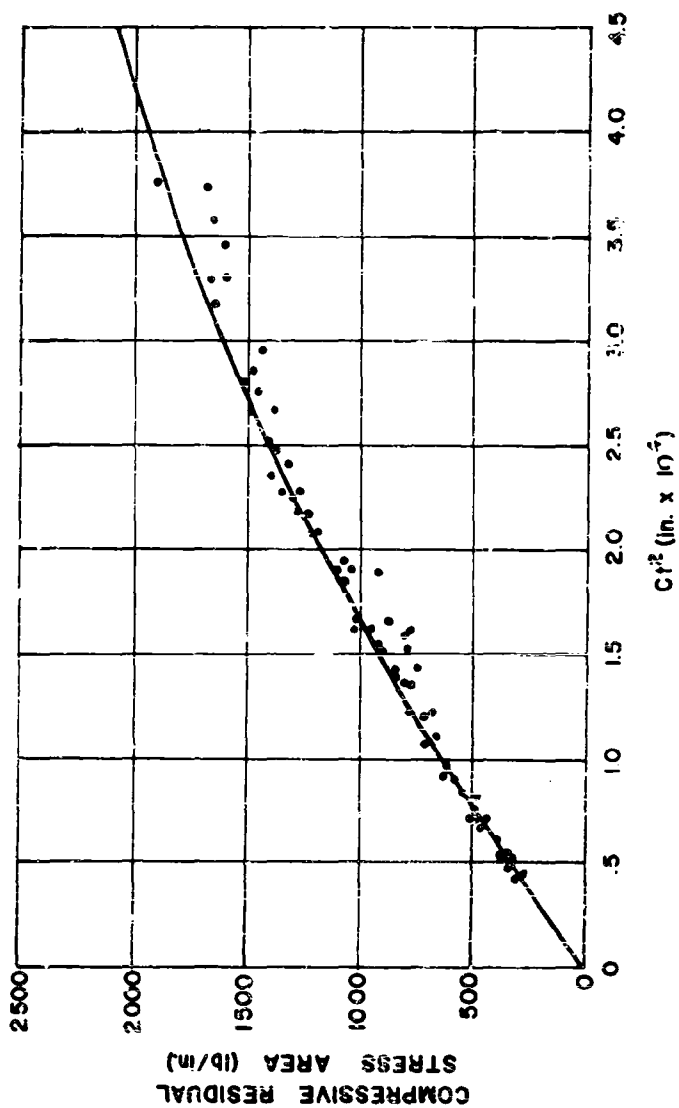
FIGURE 30. DISTORTION PARAMETER Vs. COMPRESSIVE RESIDUAL STRESS AREA
(lb/in.) FOR 4340 STEEL — Rc 31
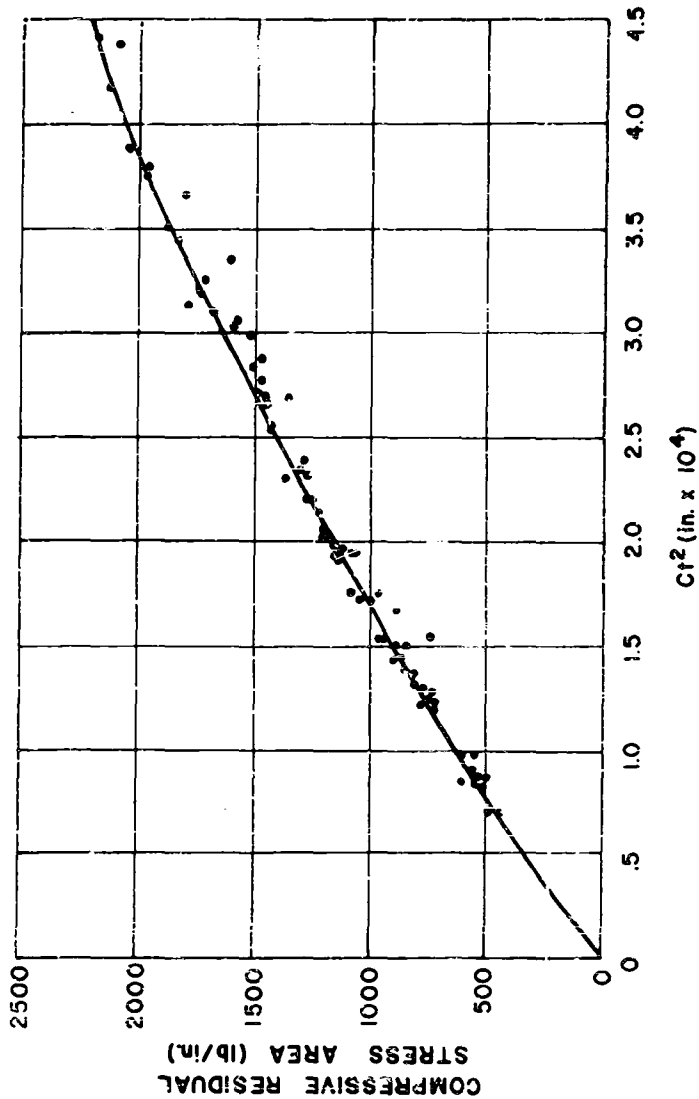
FIGURE 31. DISTORTION PARAMETER Vs. COMPRESSIVE RESIDUAL STRESS AREA (lb/in.) FOR 4340 STEEL— Rc 42
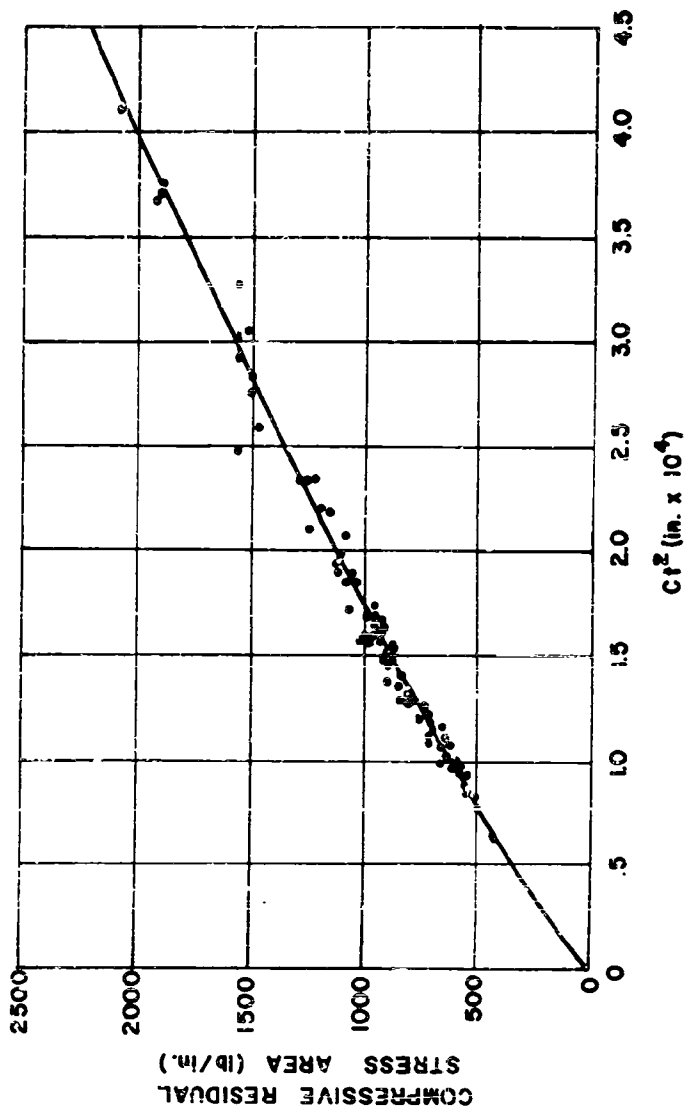
FIGURE 32. DISTORTION PARAMETER VS. COMPRESSIVE RESIDUAL STRESS AREA (lb/in.) FOR 4340 STEEL — Rc 52
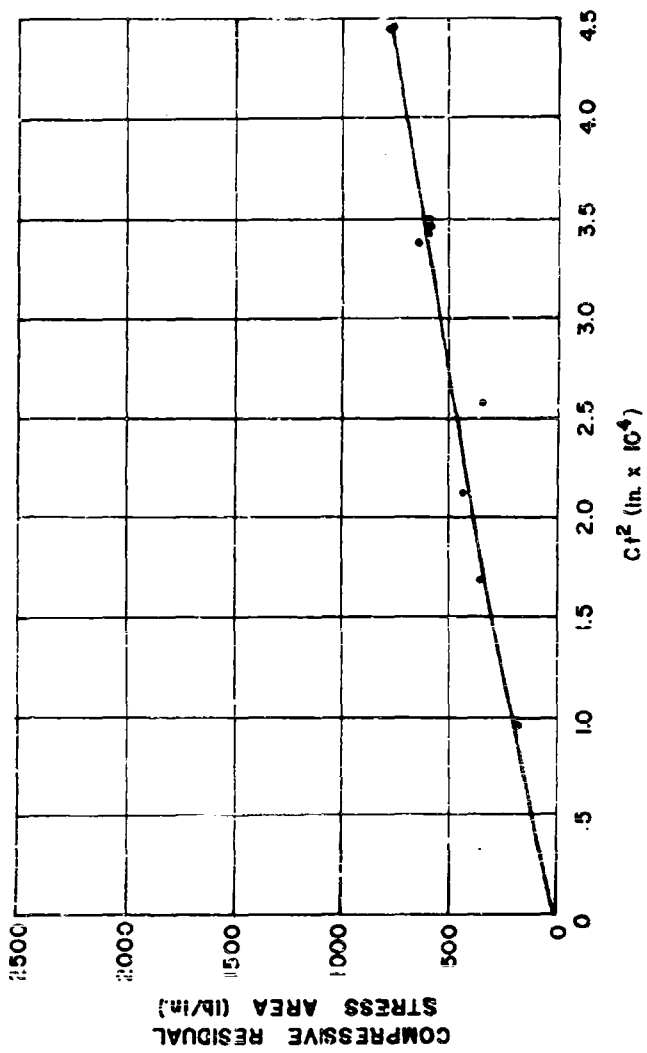
FIGURE 33. DISTORTION PARAMETER Vs. COMPRESSIVE RESIDUAL STRESS AREA (lb/in.) FOR 76S—T6 ALUMINUM

curve for aluminum and can be made to coincide with the curve for these steels by multiplying by the ratio of the elastic moduli, i. e., E_{St}/E_{Al}. These curves, when combined with the residual stress data given in WADC TR 55-56, Part 1, allow the determination of the specimen curvature to be expected from any peening condition.

It is also of interest to relate these variables to the Almen arc height observed during peening, since the latter is the common method of determining the peening conditions. Consequently, Figures 34 and 35 have been included. These are plots of the various parameters against the Almen C arc height resulting from the peening. It will be noted that the slope of Ct^2 vs. Almen C increases at an Almen C value of approximately .008 in. This is attributed to the limitation observed in low thicknesses, as was shown in Figure 27, and is a result of increased stiffness as the thin strip develops transverse curvature.

Although the maximum value of compressive stress and depth are of primary interest, the peak value of tensile residual stress immediately below the compressive layer may also be of interest in many cases. Figure 36 shows how this peak value changes with specimen thickness. It can be seen that the value of tensile stress increases as thickness decreases. This is reasonable as it is necessary to enable force and moment equilibrium to be maintained. In this connection Figure 37 shows the location of the neutral axis, that is the point at which the residual stress becomes zero after having reached its maximum value of tension. It can be seen that the position of the neutral axis is a function of thickness only, regardless of the peening conditions on a given material. The tests as shown were conducted only on R_c 42 material in which the maximum value of compressive stress is essentially constant.

A summary curve for all materials tested results from the inclusion (in the parameter Ct^2) of the modulus and the maximum compressive stress for each specimen. Figure 38 is a plot of the parameter $\dfrac{Ct^2 E}{\sigma_{c\,max}^2}$ vs. the depth of compression for all cases considered; that is for all materials, coverages, shot sizes, air pressures, and thicknesses tested. Thus, given the dimensions of the piece to be treated and knowing either the maximum compressive stress resulting from peening of that hardness or the depth of compression resulting from the peening, it is possible to determine the distortion which would result. The depth of compression can be obtained from curves for the various materials and peening conditions as given in Part 1. Because of the large number of data points available for Figure 35, only about 20% of the points have been plotted. Every fifth point was selected from a numerical listing of specimens.
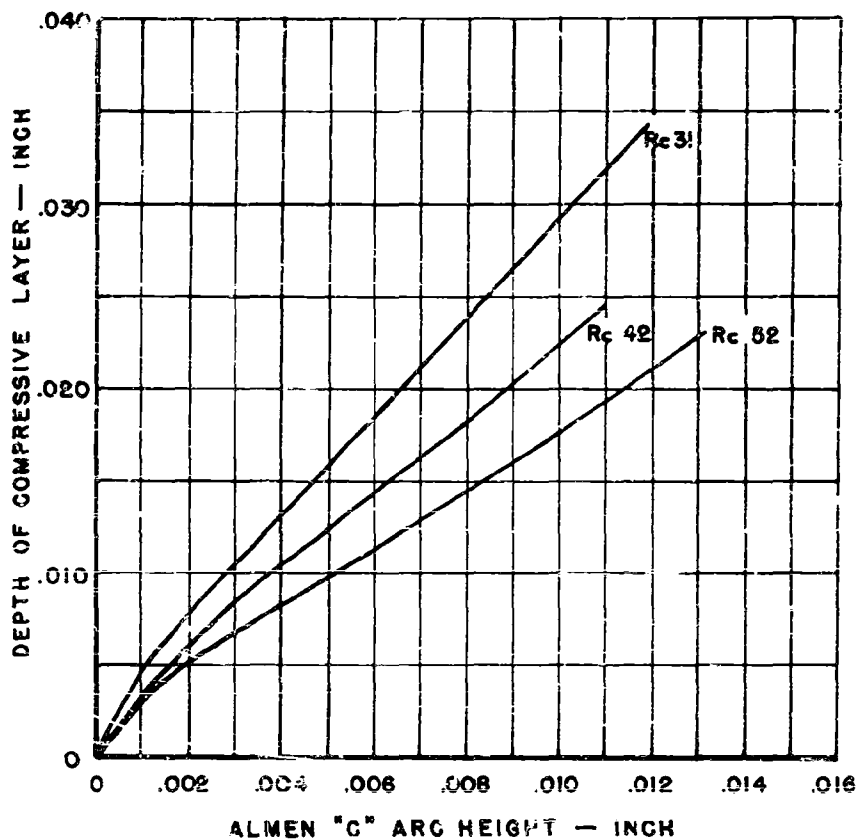
FIGURE 34. DEPTH OF COMPRESSION VS.
ALMEN ARC HEIGHT

FIGURE 35. DISTORTION PARAMETER Vs. ALMEN "C"
ARC HEIGHT
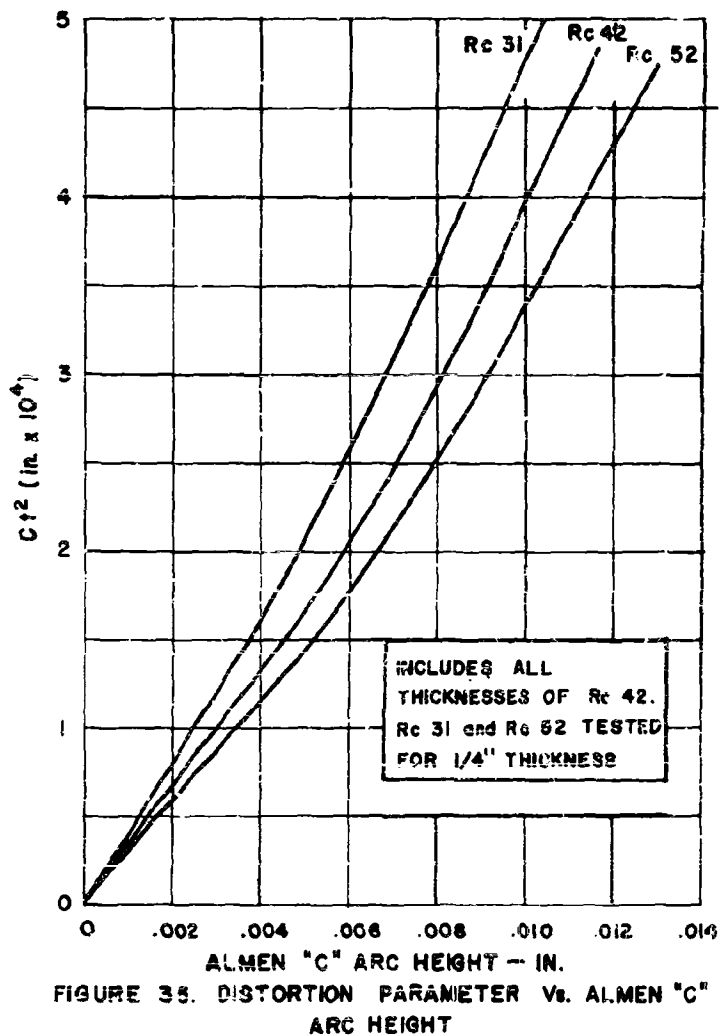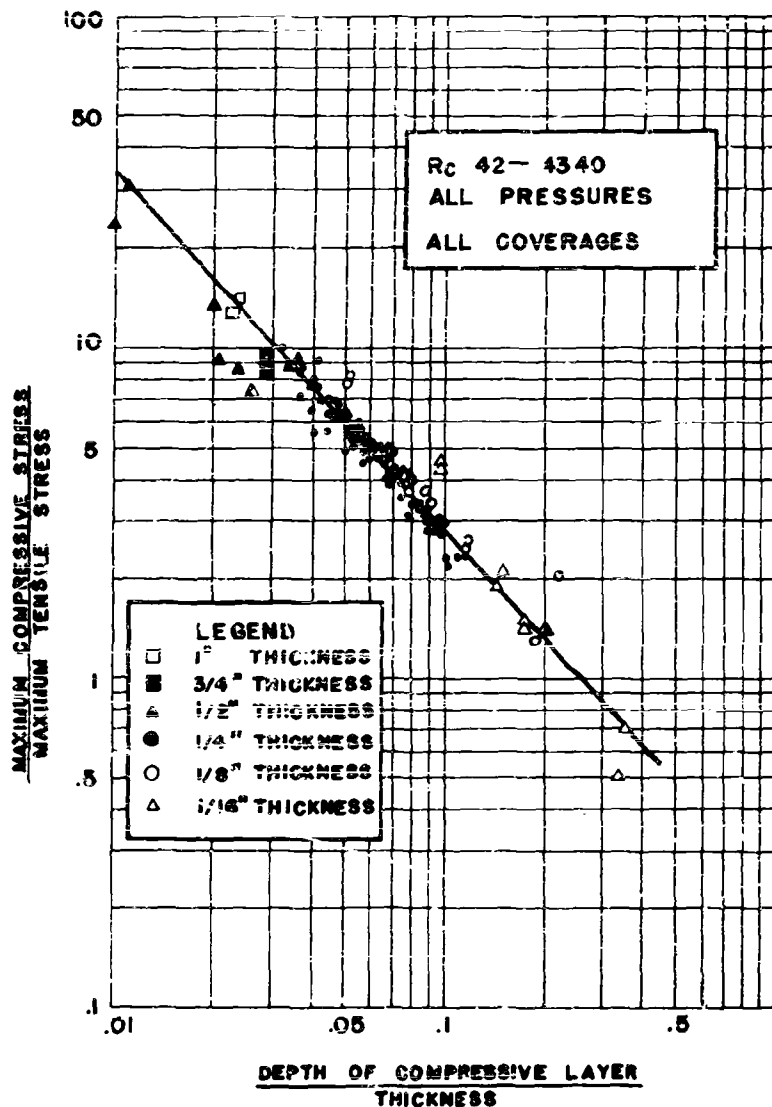
FIGURE 36. RATIO OF MAXIMUM COMPRESSIVE STRESS TO MAXIMUM TENSILE STRESS
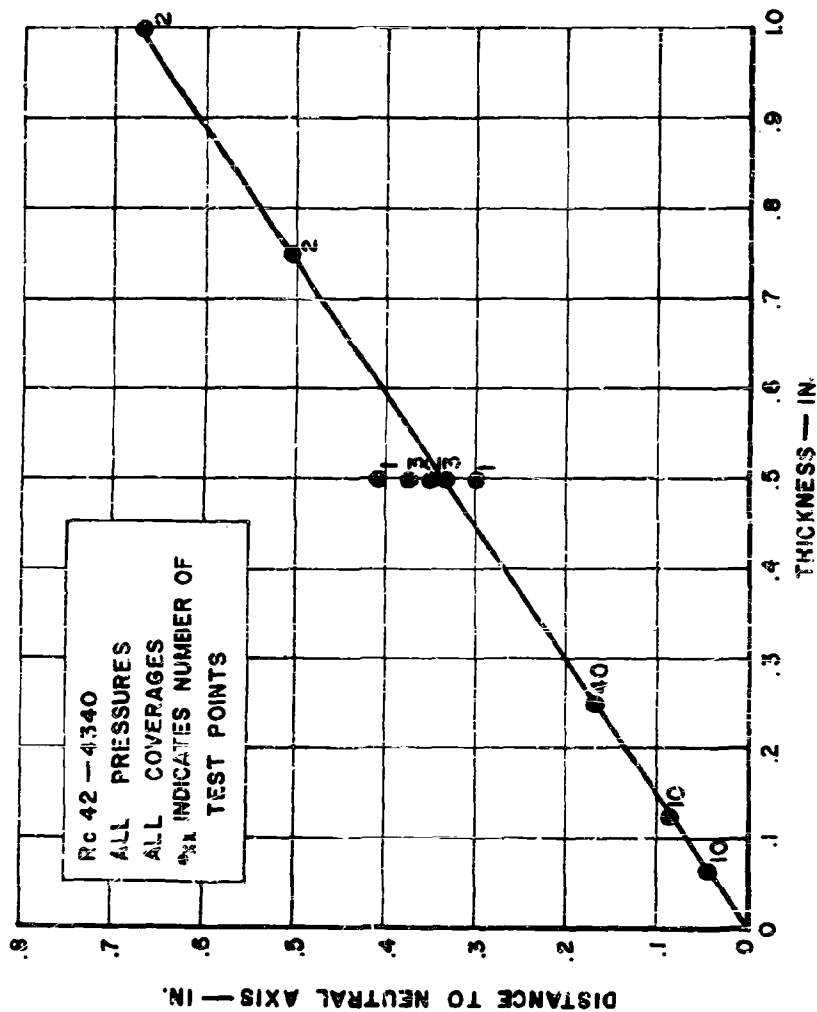
FIGURE 37. EFFECT OF THICKNESS ON LOCATION OF NEUTRAL AXIS
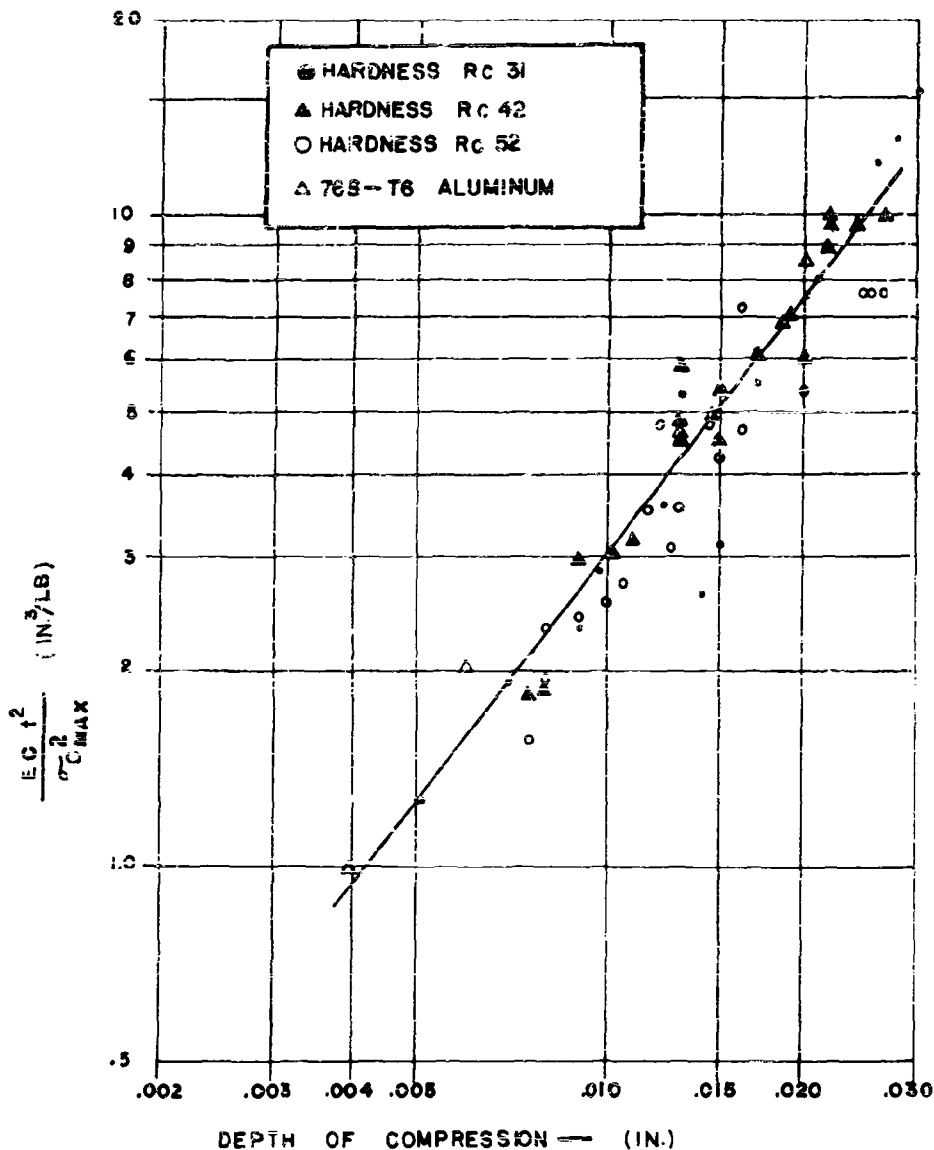
FIGURE 38. DISTORTION PARAMETER CORRECTED FOR
MATERIAL PROPERTIES

It seems theoretically probable that a more universal curve relating compressive stress and depth to the kinetic energy of the shot, either the single shot or the total shot stream, could be obtained. This relation, however, has not yet been discovered. The depth of compression can however be related for each material and shot velocity. Figure 39 shows the ratio of depth of compression/ shot diameter for R_c 42 material vs. the parameter D^3V^3, where D is the shot diameter (in.) and V is the shot velocity (ft/sec). The exact physical significance of this parameter is not clear. It would seem that the parameter D^3V^2 would be more representative of the kinetic energy of a single shot. A plot of this parameter, however, does not produce a smooth curve.

IV. MEASUREMENT OF SHOT VELOCITY

In order to correlate the results of these peening tests with shot peening as done on other equipment, it was deemed necessary to know the velocity of the shot. This was measured by means of high-speed flash photography. A high-intensity flash tube was placed in the rear of the peening cabinet. A viewing window was cut into the front of the cabinet such that the shot stream was silhouetted against the flash tube. A reference marker 1-in. long was placed adjacent to the shot stream. The flash tube was triggered by an oscillator operating either at 1800 or 2400 cps, depending on the particular run. The tube flashed 3 times, each flash being less intense than the previous one. The camera was placed at the viewing window and aimed at the flash tube with open shutter. Thus, the film was subjected to a triple exposure with a known time between exposures. This resulted in a picture wherein individual shot could be identified at 3 locations with respect to the 1-in. marker and with respect to the known time. This enabled the calculation of the velocity of shot.

Figure 40 shows the results of this test. It can be seen that the maximum velocity obtained is approximately 120 ft/sec. It can also be seen that the shot velocity is practically independent of shot size. This may be partly due to the fact that the shot and air nozzle sizes were changed with the shot size in accordance with the schedule previously reported in Part I. The values of shot velocity are somewhat lower than would be expected from a wheel—type machine. They are also somewhat lower than those reported by Coombs, Sherratt and Pope at the International Conference on Fatigue of Metals, London, 1956, but agree quite closely to some unpublished data taken on a similar cabinet.
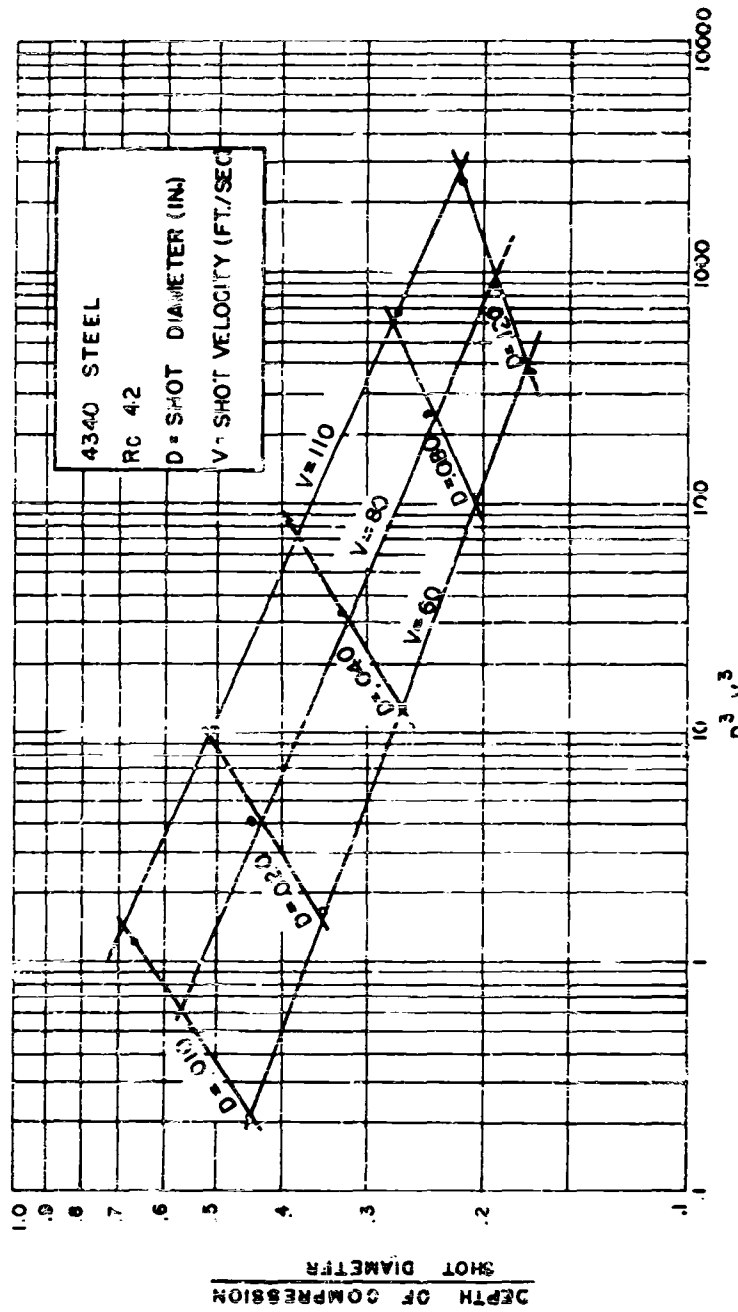
FIGURE 39. DEPENDENCE OF DEPTH OF COMPRESSION ON SHOT DIAMETER AND SHOT VELOCITY

Figure 40 can be used to convert all values of air pressure previously reported to shot velocity, enabling results on other equipment to be compared with those reported from this project.

V. CONCLUSIONS

For the case of light damage, shot peening increased the fatigue strengths of SAE 4340 steel of hardnesses R_c 51, R_c 42 and R_c 52 by 19%, 53% and 86%, respectively. The optimum ratio of depth of compression to depth of damage is about five or greater, although considerable improvement in fatigue strength of R_c 42 and R_c 52 material is achieved at a ratio as low as two.

For the case of heavy damage, shot peening increased the fatigue strengths of SAE 4340 steel at hardnesses R_c 31, R_c 42 and R_c 52 by 72%, 120%, and 133%, respectively. The figure for the R_c 31 is based on an estimated fatigue strength for the unpeened—damaged material. The optimum ratio of depth of compression to depth of damage is about five or greater, although considerable improvement in fatigue strength was noted at a ratio as low as one.

A check of the Prot slope resulted in a value which would indicate a lower endurance limit than would be indicated by WADC TR 52-234. When failure stresses and stress rates are not corrected for gouge depth, the slope is identical to that reported in WADC TR 52-234. S-N tests in general confirmed the lower values of endurance limit. The S-N tests showed considerable scatter, however, which is a natural result of scatter in the damaged specimens.

S—N tests on the harder steels failed to reveal definite fatigue strengths, a condition which has been noted by a few other investigators.

Empirical curves and parameters relating distortion of flat plates to peening conditions have been established. The parameter $\frac{C t^2 E}{\sigma_c^2}$, when plotted against the depth of compressive layer, appears to relate all peening conditions, thicknesses and materials tested.

The compressive residual stress conditions are essentially constant for thicknesses of 1/8 in. and above. On the basis of a few tests, the residual stress condition changes below 1/8 in. thickness. For a given state of compressive stress in the region of the surface, the tensile stress beneath this layer increases with decreasing thickness.
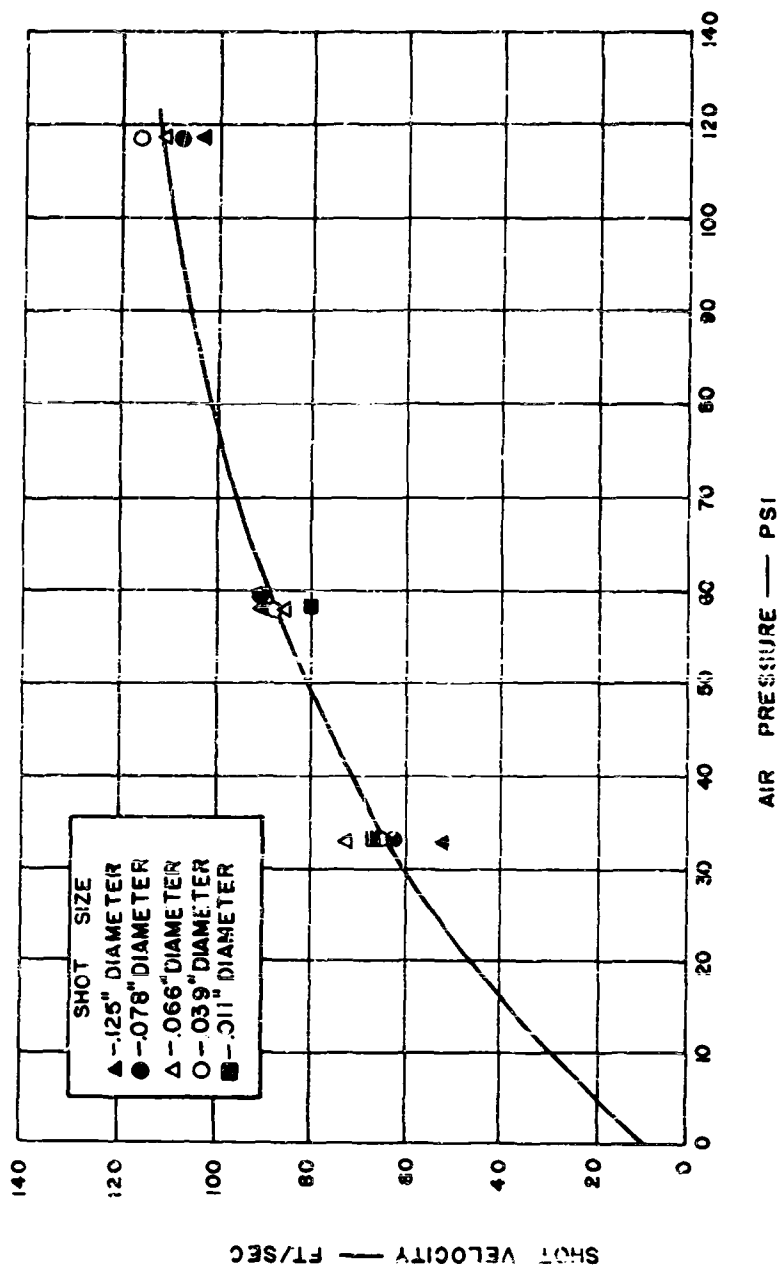
FIGURE 40. SHOT VELOCITY vs. AIR PRESSURE

APPENDIX I

FATIGUE TEST SPECIMENS

The table on the following pages lists all fatigue specimens tested, together with the peening conditions, type of damage and failure stress for each. The maximum gouge depth refers to the deepest penetration of the gouge through which failure occurred. The gouge depth at failure refers to the depth at the nucleus of the fatigue crack.

TABLE 5

FATIGUE TEST SPECIMENS

Specimen No.	Hardness R_c	Compressive Depth (in.)	Damage	Maximum Gouge Depth (in.)	Gouge Depth at Failure (in.)	Failure Stress (10^3 psi)
301	27.5	.000	Light	.002	.002	64
302	26.8	.000	Light	.002	.002	69
303	26.8	.000	Light	.003	.004	62
304	26.0	.000	Light	.000	.000 (c)	68
305	27.8	.000	Light	.000	.000 (a)	69
306	27.0	.000	Light	.006	.006	61
307	26.0	.000	Light	.000	.000 (c)	67
308	26.0	.000	Light	.001	.001	64
309	25.9	.000	Light	.000	.000 (a)	69
310	26.0	.000	Light	.000	.000 (c)	66
311	26.0	.000	Light	.005	.005	65
312	25.8	.000	Light	.000	.000 (c)	62
313	28.0	.000	Light	.000	.000 (a)	66
314	27.8	.000	Light	.006	.006	64
315	26.0	.017	Light	.010	.010	60
316	27.0	.017	Light	.010	.010	65
317	26.5	.017	Light	.010	.004	72
318	27.0	.017	Light	.004	.009	65
319	26.5	.017	Light	.009	.006	74
320	26.5	.017	Light	.012	.012	60
321	25.8	.017	Light	.006	.006	71
322	26.0	.017	Light	.004	.004	73
323	27.0	.017	Light	.006	.006	68
324	26.0	.017	Light	.006	.006	67
325	27.0	.017	Light	.000	.000 (c)	74
326	26.5	.017	Light	.004	.004	70
327	27.0	.017	Light	.006	.006	77
328	27.5	.017	Light	.002	.002	75
329	30.0	.017	Heavy	.013	.000 (b)	66
330	30.0	.017	Heavy	.013	.003	71
331	30.8	.017	Heavy	.041	.000 (b)	70
332	29.8	.017	Heavy	.008	.008	64
333	30.0	.017	Heavy	.027	.000 (b)	74

(a) Did not fail through gouge
(b) Failed at entry or exit of gouge
(c) Failed at surface scratch less than .001 in. deep

TABLE 5 (CONTINUED)

FATIGUE TEST SPECIMENS

Specimen No.	Hardness R_c	Compressive Depth (in.)	Damage	Maximum Gouge Depth (in.)	Gouge Depth of Failure (in.)	Failure Stress (10^3 psi)
334	29.5	.017	Heavy	.017	.000 (b)	71
335	30.0	.017	Heavy	.006	.006	68
336	30.0	.017	Heavy	.019	.000 (b)	73
337	31.0	.017	Heavy	.064	.004	51
338	30.0	.017	Heavy	.020	.020	58
339	31.0	.017	Heavy	.009	.004	68
340	30.5	.017	Heavy	.005	.002	70
341	30.0	.017	Heavy	.021	.020	58
342	30.0	.017	Heavy	.018	.012	61
343	29.8	.017	Heavy	.006	.006	69
344	30.0	.017	Heavy	.022	.011	63
345	30.0	.017	Heavy	.014	.007	66
346	31.0	.017	Heavy	.055	.037	41
347	29.5	.017	Heavy	.051	.017	59
348	29.5	.017	Heavy	.048	.024	56
349	30.0	.017	Heavy	.032	.016	59
350	30.0	.017	Heavy	.009	.007	70
351	30.0	.017	Heavy	.021	.014	66
352	29.0	.000	Heavy	.001	.000 (c)	53*
353	30.0	.041	Heavy	.024	.024	58
354	30.0	.041	Heavy	.030	.030	57
355	30.0	.041	Heavy	.013	.007	69
356	30.0	.041	Heavy	.008	.008	69
357	29.4	.041	Heavy	.015	.015	67
358	29.8	.041	Heavy	.030	.015	65
359	30.0	.041	Heavy	.024	.012	67
360	30.5	.041	Heavy	.014	.009	70
361	30.5	.041	Heavy	.015	.015	62
362	30.0	.041	Heavy	.009	.009	73
363	30.0	.041	Heavy	.019	.019	73
364	30.0	.041	Heavy	.012	.012	67
365	30.0	.041	Heavy	.021	.018	62
366	29.5	.041	Heavy	.063	.051	39
367	30.0	.041	Heavy	.014	.014	71
368	30.0	.041	Heavy	.003	.003	73

---

* Not Peened

TABLE 5 (CONTINUED)

FATIGUE TEST SPECIMENS

Specimen No.	Hardness R_C	Compressive Depth (in.)	Damage	Maximum Gouge Depth (in.)	Gouge Depth of Failure (in.)	Failure Stress (10^3 psi)
369	30.0	.041	Heavy	.009	.009	72
370	30.0	.041	Heavy	.012	.012	69
371	30.0	.041	Heavy	.030	.015	62
372	30.0	.041	Heavy	.018	.009	71
373	29.5	.041	Heavy	.005	.005	74
374	30.0	.041	Heavy	.008	.008	71
375	29.8	.041	Heavy	.032	.032	70
376	29.5	.041	Heavy	.069	.015	60
377	42.0	.000	Light	.002	.002	69
378	42.0	.000	Light	.004	.004	56
379	42.0	.000	Light	.004	.004	53
380	42.0	.000	Light	.006	.006	59
381	41.0	.000	Light	.004	.004	73
382	42.0	.000	Light	.001	.001	58
383	42.0	.000	Light	.005	.005	56
384	42.0	.000	Light	.007	.007	46
385	43.0	.000	Light	.002	.002	63
386	43.0	.000	Light	.002	.002	58
387	42.0	.000	Light	.009	.009	57
388	42.5	.000	Light	.004	.004	53
389	42.0	.000	Light	.003	.003	61
390	42.5	.000	Light	.003	.003	56
391	42.0	.000	Light	.006	.006	62
392	42.0	.000	Light	.008	.008	49
393	42.0	.000	Light	.004	.004	61
394	42.0	.000	Light	.000	.000 (a)	70
395	42.0	.000	Light	.003	.003	67
396	42.0	.000	Light	.006	.006	56
397	42.0	.000	Light	.003	.003	70
398	42.0	.000	Light	.000	.000 (a)	79
399	42.0	.000	Light	.006	.006	64
400	42.0	.000	Light	.007	.007	63
401	41.5	.000	Heavy	.024	.024	62
402	41.0	.000	Heavy	.009	.004	49
403	42.0	.000	Heavy	.006	.000 (c)	48
404	42.0	.000	Heavy	.049	.032	36
405	42.0	.000	Heavy	.007	.007	46
406	42.0	.000	Heavy	.005	.000 (b)	53
407	42.0	.000	Heavy	.004	.000 (a)	51
408	42.0	.000	Heavy	.002	.000 (a)	53
409	42.0	.000	Heavy	.018	.018	40

TABLE 5 (CONTINUED)

FATIGUE TEST SPECIMENS

Specimen No.	Hardness R_c	Compressive Depth (in.)	Damage	Maximum Gouge Depth (in.)	Gouge Depth of Failure (in.)	Failure Stress (10^3 psi)
410	42.0	.000	Heavy	.027	.027	42
411	42.0	.000	Heavy	.046	.035	34
412	42.0	.000	Heavy	.006	.000 (a)	56
413	42.0	.000	Heavy	.007	.000 (c)	54
114	42.0	.000	Heavy	.008	.000 (c)	50
415	43.0	.000	Heavy	.022	.022	44
416	42.0	.000	Heavy	.006	.000 (c)	53
417	42.0	.000	Heavy	.004	.004	59
418	42.0	.000	Heavy	.016	.000 (a)	55
419	43.0	.000	Heavy	.004	.000 (c)	52
420	41.0	.000	Heavy	.006	.006	51
421	42.0	.000	Heavy	.008	.008	45
422	42.0	.000	Heavy	.006	.000 (c)	58
423	41.5	.000	Heavy	.021	.021	50
424	42.0	.000	Heavy	.005	.005	48
425	42.0	.017	Light	.000	.000 (a)	90
426	42.0	.017	Light	.000	.000 (a)	94
427	42.0	.017	Light	.000	.000 (a)	88
428	42.0	.017	Light	.000	.000 (a)	95
429	41.0	.017	Light	.000	.000 (a)	94
430	42.0	.017	Light	.000	.000 (a)	91
431	42.0	.017	Light	.000	.012	85
432	42.0	.017	Light	.012	.000 (a)	80
433	42.0	.017	Light	.012	.000 (a)	95
434	42.0	.017	Light	Failed	Outside	Peening
435	42.0	.017	Light	.012	.000 (a)	89
436	42.0	.017	Light	.012	.000 (a)	94
437	41.0	.017	Light	.012	.000 (a)	95
438	41.0	.017	Light	.012	.000 (a)	96
439	42.0	.017	Light	.012	.000 (a)	94
440	42.0	.017	Light	.012	.000 (a)	98
441	42.0	.017	Light	.012	.000 (a)	98
442	41.0	.017	Light	.012	.000 (a)	96
443	42.0	.017	Light	.006	.006	91
444	42.0	.017	Light	.006	.000 (a)	97
445	42.0	.017	Light	.006	.000 (a)	95
446	42.0	.017	Light	.006	.000 (a)	92
447	42.0	.017	Light	.006	.000 (a)	93
448	42.0	.017	Light	.006	.000 (a)	96
449	43.0	.017	Heavy	.005	.005	87
450	42.0	.017	Heavy	.020	.020	73

TABLE 5 (CONTINUED)

FATIGUE TEST SPECIMENS

Specimen No.	Hardness R_c	Compressive Depth (in.)	Damage	Maximum Gouge Depth (in.)	Gouge Depth of Failure (in.)	Failure Stress (10^3 psi)
451	41.0	.017	Heavy	.008	.008	90
452	42.0	.017	Heavy	.046	.046	46
453	42.0	.017	Heavy	.031	.031	62
454	41.0	.017	Heavy	.000	.000 (c)	102
455	42.0	.017	Heavy	.003	.003	97
456	43.0	.017	Heavy	.006	.004	95
457	42.0	.017	Heavy	.006	.006	91
458	42.0	.017	Heavy	.024	.008	78
459	42.0	.017	Heavy	.005	.005	91
460	42.0	.017	Heavy	.007	.007	91
461	42.0	.017	Heavy	.018	.012	78
462	42.0	.017	Heavy	.009	.006	89
463	41.0	.017	Heavy	.032	.032	68
464	41.0	.017	Heavy	.006	.006	93
465	42.0	.017	Heavy	.009	.006	91
466	42.0	.017	Heavy	.037	.037	47
467	41.0	.017	Heavy	.011	.011	83
468	41.0	.017	Heavy	.038	.019	60
469	43.0	.017	Heavy	.008	.008	89
470	42.0	.017	Heavy	.002	.000 (a)	99
471	42.0	.017	Heavy	.038	.038	53
472	42.0	.017	Heavy	.026	.026	70
473	41.0	.021	Heavy	.000	.000 (c)	92
474	42.0	.021	Heavy	.009	.009	88
475	42.0	.021	Heavy	.000	.000 (a)	99
476	42.0	.021	Heavy	.027	.000 (b)	85
477	42.0	.021	Heavy	.009	.009	86
478	41.0	.021	Heavy	.009	.009	90
479	42.0	.021	Heavy	.006	.000 (b)	98
480	42.0	.021	Heavy	.006	.006	90
481	42.0	.021	Heavy	.009	.009	87
482	42.0	.021	Heavy	.012	.012	90
483	41.5	.021	Heavy	.012	.012	85
484	42.0	.021	Heavy	.000	.000 (c)	99
485	42.0	.021	Heavy	.003	.000 (b)	96
486	42.0	.021	Heavy	.006	.006	92
487	42.0	.021	Heavy	.012	.006	96
488	42.0	.021	Heavy	.006	.006	94
489	42.0	.021	Heavy	.009	.006	94
490	41.0	.021	Heavy	.023	.023	75
491	42.0	.021	Heavy	.009	.000 (b)	98

TABLE 5 (CONTINUED)

FATIGUE TEST SPECIMENS

Specimen No.	Hardness R_c	Compressive Depth (in.)	Damage	Maximum Gouge Depth (in.)	Gouge Depth of Failure (in.)	Failure Stress (10^3 psi)
492	42.0	.021	Heavy	.003	.003	95
493	42.0	.021	Heavy	.012	.000 (b)	99
494	42.0	.021	Heavy	.006	.006	95
495	41.5	.021	Heavy	.006	.006	95
496	42.0	.021	Heavy	.026	.000 (a)	99
497	41.5	.027	Heavy	.000	.000 (c)	91
498	42.0	.027	Heavy	.001	.000 (a)	102
499	42.0	.027	Heavy	.000	.000 (c)	93
500	42.0	.027	Heavy	.000	.000 (a)	95
501	41.5	.027	Heavy	.000	.000 (b)	84
502	42.0	.027	Heavy	.000	.000 (b)	96
503	42.0	.027	Heavy	.000	.000 (c)	92
504	43.0	.027	Heavy	.000	.000 (a)	89
505	42.0	.027	Heavy	.000	.000 (c)	95
506	42.0	.027	Heavy	.000	.000 (b)	96
507	42.0	.027	Heavy	.000	.000 (b)	101
508	41.0	.027	Heavy	.015	.015	86
509	41.0	.027	Heavy	.000	.000 (a)	101
510	42.0	.027	Heavy	.000	.000 (a)	100
511	42.0	.027	Heavy	.024	.000 (b)	92
512	42.0	.027	Heavy	.051	.024	55
513	43.0	.027	Heavy	.000	.009	94
514	42.0	.021	Heavy	.000	.000 (c)	89
515	41.0	.027	Heavy	.006	.006	107
516	42.5	.027	Heavy	Not	Visible	—
517	42.0	.027	Heavy	.012	.000 (b)	98
518	42.0	.027	Heavy	.030	.030	65
519	42.0	.027	Heavy	.002	.000 (c)	95
520	42.0	.027	Heavy	.033	.033	63
521	50.0	.000	Light	.003	.003	72
522	50.0	.000	Light	.000 (c)	.000 (c)	69
523	50.0	.000	Light	.002	.002	80
524	50.2	.000	Light	.002	.002	72
525	50.5	.000	Light	.003	.003	72
526	50.8	.000	Light	.000	.000 (c)	80
527	50.0	.000	Light	.000	.000 (c)	67
528	51.0	.000	Light	.002	.002	74
529	50.5	.000	Light	.003	.003	86
530	50.0	.000	Light	.003	.003	76
531	50.5	.000	Light	.000	.000 (c)	66
532	51.0	.000	Light	.003	.003	79
533	50.5	.000	Light	.000	.000 (c)	78

TABLE 5 (CONTINUED)

FATIGUE TEST SPECIMENS

Specimen No.	Hardness R_c	Compressive Depth (in.)	Damage	Maximum Gouge Depth (in.)	Gouge Depth of Failure (in.)	Failure Stress $(10^3$ psi)
534	51.0	.000	Light	.002	.002	85
535	49.5	.000	Heavy	.005	.000 (c)	69
536	50.0	.000	Heavy	.005	.002	58
537	49.5	.000	Heavy	.004	.002	51
538	49.0	.000	Heavy	.002	.000 (c)	57
539	49.0	.000	Heavy	.004	.000 (c)	58
540	49.5	.000	Heavy	.000	.000 (c)	63
541	49.5	.000	Heavy	.005	.000 (c)	53
542	49.0	.000	Heavy	.005	.001	56
543	49.5	.000	Heavy	.004	.000 (c)	57
544	49.0	.000	Heavy	.004	.002	52
545	49.0	.000	Heavy	.000	.000 (c)	74
546	49.5	.000	Heavy	.004	.000 (c)	61
547	49.0	.000	Heavy	.004	.000 (c)	55
548	49.0	.000	Heavy	.005	.000 (c)	56
549	48.5	.000	Heavy	.004	.000 (c)	59
550	49.5	.000	Heavy	.007	.000 (c)	57
551	49.0	.000	Heavy	.021	.002	81
552	49.0	.000	Heavy	.002	.000 (c)	54
553	49.0	.000	Heavy	.004	.000 (c)	51
554	49.0	.000	Heavy	.004	.000 (c)	55
555	49.5	.000	Heavy	.019	.019	63
556	49.0	.000	Heavy	.057	.000 (c)	53
557	49.0	.000	Heavy	.001	.000 (c)	66
558	49.5	.000	Heavy	.005	.000 (c)	55
559	49.5	.011	Light	Failed Outside Peening		
560	50.0	.011	Light	.000	.000 (a)	125
561	49.0	.011	Light	.000	.000 (a)	121
562	50.0	.011	Light	.000	.000 (a)	96
563	50.2	.011	Light	.000	.000 (a)	126
564	49.5	.011	Light	.000	.000 (a)	118
565	50.5	.011	Light	.000	.000 (a)	127
566	49.0	.011	Light	.000	.000 (a)	121
567	50.5	.011	Light	.000	.000 (a)	117
568	50.5	.011	Light	. Failed Outside Peening		
569	50.0	.011	Light	.000	.000 (c)	128
570	51.0	.011	Light	.003	.003	125
571	50.5	.011	Light	.000	.000 (a)	119
572	50.8	.011	Light	.000	.000 (a)	115
573	49.0	.011	Heavy	.003	.003	107

TABLE 5 (CONTINUED)

FATIGUE TEST SPECIMENS

Specimen No.	Hardness R_c	Compressive Depth (in.)	Damage	Maximum Gouge Depth (in.)	Gouge Depth of Failure (in.)	Failure Stress $(10^3$ psi)
574	49.0	.011	Heavy	.000	.000 (c)	115
575	49.0	.011	Heavy	.043	.000 (a)	105
576	49.0	.011	Heavy	.002	.002	105
577	49.5	.011	Heavy	.006	.006	101
578	49.0	.011	Heavy	Failed	Outside	Peening
579	49.0	.011	Heavy	.007	.007	96
580	49.0	.011	Heavy	.004	.004	107
581	49.0	.011	Heavy	.025	.025	85
582	49.0	.011	Heavy	.006	.006	98
583	49.0	.011	Heavy	.006	.006	99
584	49.0	.011	Heavy	.006	.006	93
585	49.0	.011	Heavy	.004	.004	106
586	49.0	.011	Heavy	.003	.003	112
587	49.5	.011	Heavy	.000	.000 (c)	117
588	49.5	.011	Heavy	.003	.003	109
589	48.5	.011	Heavy	.033	.000 (b)	104
590	49.0	.011	Heavy	.006	.006	103
591	50.0	.011	Heavy	.004	.004	113
592	49.5	.011	Heavy	.009	.009	101
593	49.0	.011	Heavy	.012	.012	103
594	49.0	.011	Heavy	.033	.033	58
595	49.0	.011	Heavy	.024	.024	83
596	49.0	.011	Heavy	.006	.006	103
597	49.7	.018	Heavy	.002	.000 (a)	120
598	50.0	.018	Heavy	.006	.000 (a)	117
599	49.2	.018	Heavy	.003	.000 (a)	113
600	49.2	.018	Heavy	.005	.000 (a)	113
601	49.1	.018	Heavy	.001	.000 (a)	110
602	49.4	.018	Heavy	.003	.000 (a)	118
603	48.7	.018	Heavy	.003	.000 (a)	113
604	49.3	.018	Heavy	.003	.000 (a)	119
605	49.7	.018	Heavy	.002	.000 (a)	120
606	50.0	.018	Heavy	.003	.000 (a)	107
607	48.9	.018	Heavy	.003	.000 (a)	111
608	49.9	.018	Heavy	.003	.000 (a)	109
609	49.3	.018	Heavy	.003	.000 (a)	114
610	49.0	.018	Heavy	.002	.000 (a)	106
611	49.8	.018	Heavy	.003	.000 (a)	113
612	49.2	.018	Heavy	.002	.000 (a)	114
613	49.1	.018	Heavy	.002	.000 (a)	112
614	49.4	.018	Heavy	.002	.000 (a)	115

TABLE 5 (CONTINUED)

FATIGUE TEST SPECIMENS

Specimen No.	Hardness R_c	Compressive Depth (in.)	Damage	Maximum Gouge Depth (in.)	Gouge Depth of Failure (in.)	Failure Stress (10^3 psi)
615	49.0	.018	Heavy	.003	.000 (a)	112
616	49.7	.018	Heavy	.003	.000 (a)	117
617	49.0	.018	Heavy	.003	.000 (a)	118
618	49.5	.018	Heavy	.003	.000 (a)	113
619	49.0	.018	Heavy	.002	.000 (a)	108
620	49.1	.018	Heavy	.002	.000 (a)	124
621	49.7	.025	Heavy	.003	.000 (a)	115
622	49.4	.025	Heavy	.003	.000 (a)	109
623	49.0	.025	Heavy	.003	.000 (a)	106
624	49.0	.025	Heavy	.003	.000 (a)	118
625	49.1	.025	Heavy	.001	.000 (a)	111
626	49.9	.025	Heavy	.003	.000 (a)	107
627	49.3	.025	Heavy	.003	.000 (a)	109
628	49.7	.025	Heavy	.003	.000 (a)	103
629	49.4	.025	Heavy	.003	.000 (a)	114
630	49.9	.025	Heavy	.007	.000 (a)	116
631	49.3	.025	Heavy	.003	.000 (a)	110
632	49.8	.025	Heavy	.002	.000 (a)	98
633	49.4	.025	Heavy	.004	.000 (a)	109
634	49.8	.025	Heavy	.005	.000 (a)	109
635	50.2	.025	Heavy	.003	.000 (a)	114
636	48.7	.025	Heavy	.003	.000 (a)	115
637	49.0	.025	Heavy	.003	.000 (a)	114
638	49.6	.025	Heavy	.008	.000 (a)	112
639	50.0	.025	Heavy	.003	.000 (a)	110
640	50.1	.025	Heavy	.005	.000 (a)	107
641	49.5	.025	Heavy	.004	.000 (a)	114
642	49.1	.025	Heavy	.012	.000 (a)	109
643	50.0	.025	Heavy	.006	.000 (a)	102
644	49.7	.025	Heavy	.005	.000 (a)	116
645	41.0	.000	None	.000	.000 (a)	80
646	41.0	.000	None	.000	.000 (a)	74
647	41.5	.000	None	.000	.000 (a)	75
648	40.5	.000	None	.000	.000 (a)	73
649	41.5	.000	None	.000	.000 (a)	72
650	40.0	.000	None	.000	.000 (a)	75
651	42.0	.000	None	.000	.000 (a)	84
652	42.0	.000	None	.000	.000 (a)	82
653	42.0	.000	None	.000	.000 (a)	80
654	41.0	.000	None	.000	.000 (a)	81

TABLE 5 (CONTINUED)

FATIGUE TEST SPECIMENS

Specimen No.	Hardness R_c	Compressive Depth (in.)	Damage	Maximum Gouge Depth (in.)	Gouge Depth of Failure (in.)	Failure Stress (10^3 psi)
655	41.0	.000	None	.000	.000 (a)	74
656	42.0	.000	None	.000	.000 (a)	80
657	39.0	.017	Light	.000	.000 (c)	120
658	39.0	.017	Light	.003	.003	98
659	40.0	.017	Light	.007	.007	103
660	40.0	.017	Light	.015	.015	84
661	40.0	.017	Light	.006	.006	86
662	40.0	.017	Light	.004	.004	87
663	41.0	.017	Light	.000	.000 (a)	86
664	40.0	.017	Light	.000	.000 (c)	85
665	40.0	.017	Light	No	Failure	84
666	40.0	.017	Light	No	Failure	85
667	42.0	.017	Light	.000	.000 (a)	87
669	50.0	.000	None	.000	.000 (a)	110
670	49.0	.000	None	.000	.000 (a)	100
671	51.0	.000	None	.000	.000 (a)	90
672	51.0	.000	None	.000	.000 (a)	80
673	49.0	.000	None	.000	.000 (a)	77
674	49.0	.000	None	.000	.000 (a)	74
675	49.0	.000	None	.000	.000 (a)	72
676	52.0	.000	None	.000	.000 (a)	70
677	47.0	.000	None	.000	.000 (a)	70
678	48.0	.000	None	.000	.000 (a)	68
679	49.0	.000	None	.000	.000 (a)	66
680	49.0	.000	None	.000	.000 (a)	66
681	48.0	.011	Light	.000	.000 (a)	140
682	47.0	.011	Light	.000	.000 (a)	127
683	47.0	.011	Light	.003	.003	117
684	49.0	.011	Light	.000	.000 (a)	110
685	49.0	.011	Light	.000	.000 (a)	110
686	48.0	.011	Light	.005	.005	115
687	49.0	.011	Light	.000	.000 (a)	106
688	49.0	.011	Light	.002	.002	103
689	49.0	.011	Light	.000	.000 (a)	92
690	47.0	.011	Light	.000	.000 (a)	——
691	48.0	.011	Light	.000	.000 (c)	104
692	51.0	.011	Light	.000	.000 (a)	106

APPENDIX II

RESIDUAL STRESS RESULTS

The following pages give the detailed residual stress distributions for specimens tested in connection with the study of distortion. Table 2 outlines the various test conditions from which these distributions resulted. Table 6 in Appendix III contains the data from which the stress distributions were calculated. A sample calculation was presented in WADC TR 55-56, Part 1.
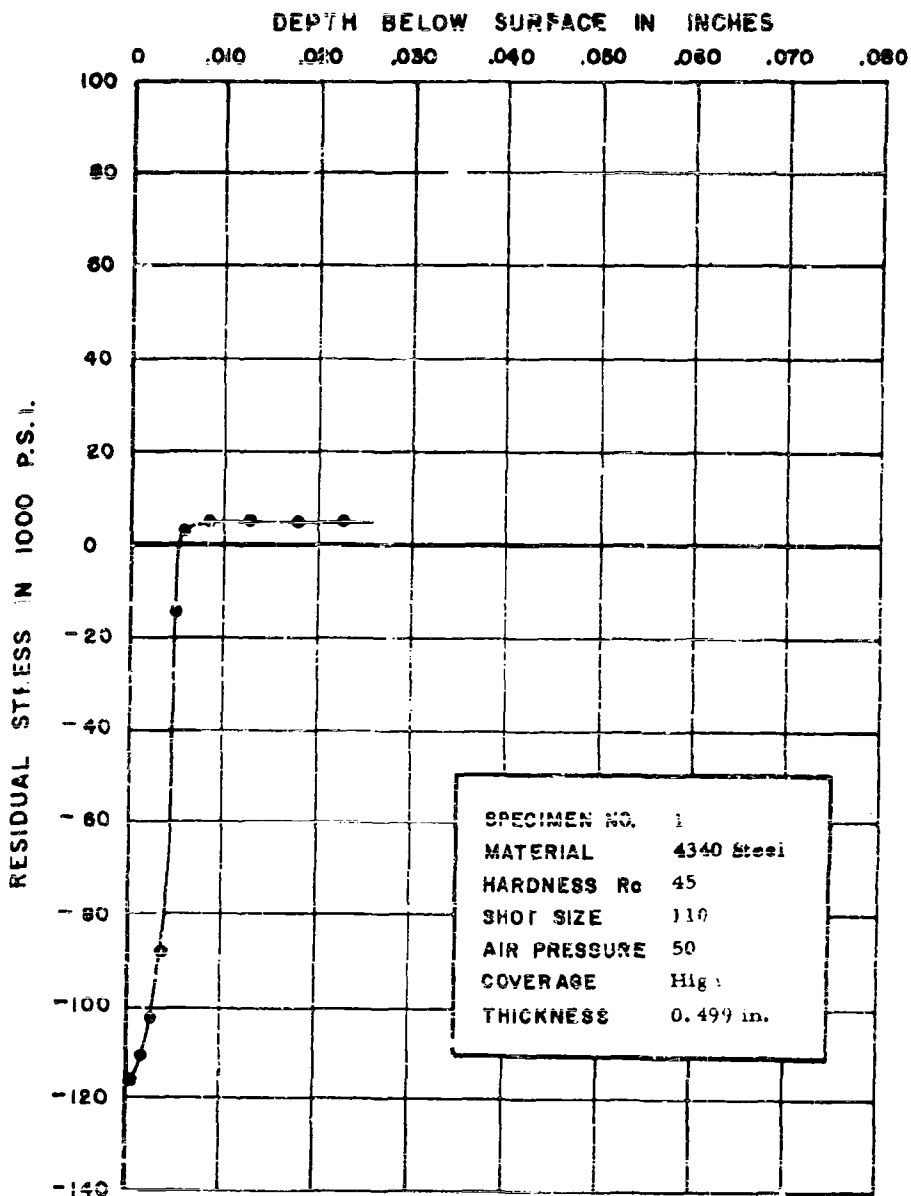
FIGURE 41.   RESIDUAL STRESS DISTRIBUTION
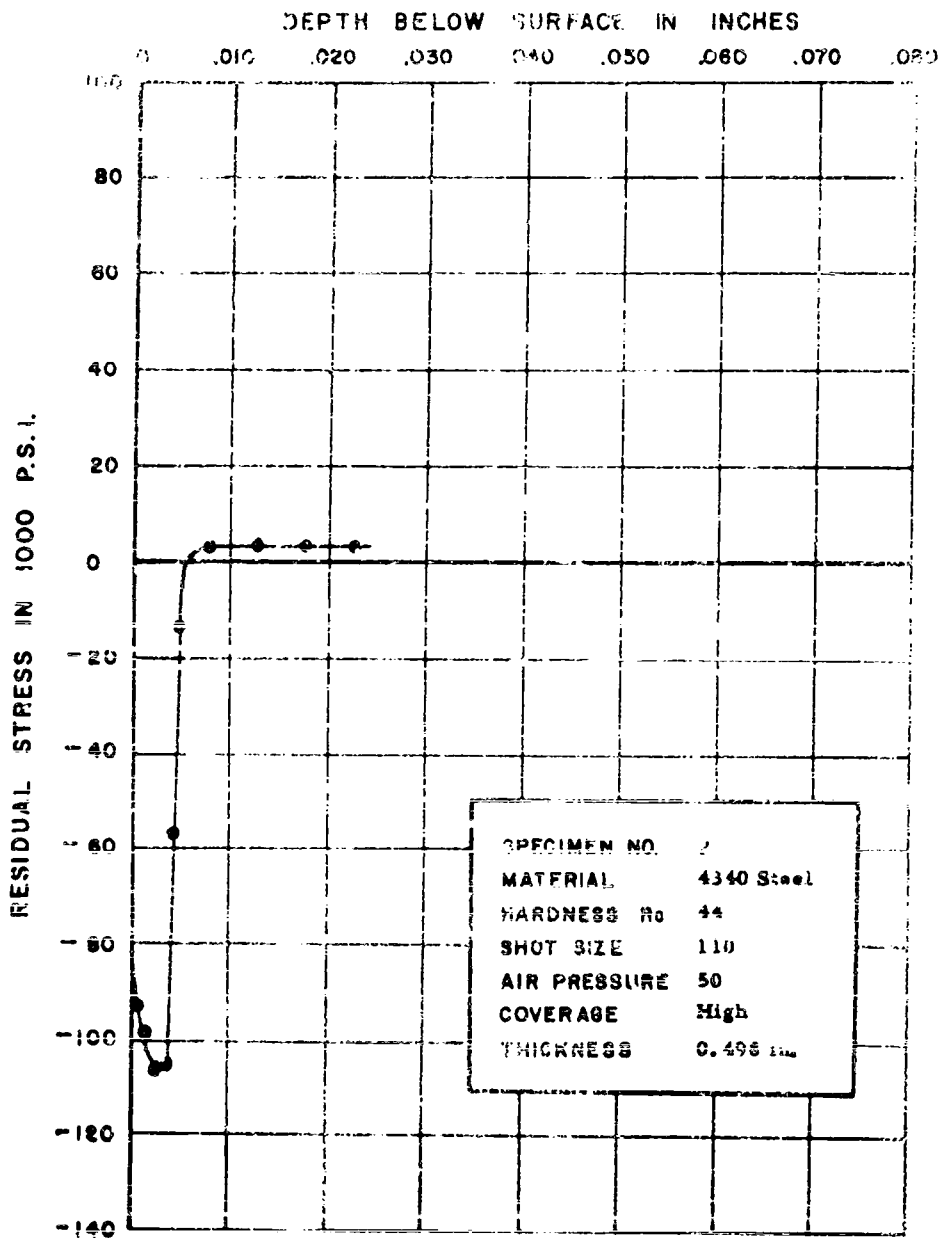
FIGURE 42. RESIDUAL STRESS DISTRIBUTION
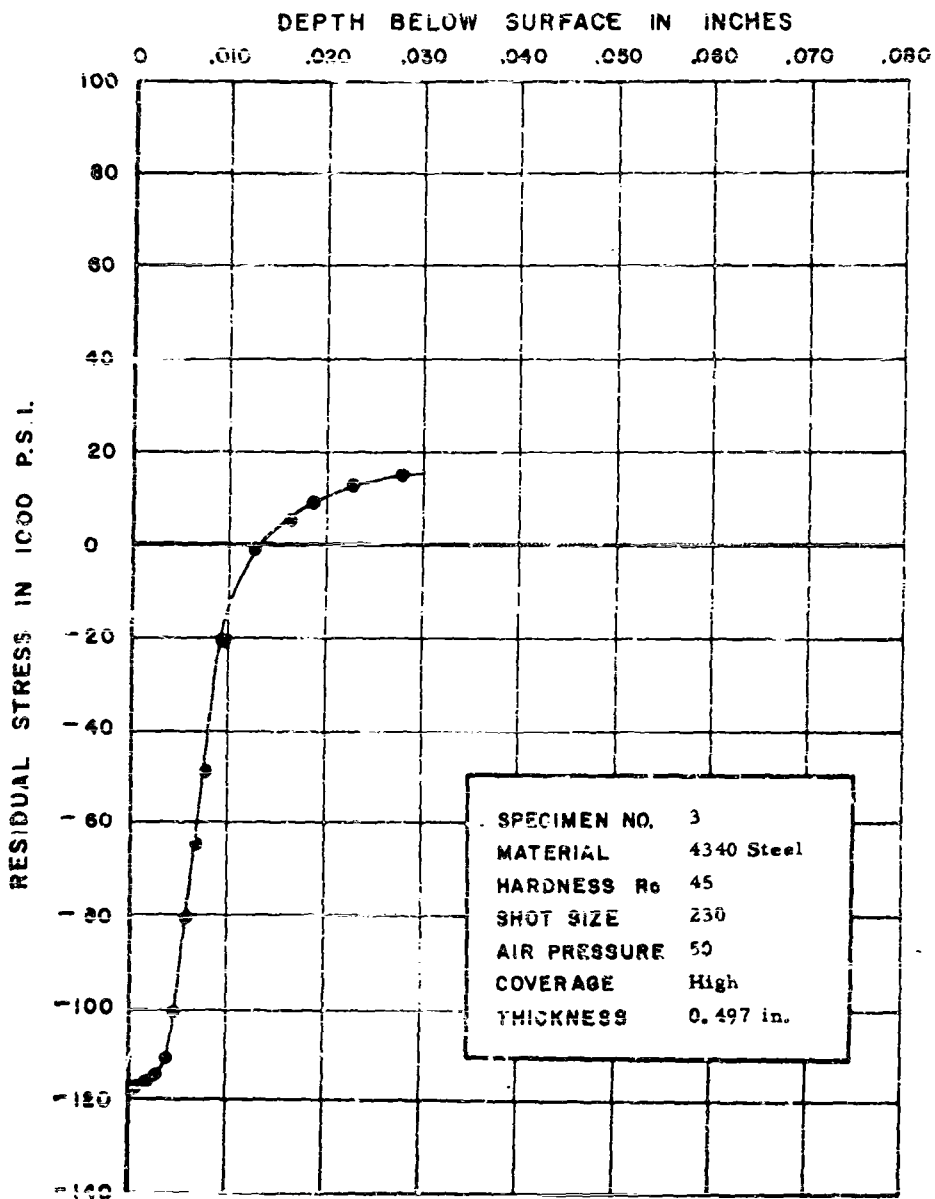
FIGURE 45. RESIDUAL STRESS DISTRIBUTION
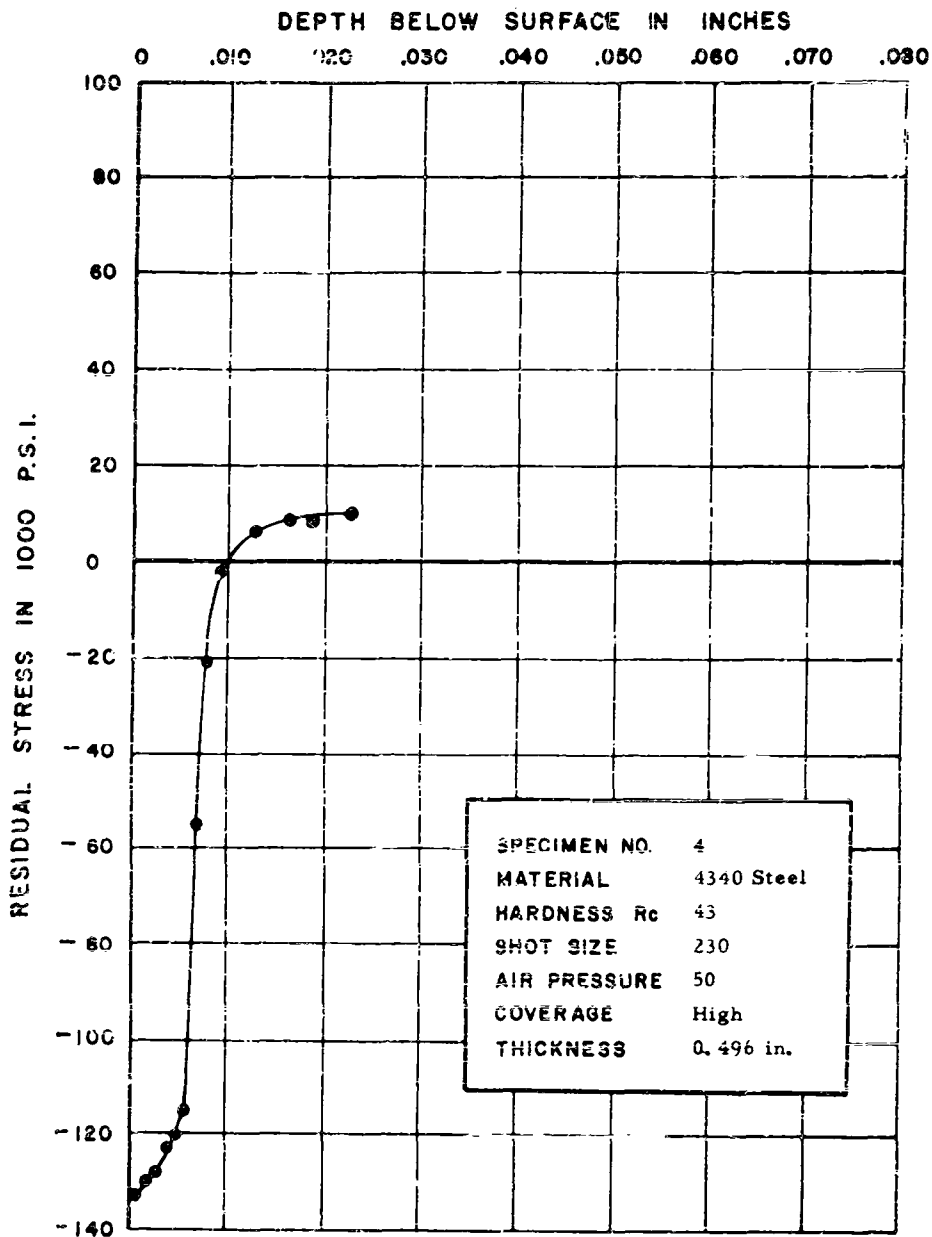
FIGURE 44. RESIDUAL STRESS DISTRIBUTION
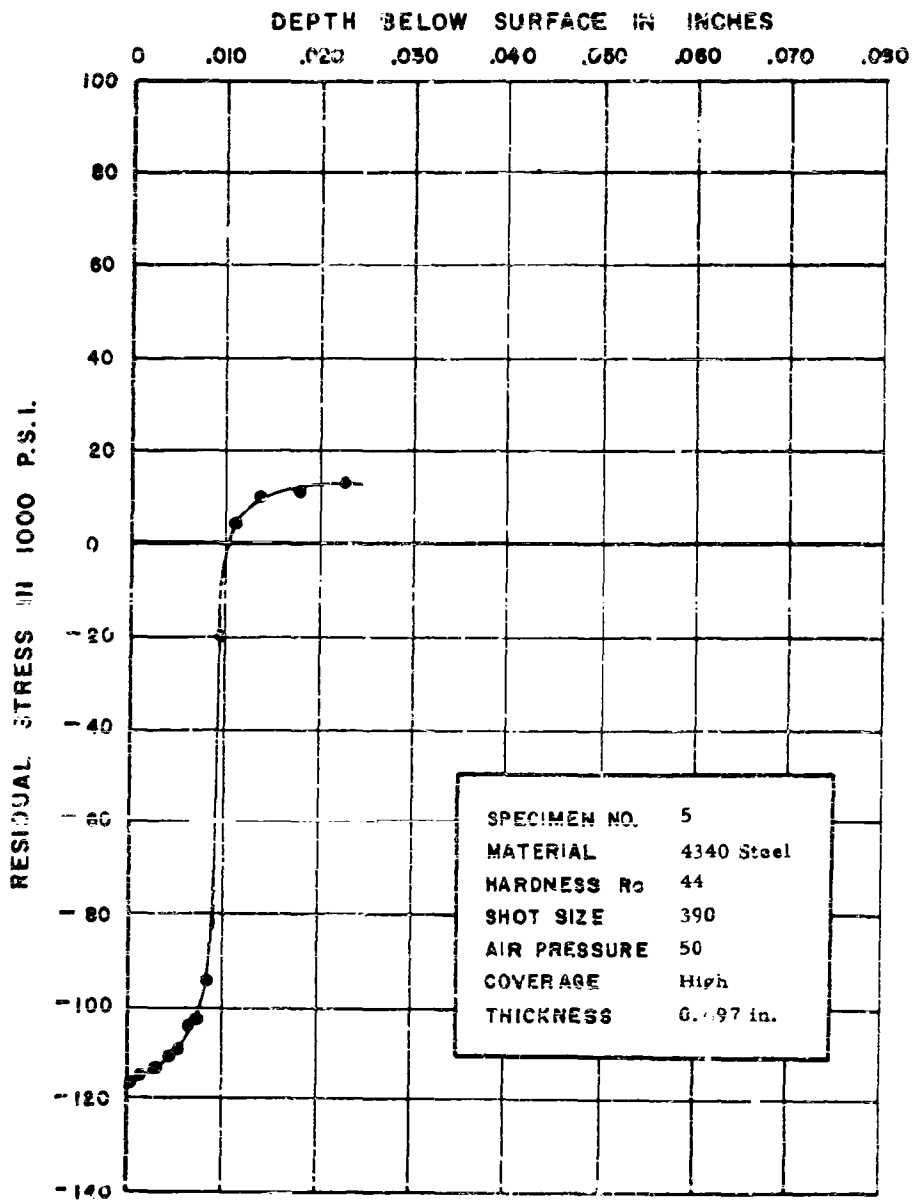
FIGURE 45. RESIDUAL STRESS DISTRIBUTION
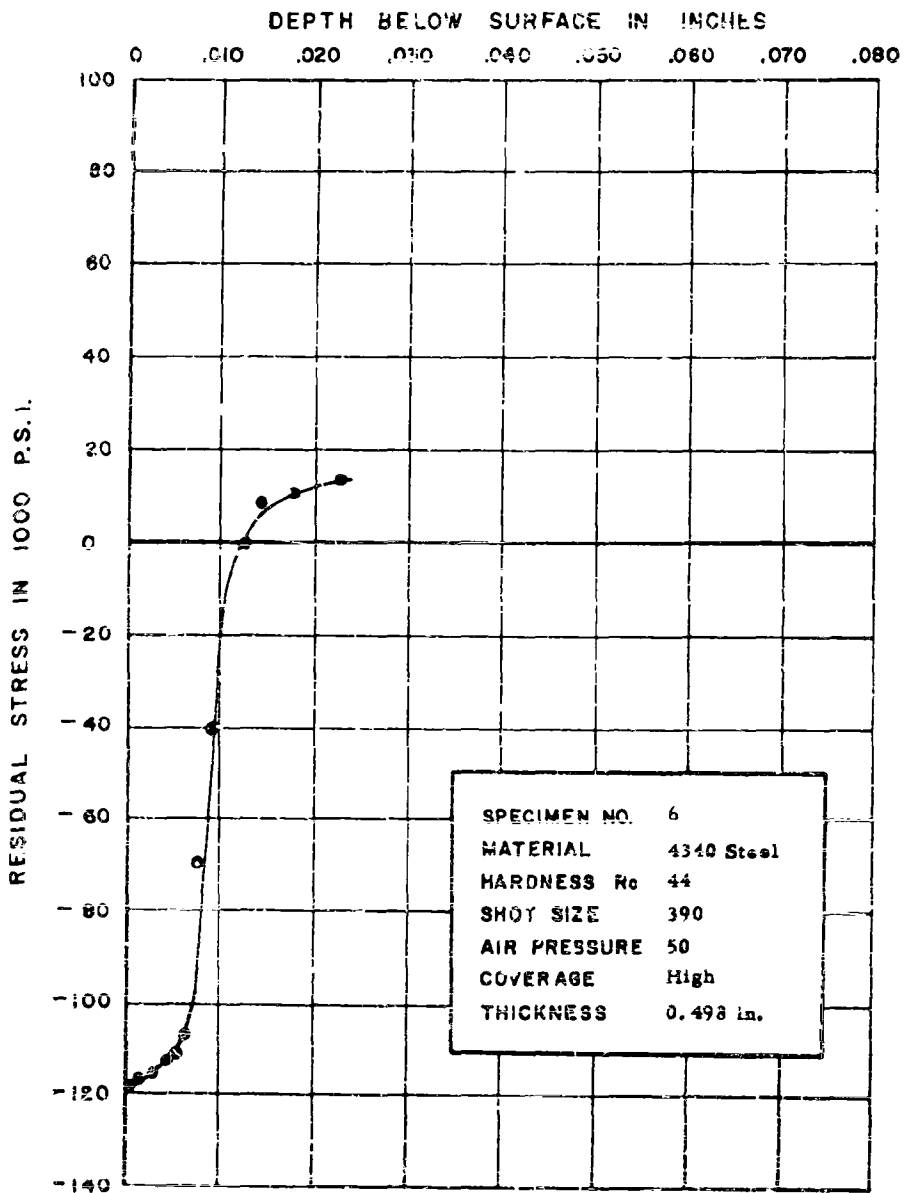
FIGURE 46. RESIDUAL STRESS DISTRIBUTION

Specimen data:

SPECIMEN NO.	6
MATERIAL	4340 Steel
HARDNESS Rc	44
SHOT SIZE	390
AIR PRESSURE	50
COVERAGE	High
THICKNESS	0.498 in.
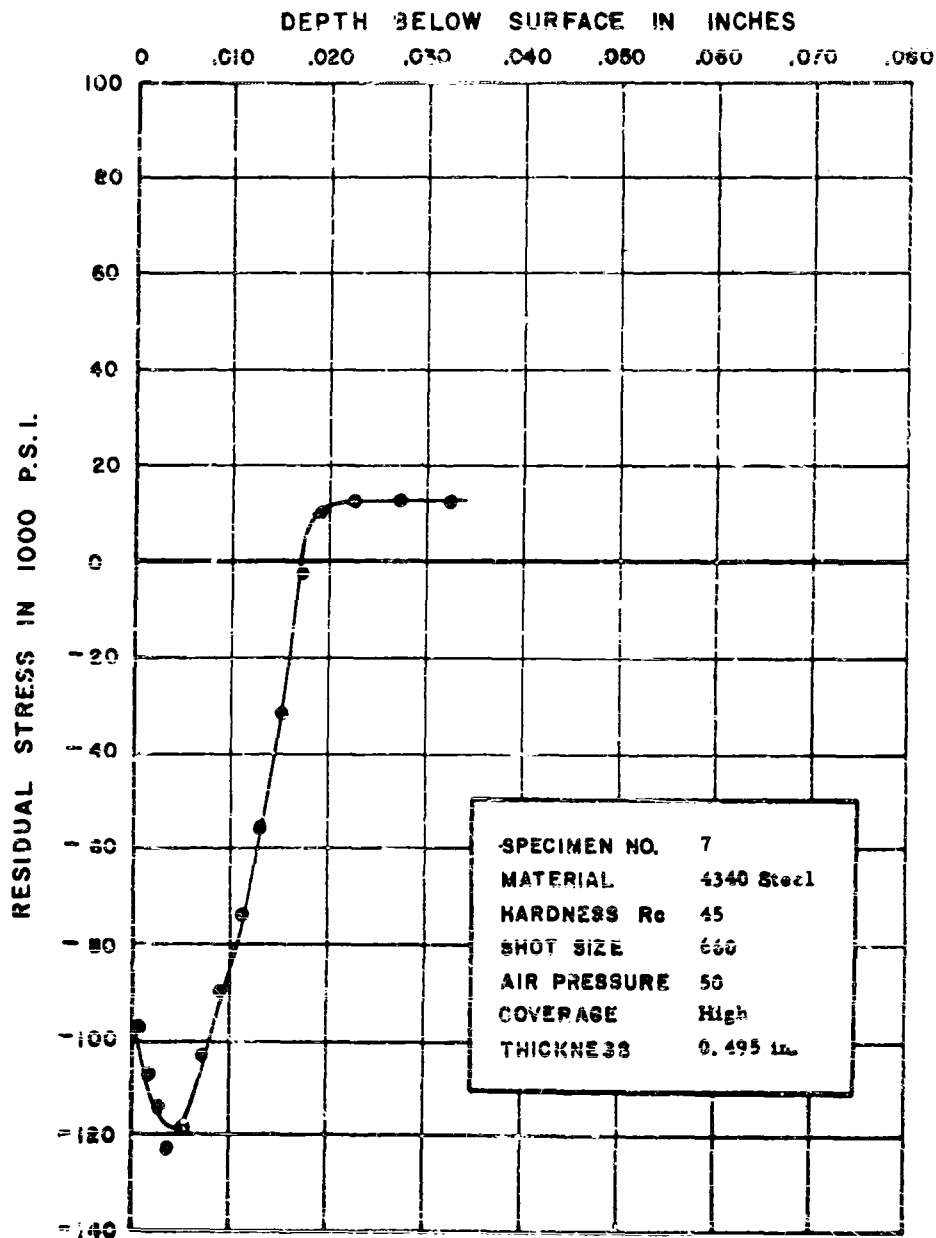
FIGURE 47. RESIDUAL STRESS DISTRIBUTION
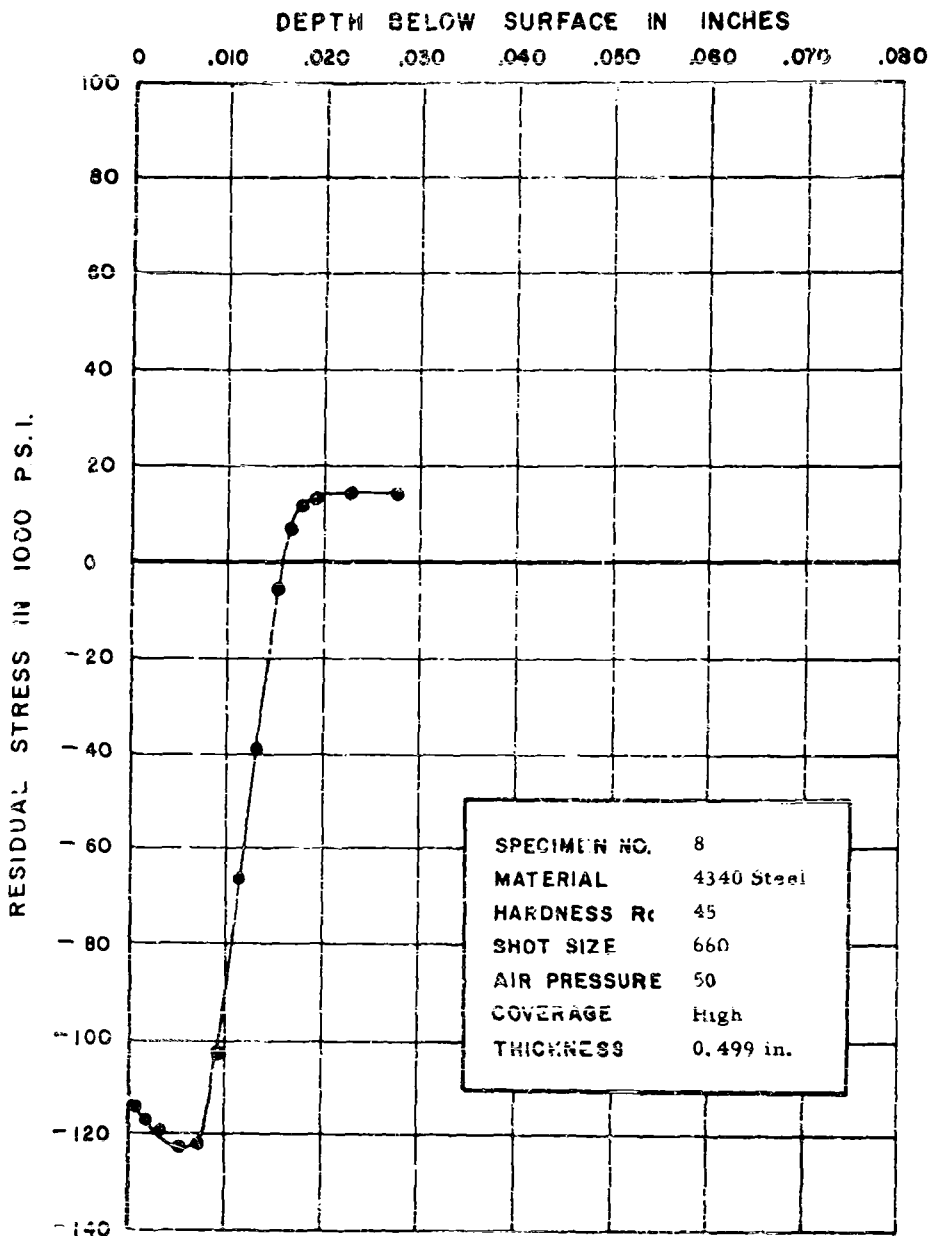
FIGURE 48. RESIDUAL STRESS DISTRIBUTION

The figure shows a plot of "RESIDUAL STRESS IN 1000 P.S.I." (vertical axis, ranging from -140 to 100) versus "DEPTH BELOW SURFACE IN INCHES" (horizontal axis, ranging from 0 to .080).

SPECIMEN NO. 8
MATERIAL 4340 Steel
HARDNESS Rc 45
SHOT SIZE 660
AIR PRESSURE 50
COVERAGE High
THICKNESS 0.499 in.
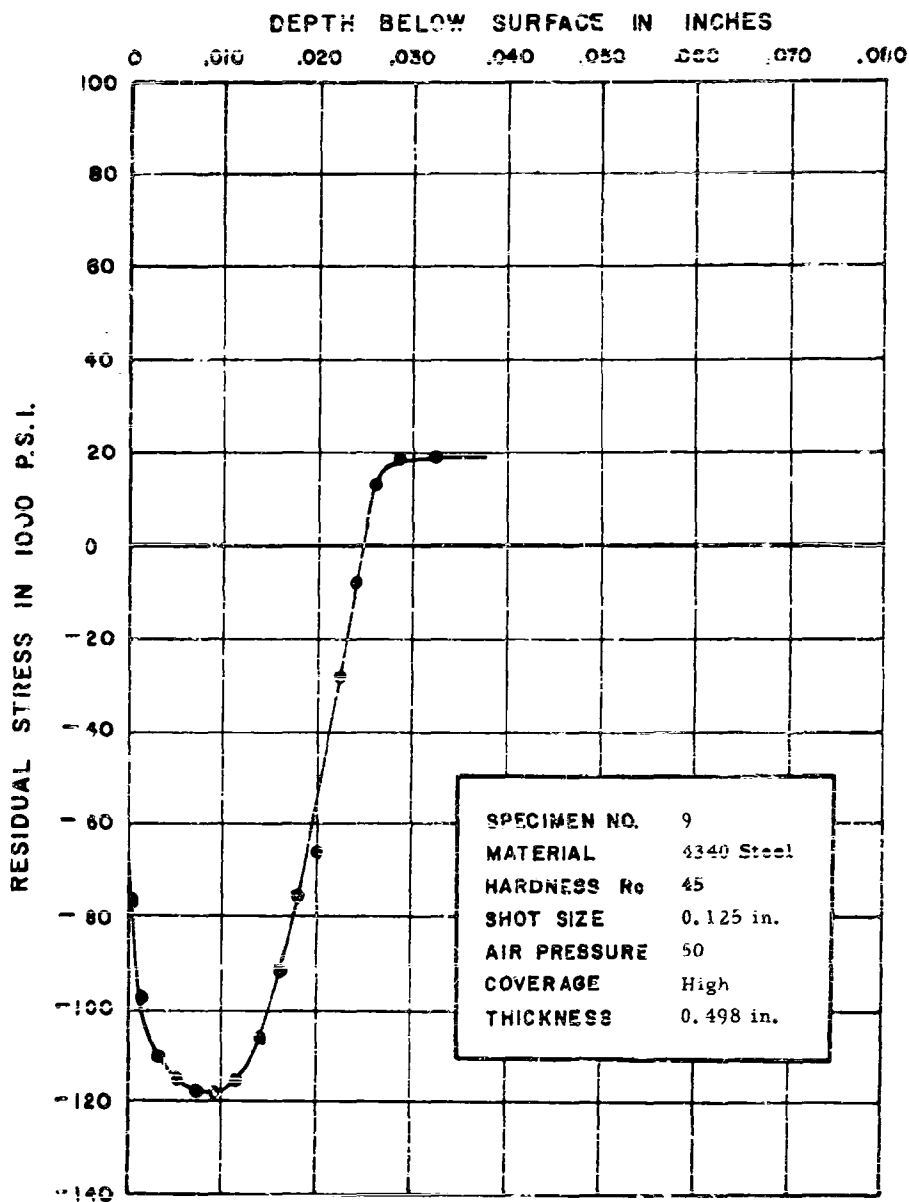
FIGURE 49. RESIDUAL STRESS DISTRIBUTION
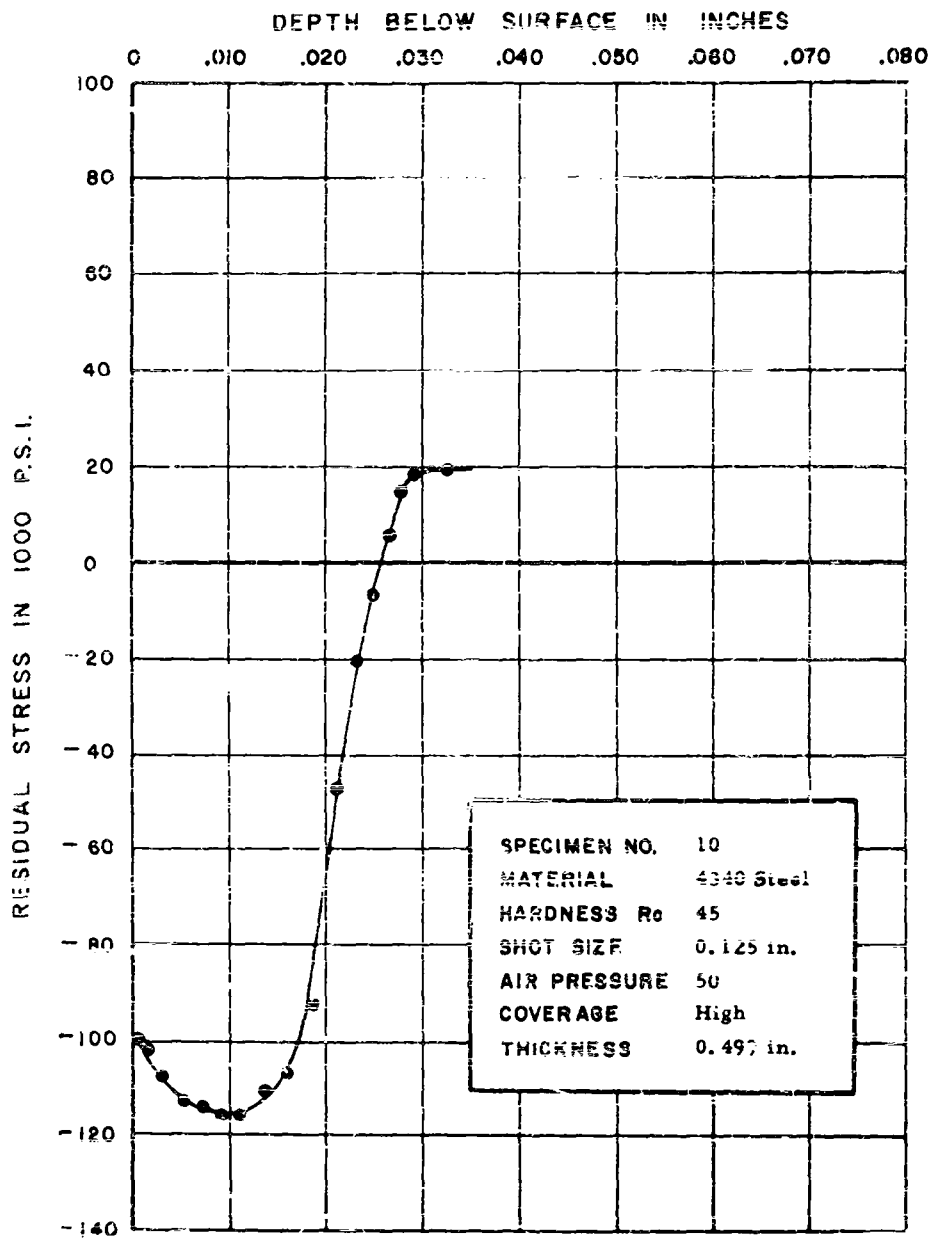
FIGURE 50.   RESIDUAL STRESS DISTRIBUTION

DEPTH BELOW SURFACE IN INCHES
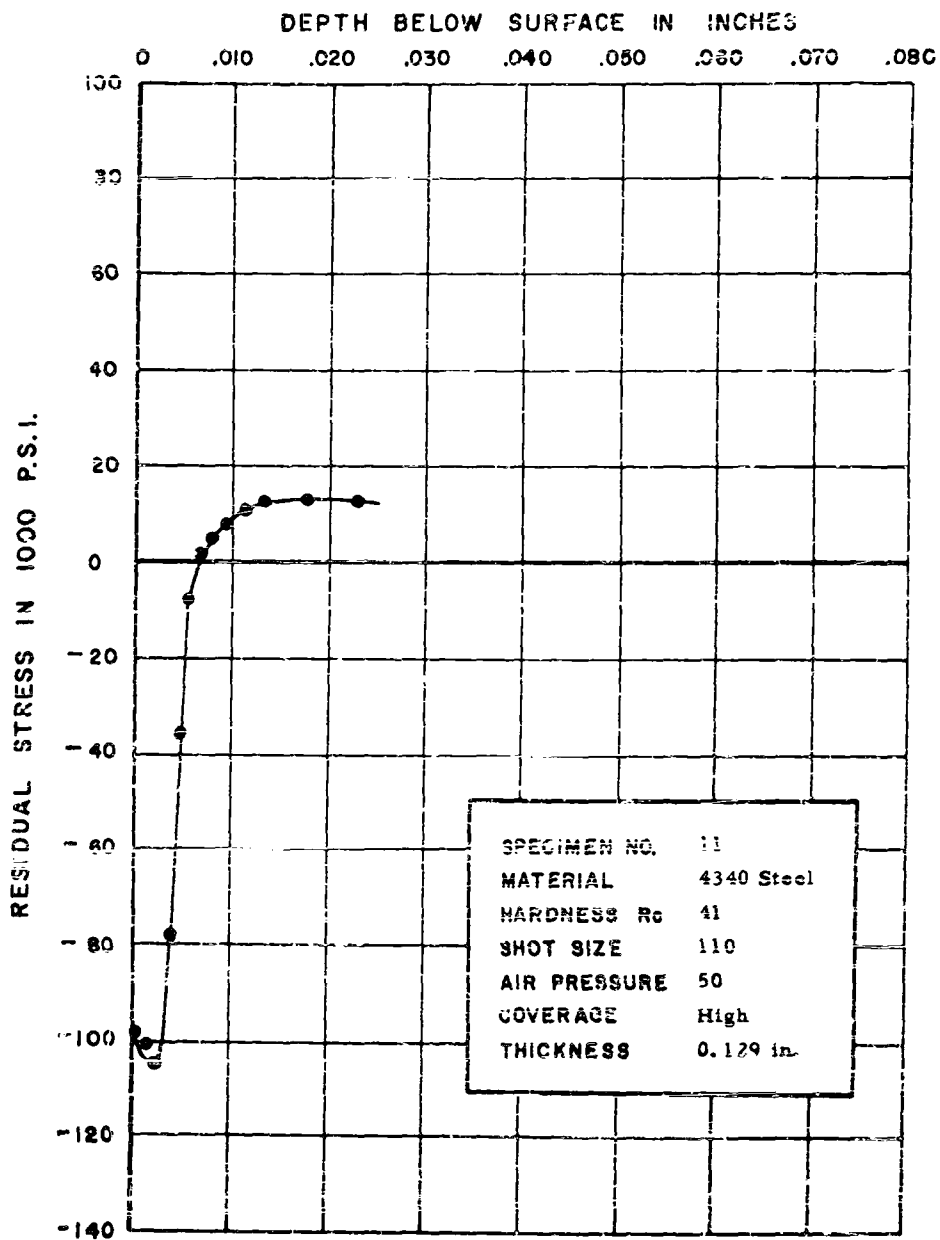
FIGURE 51. RESIDUAL STRESS DISTRIBUTION

SPECIMEN NO. 11
MATERIAL 4340 Steel
HARDNESS Rc 41
SHOT SIZE 110
AIR PRESSURE 50
COVERAGE High
THICKNESS 0.129 in.

FIGURE 52.   RESIDUAL STRESS DISTRIBUTION

FIGURE 53.   RESIDUAL STRESS DISTRIBUTION

DEPTH BELOW SURFACE IN INCHES

FIGURE 54. RESIDUAL STRESS DISTRIBUTION

SPECIMEN NO. 14
MATERIAL 4340 Steel
HARDNESS Rc 41
SHOT SIZE 230
AIR PRESSURE 50
COVERAGE High
THICKNESS 0.129 in.

DEPTH BELOW SURFACE IN INCHES

FIGURE 55. RESIDUAL STRESS DISTRIBUTION

SPECIMEN NO.	15
MATERIAL	4340 Steel
HARDNESS Rc	41
SHOT SIZE	390
AIR PRESSURE	50
COVERAGE	High
THICKNESS	0.129 in.

FIGURE 56.   RESIDUAL STRESS DISTRIBUTION
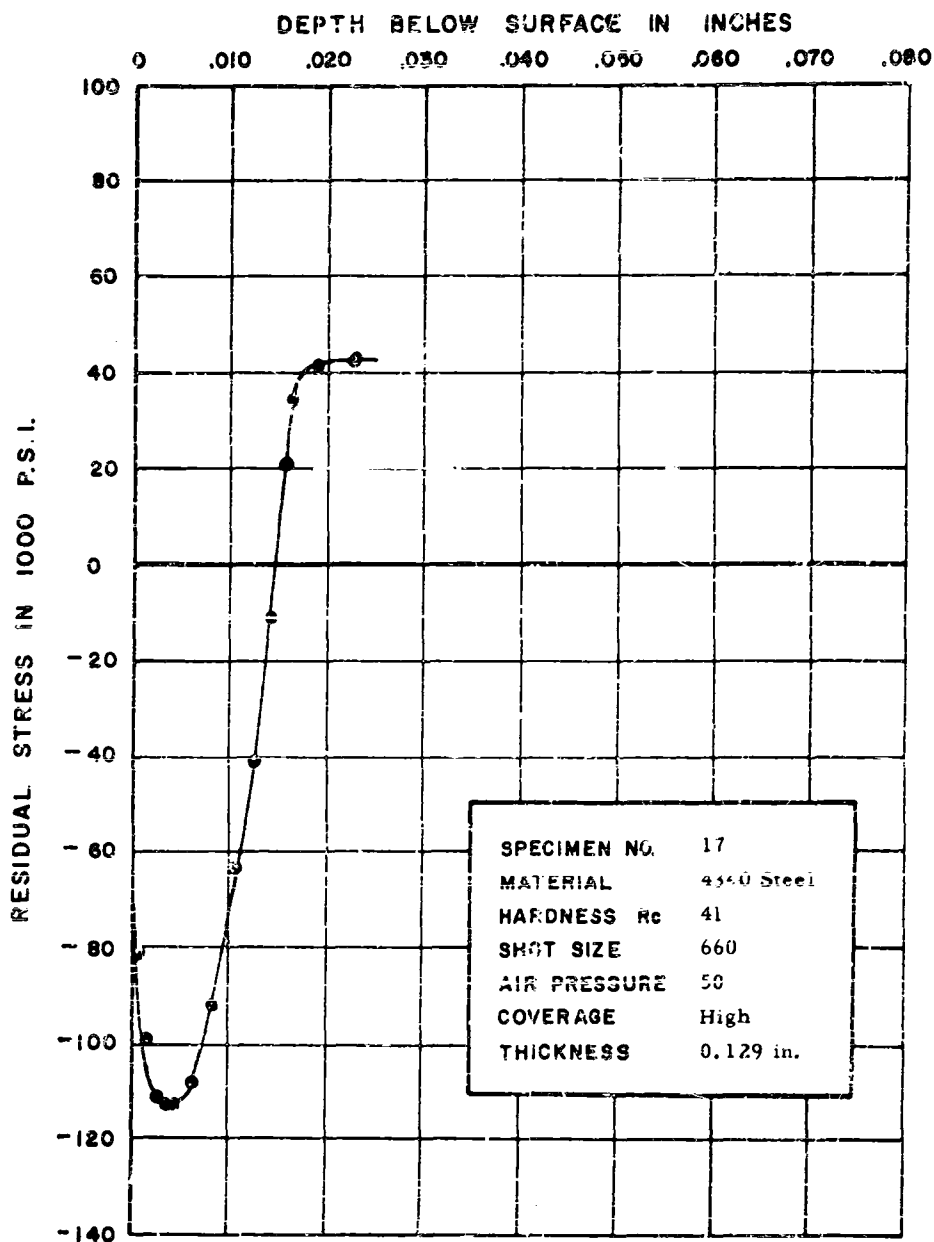
FIGURE 57. RESIDUAL STRESS DISTRIBUTION

The figure contains the following data box:

SPECIMEN NO. 17
MATERIAL 4340 Steel
HARDNESS Rc 41
SHOT SIZE 660
AIR PRESSURE 50
COVERAGE High
THICKNESS 0.129 in.

Chart axes:
DEPTH BELOW SURFACE IN INCHES
RESIDUAL STRESS IN 1000 P.S.I.

DEPTH BELOW SURFACE IN INCHES
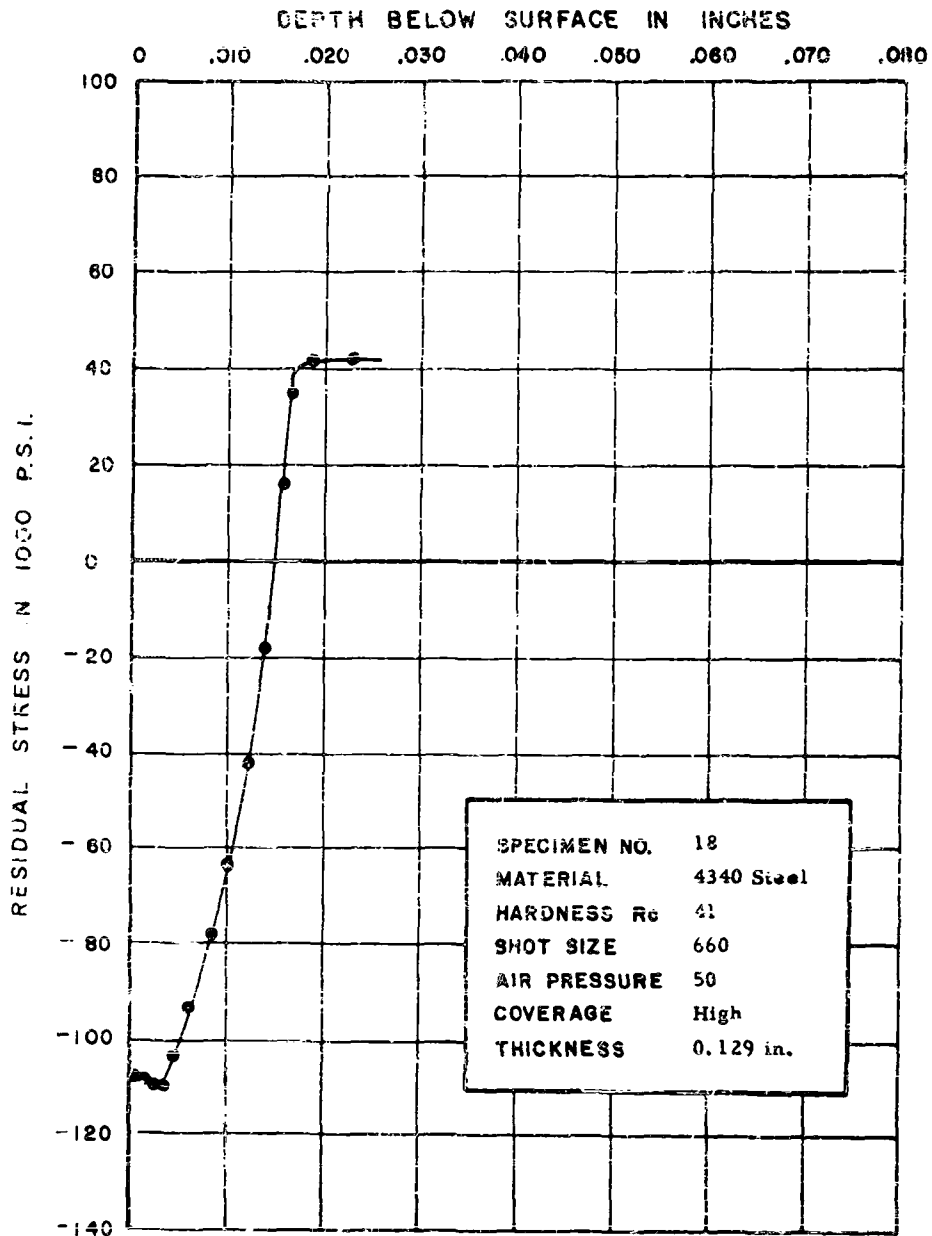
FIGURE 58. RESIDUAL STRESS DISTRIBUTION

SPECIMEN NO. 18
MATERIAL 4340 Steel
HARDNESS Rc 41
SHOT SIZE 660
AIR PRESSURE 50
COVERAGE High
THICKNESS 0.129 in.
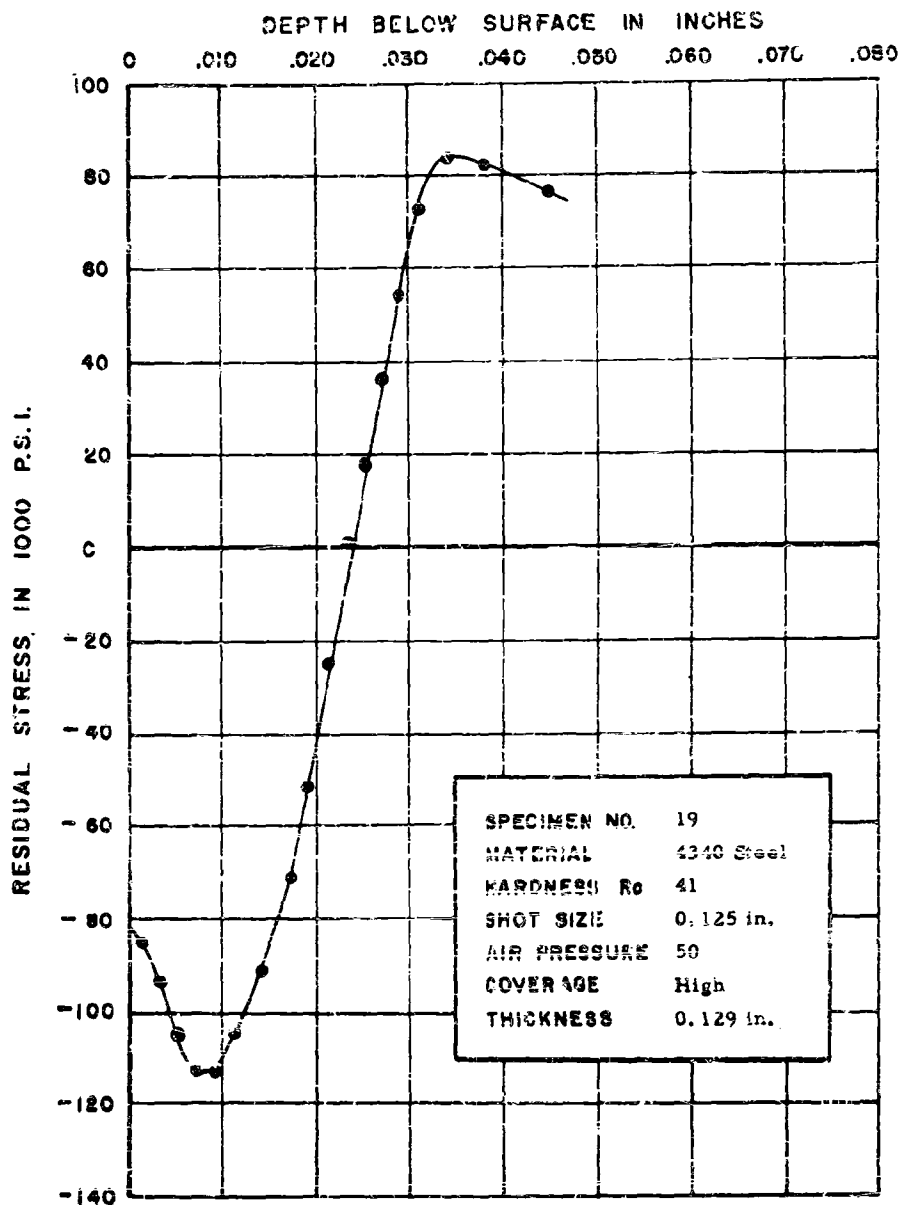
FIGURE 59. RESIDUAL STRESS DISTRIBUTION

The figure is a graph titled "DEPTH BELOW SURFACE IN INCHES" (x-axis, ranging from 0 to .080) versus "RESIDUAL STRESS, IN 1000 P.S.I." (y-axis, ranging from -140 to 100). Data legend:

SPECIMEN NO.   19
MATERIAL   4340 Steel
HARDNESS Rc   41
SHOT SIZE   0.125 in.
AIR PRESSURE   50
COVERAGE   High
THICKNESS   0.129 in.

DEPTH BELOW SURFACE IN INCHES
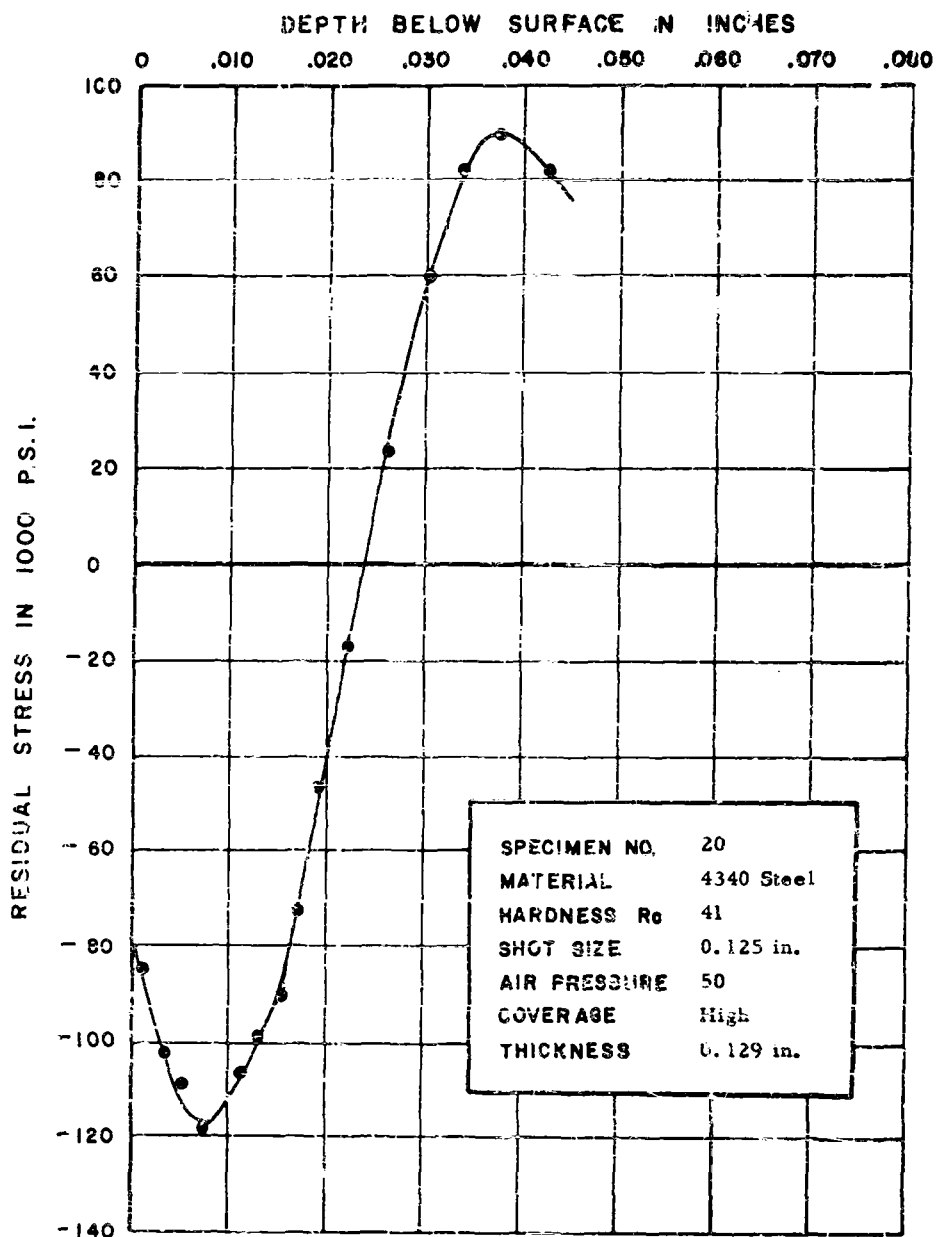
FIGURE 60. RESIDUAL STRESS DISTRIBUTION

SPECIMEN NO. 20
MATERIAL 4340 Steel
HARDNESS Rc 41
SHOT SIZE 0.125 in.
AIR PRESSURE 50
COVERAGE High
THICKNESS 0.129 in.
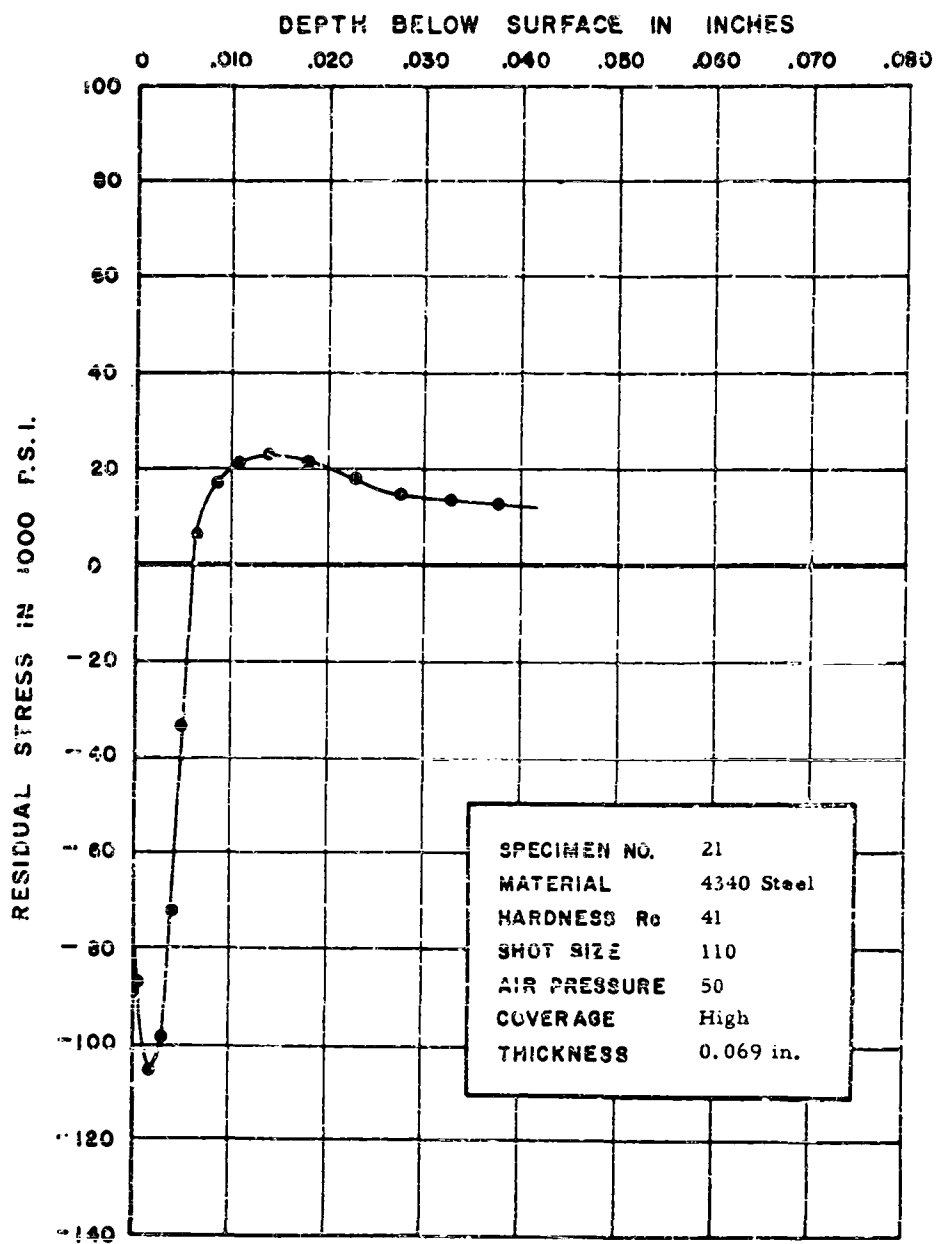
FIGURE 61.   RESIDUAL STRESS DISTRIBUTION

DEPTH BELOW SURFACE IN INCHES
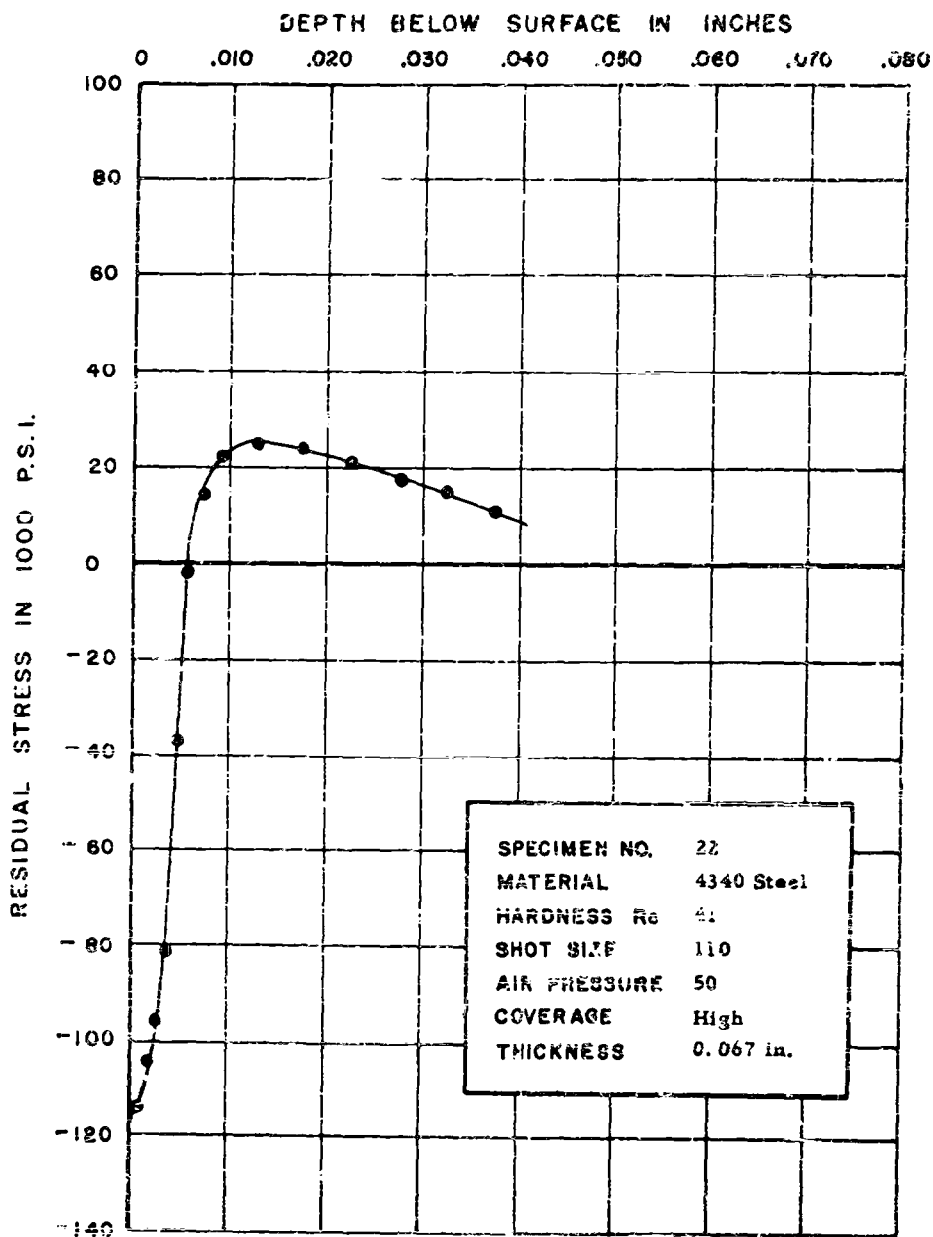
FIGURE 62.　RESIDUAL STRESS DISTRIBUTION

SPECIMEN NO.　22
MATERIAL　4340 Steel
HARDNESS Rc　4?
SHOT SIZE　110
AIR PRESSURE　50
COVERAGE　High
THICKNESS　0.067 in.

DEPTH BELOW SURFACE IN INCHES
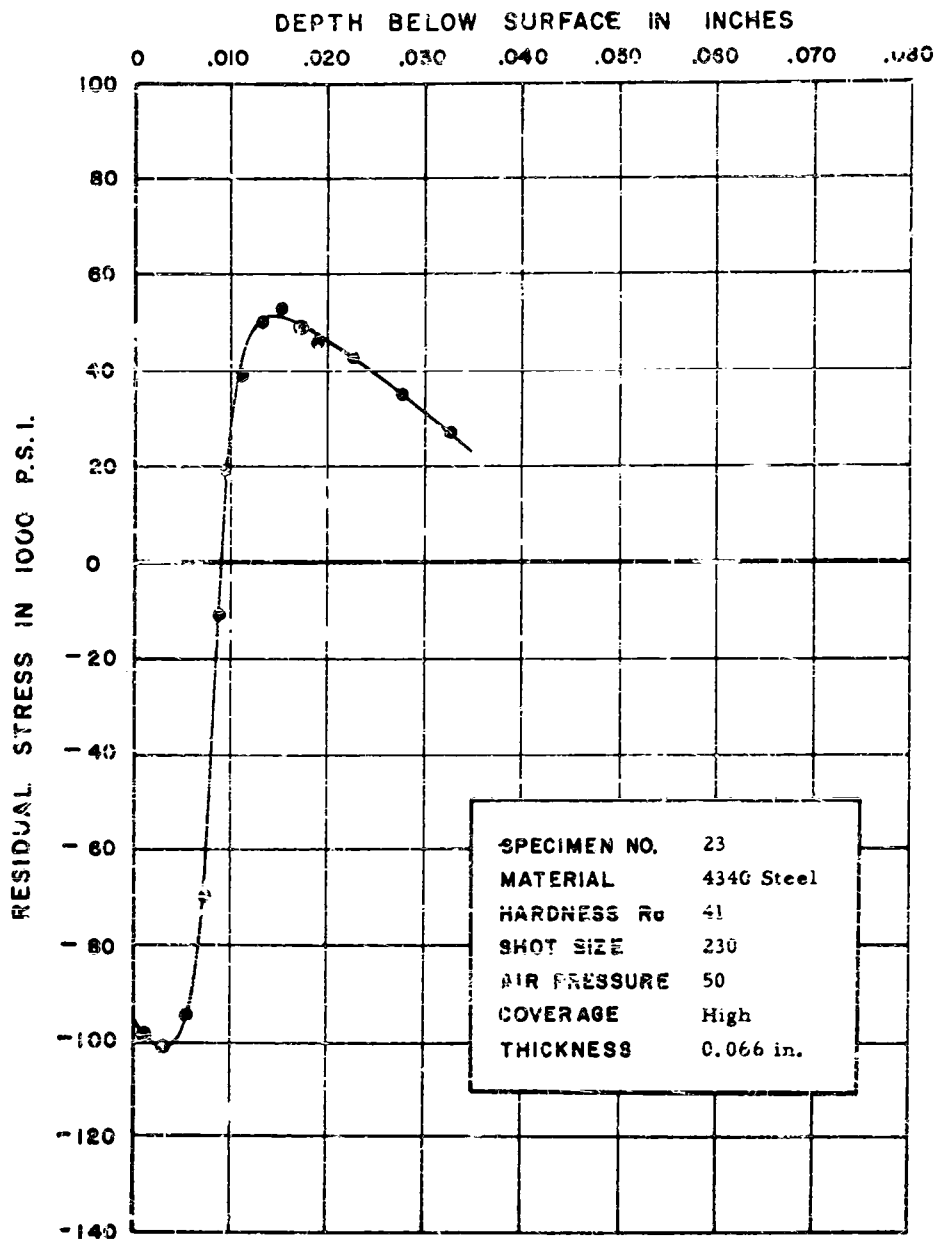
FIGURE 63. RESIDUAL STRESS DISTRIBUTION

SPECIMEN NO.	23
MATERIAL	4340 Steel
HARDNESS R_C	41
SHOT SIZE	230
AIR PRESSURE	50
COVERAGE	High
THICKNESS	0.066 in.
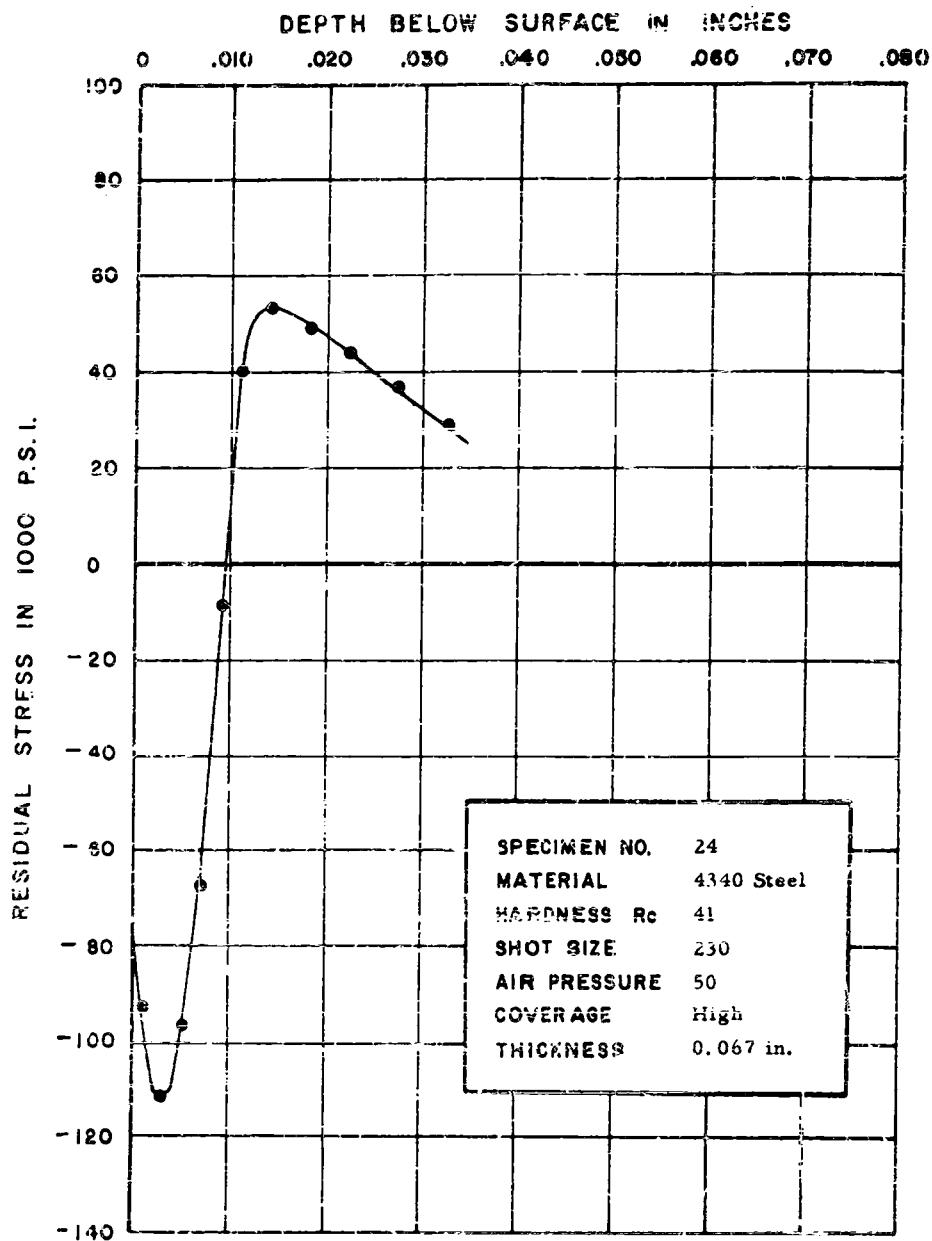
FIGURE 64.   RESIDUAL STRESS DISTRIBUTION
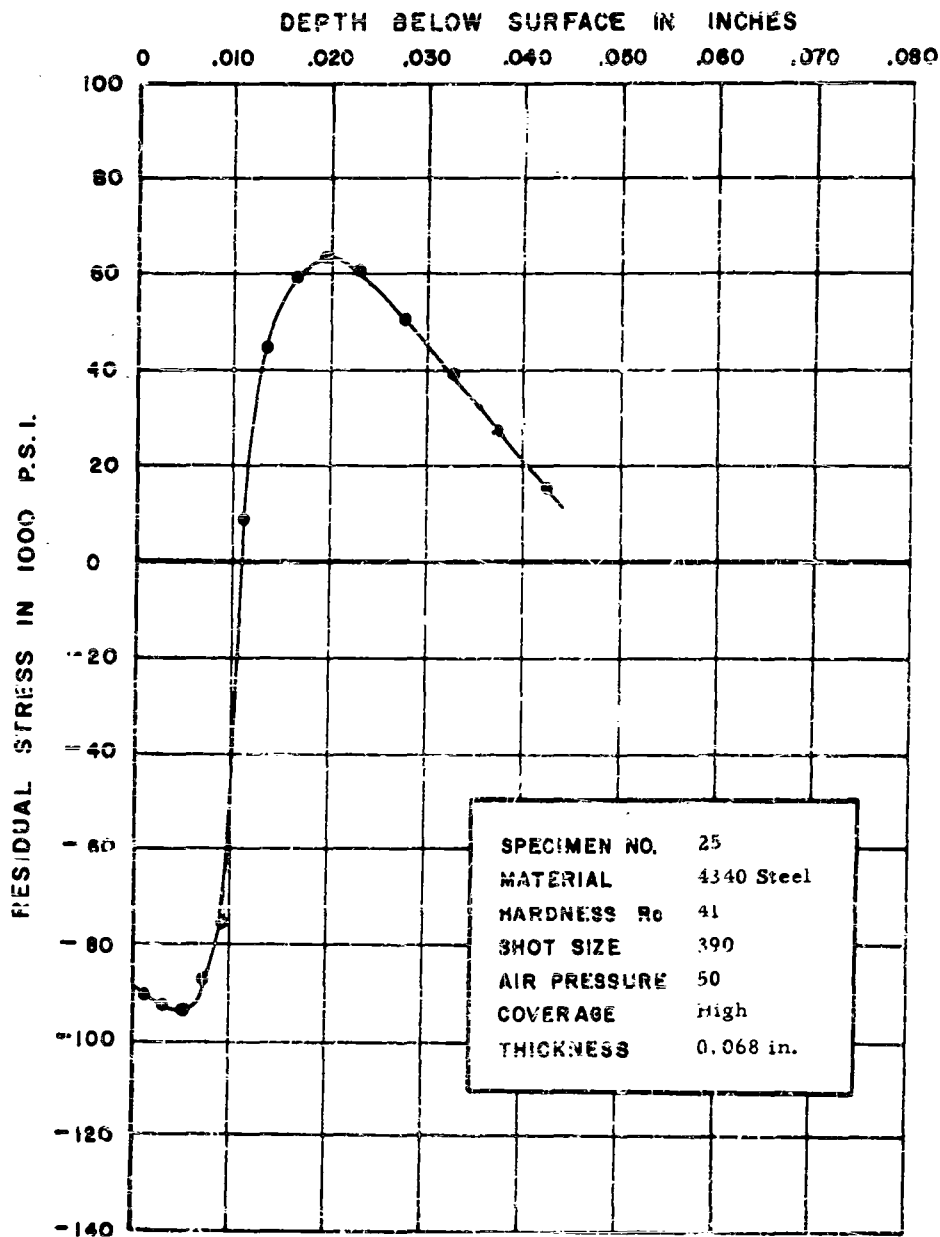
FIGURE 65.   RESIDUAL STRESS DISTRIBUTION

DEPTH BELOW SURFACE IN INCHES

SPECIMEN NO.	26
MATERIAL	4340 Steel
HARDNESS R$_c$	41
SHOT SIZE	390
AIR PRESSURE	50
COVERAGE	High
THICKNESS	0.066 in.
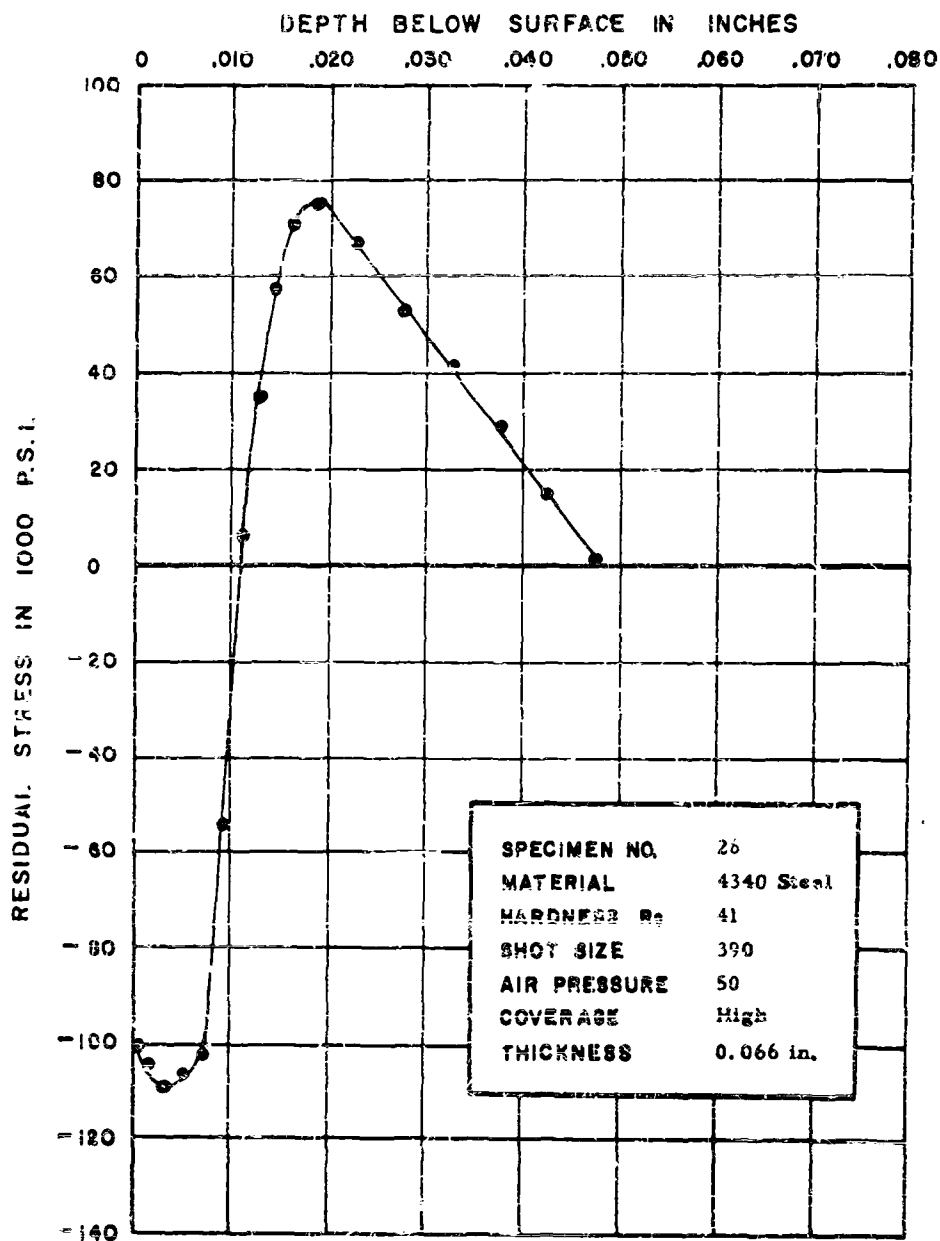
FIGURE 66. RESIDUAL STRESS DISTRIBUTION
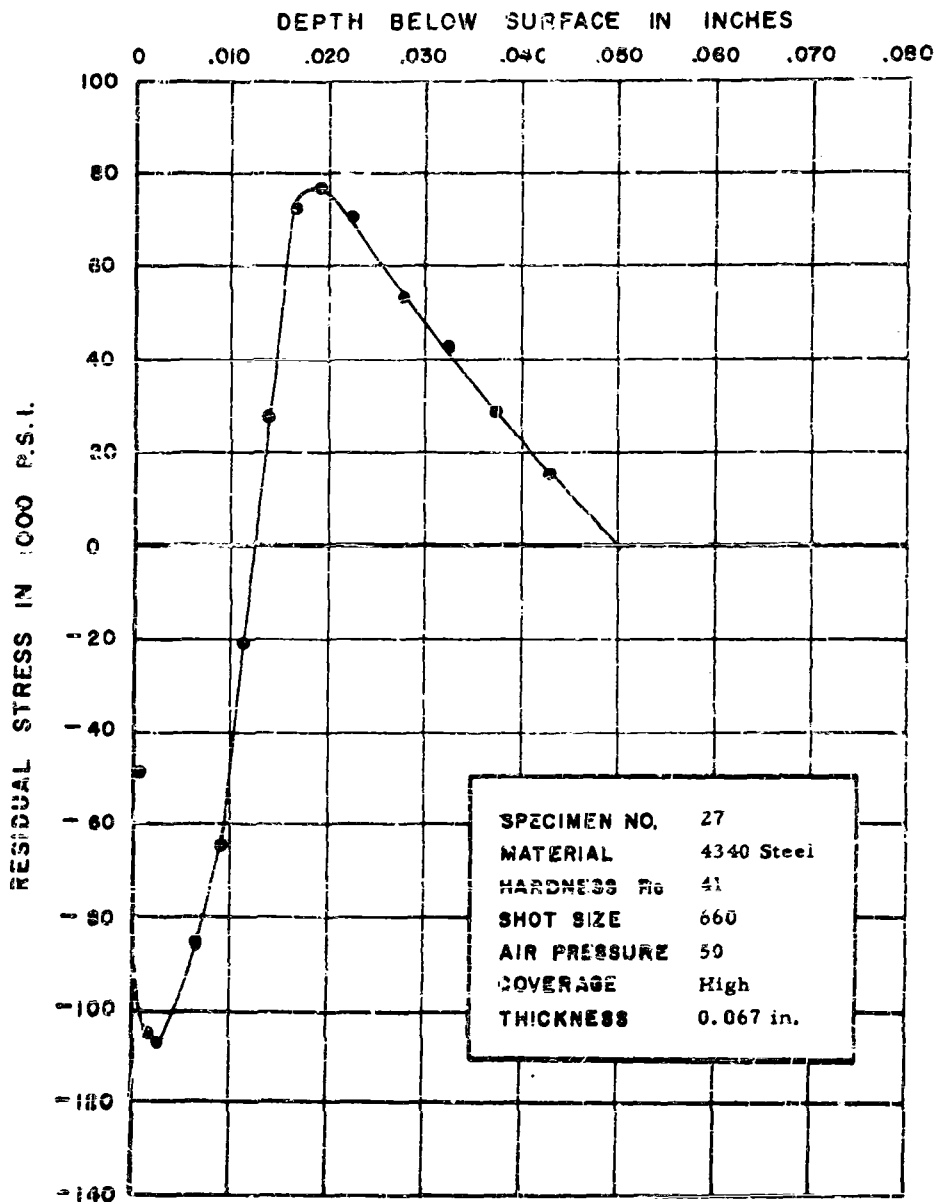
FIGURE 67. RESIDUAL STRESS DISTRIBUTION

DEPTH BELOW SURFACE IN INCHES
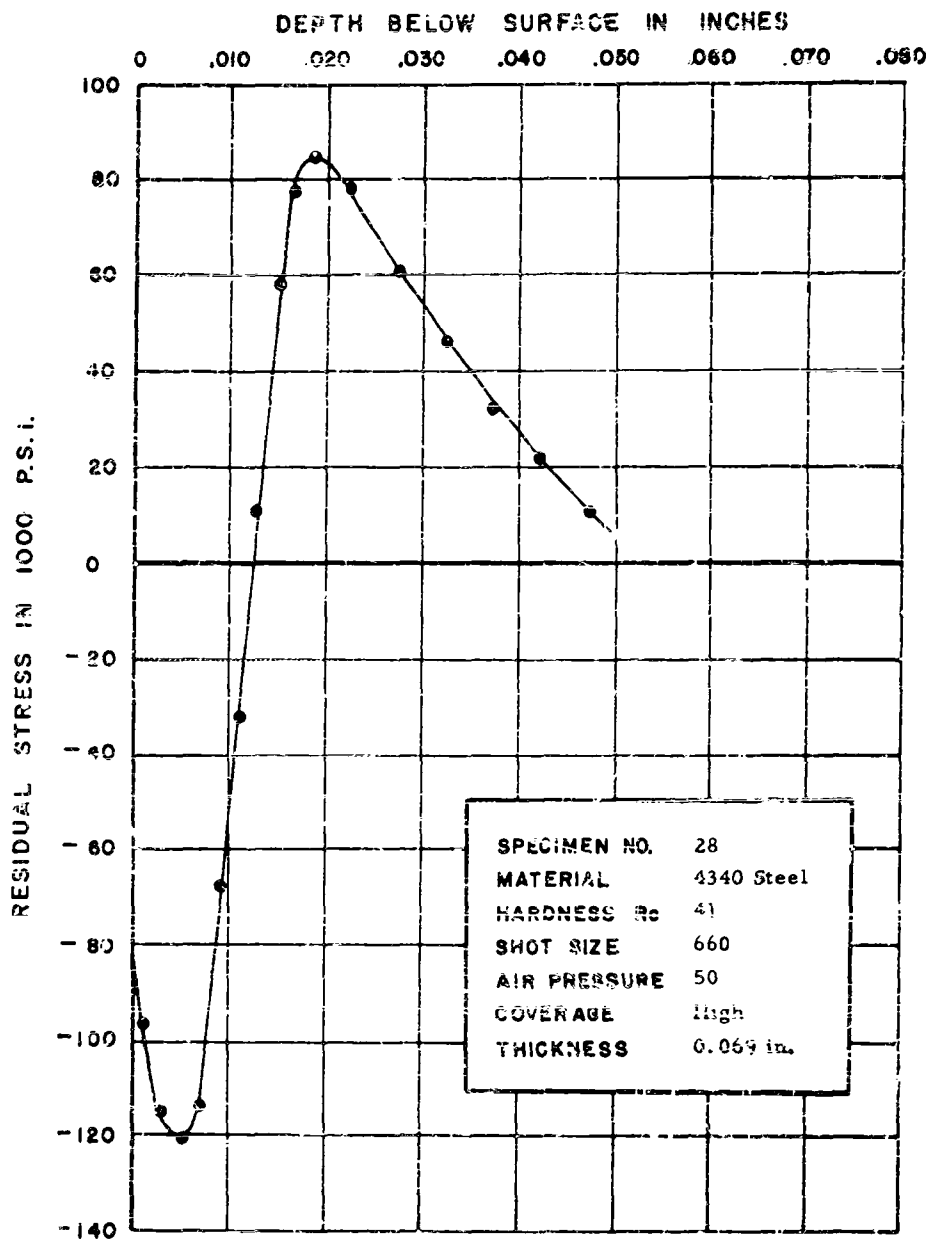
FIGURE 68. RESIDUAL STRESS DISTRIBUTION

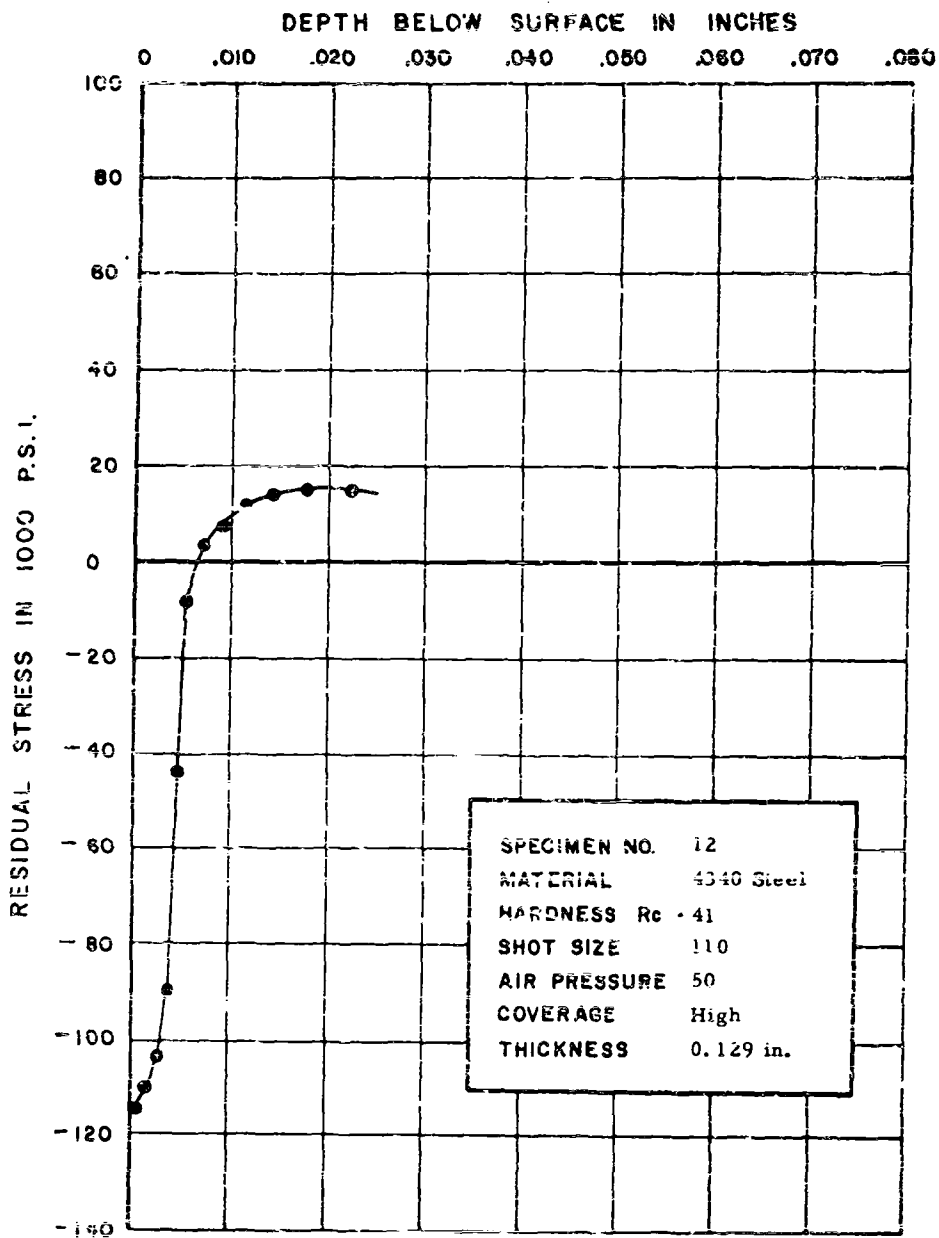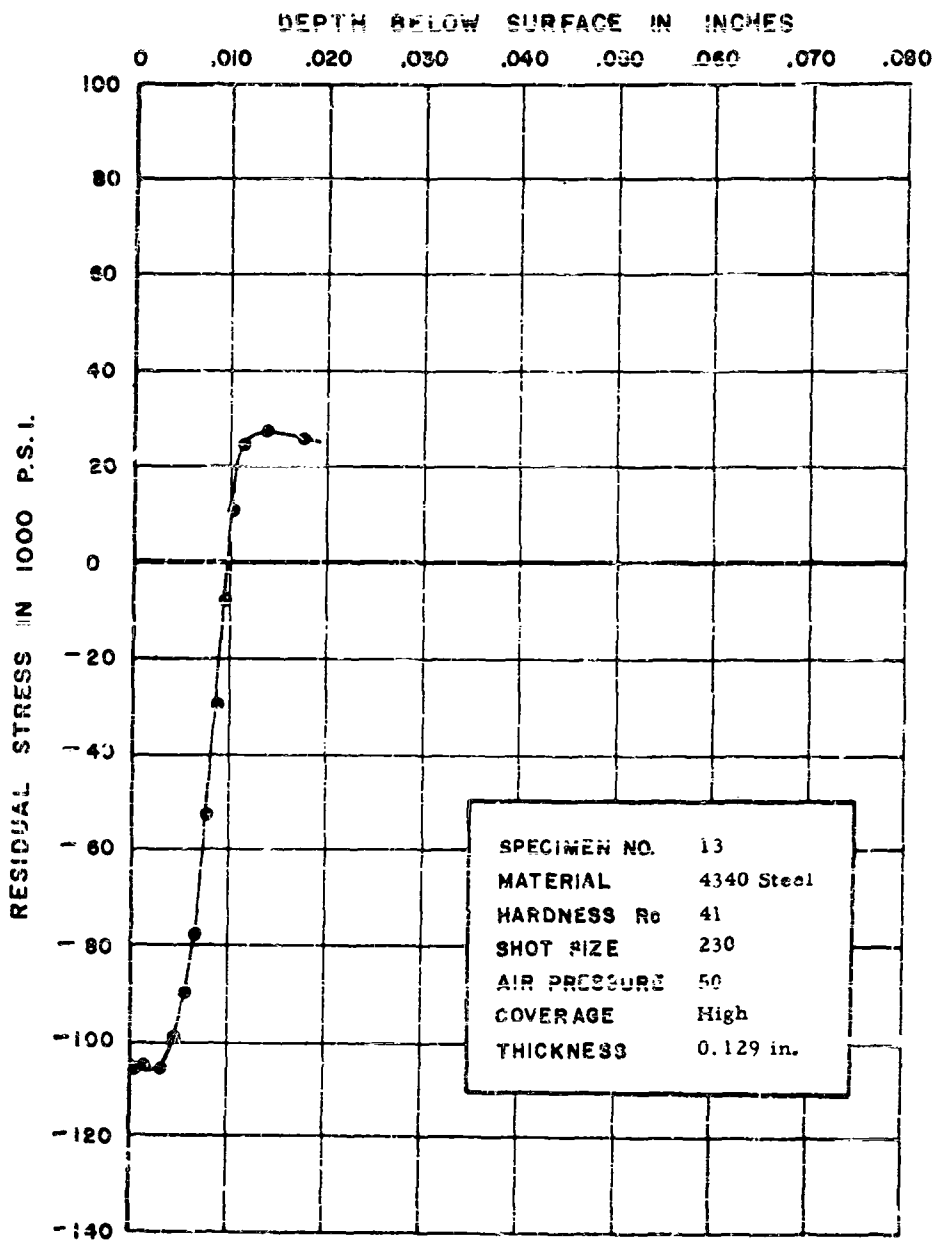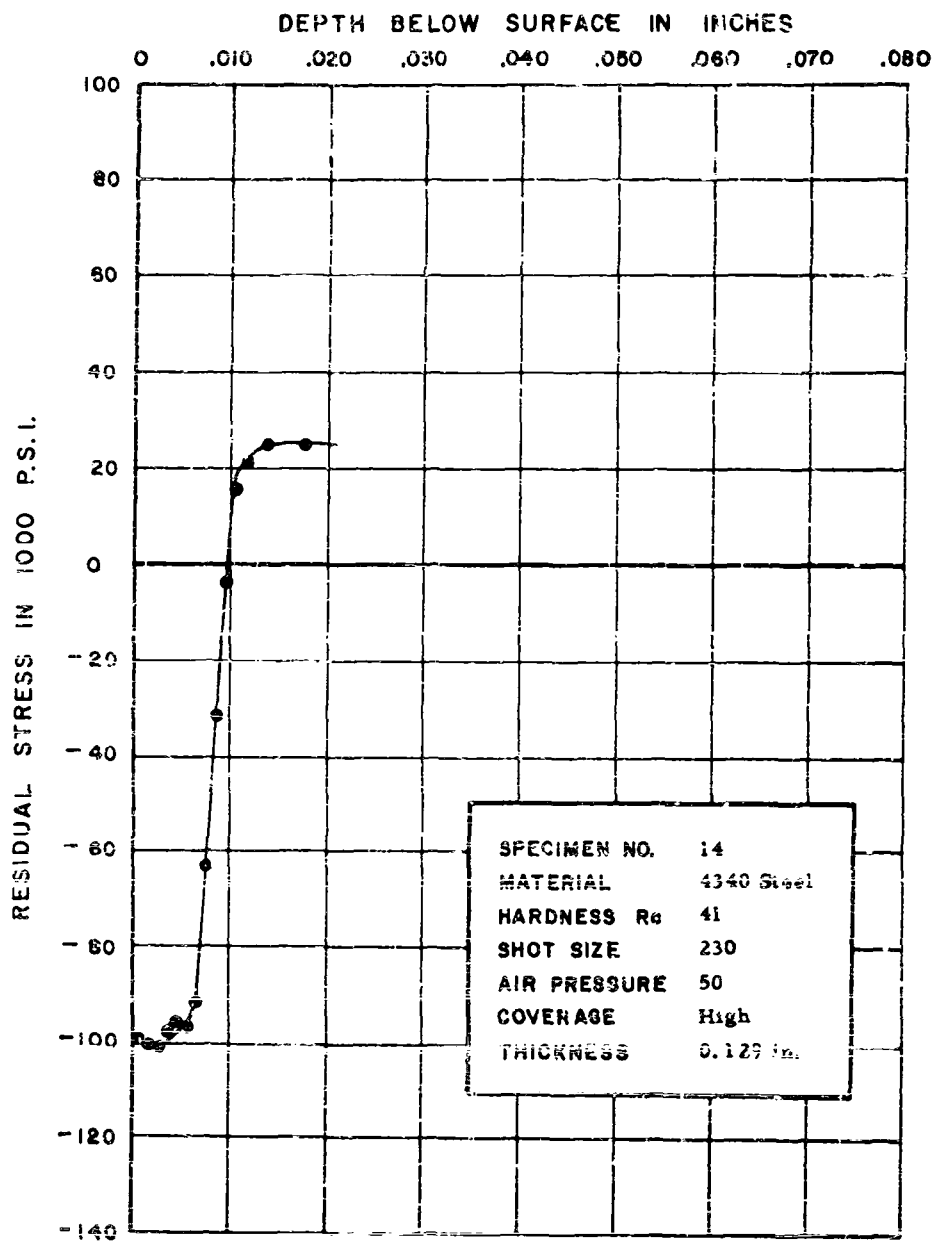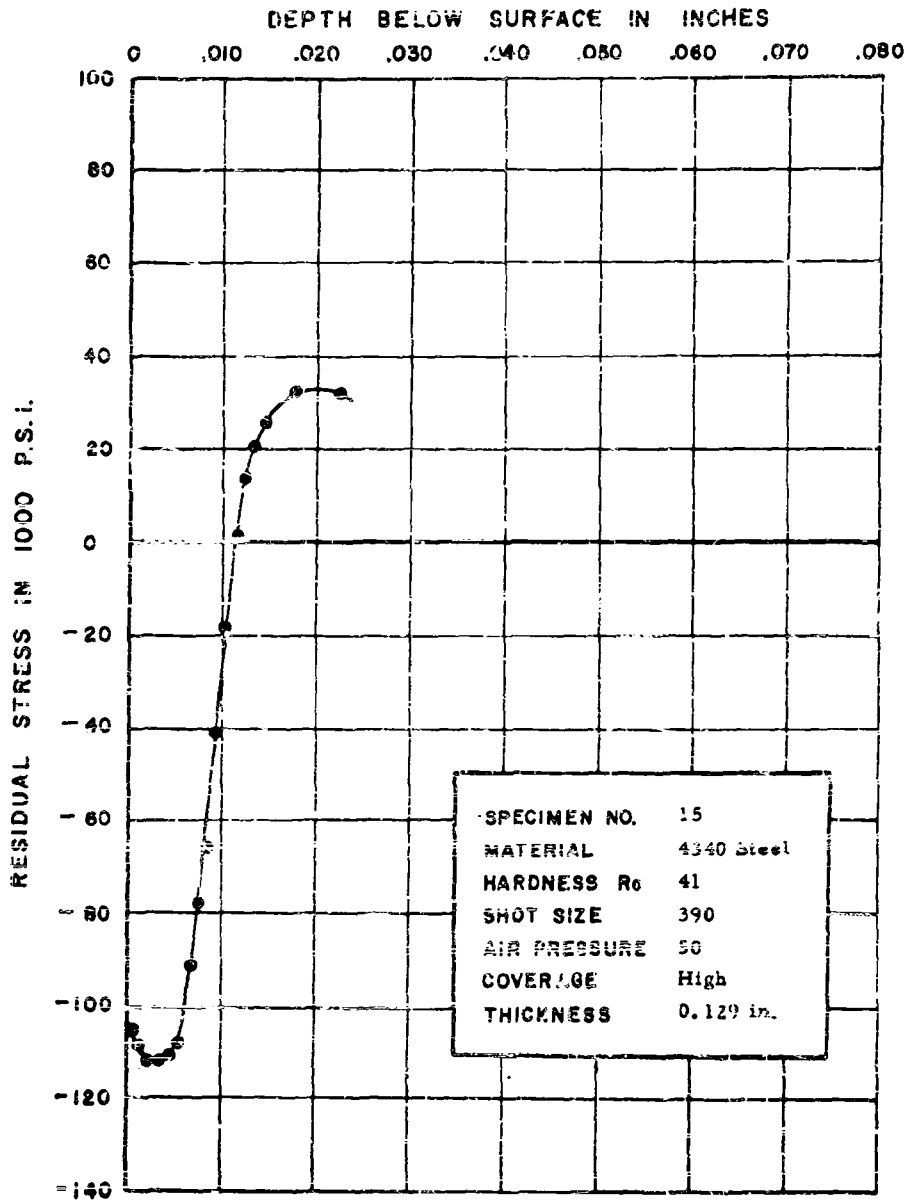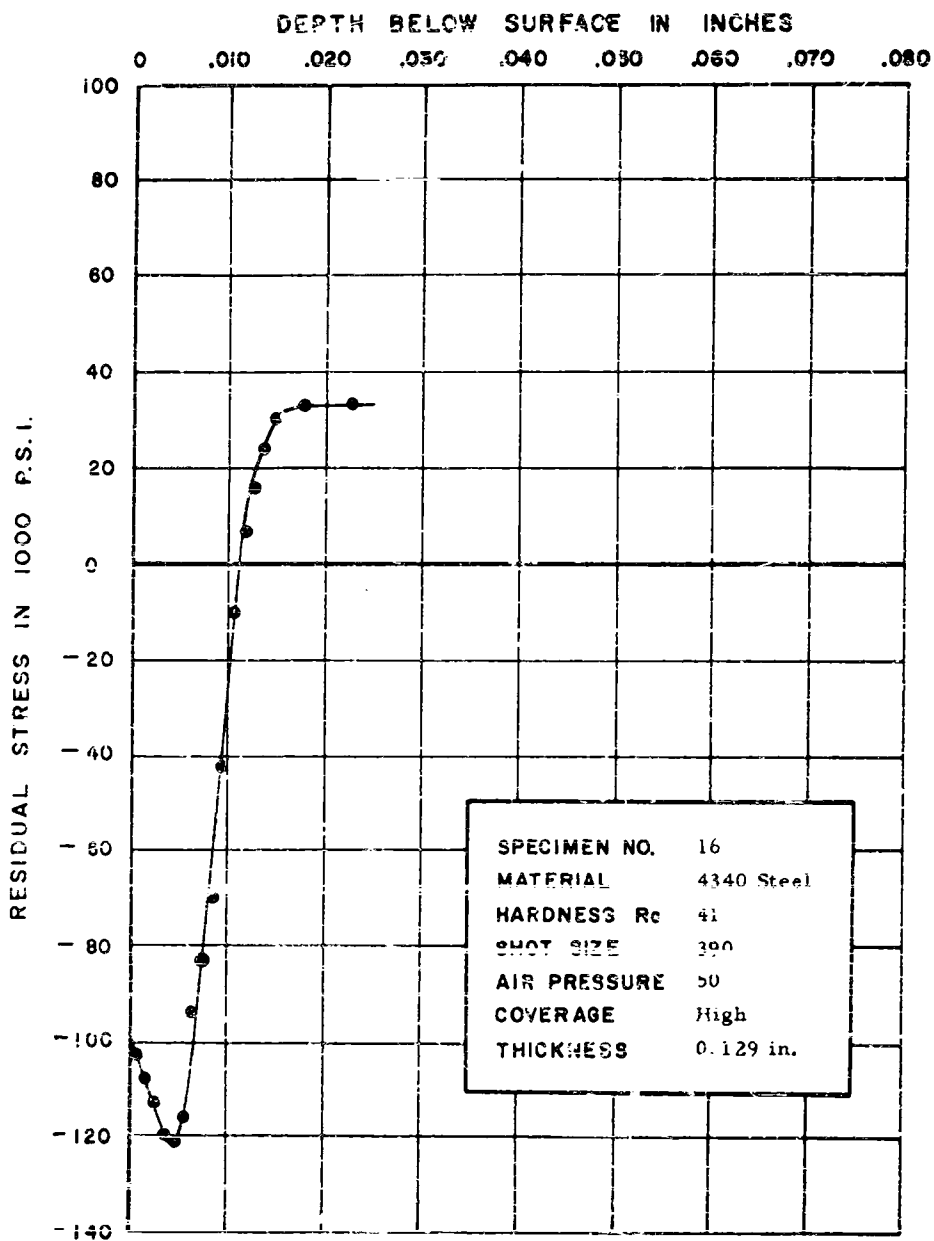| SPECIMEN NO. | 28 |
MATERIAL	4340 Steel
HARDNESS Rc	41
SHOT SIZE	660
AIR PRESSURE	50
COVERAGE	High
THICKNESS	0.069 in.
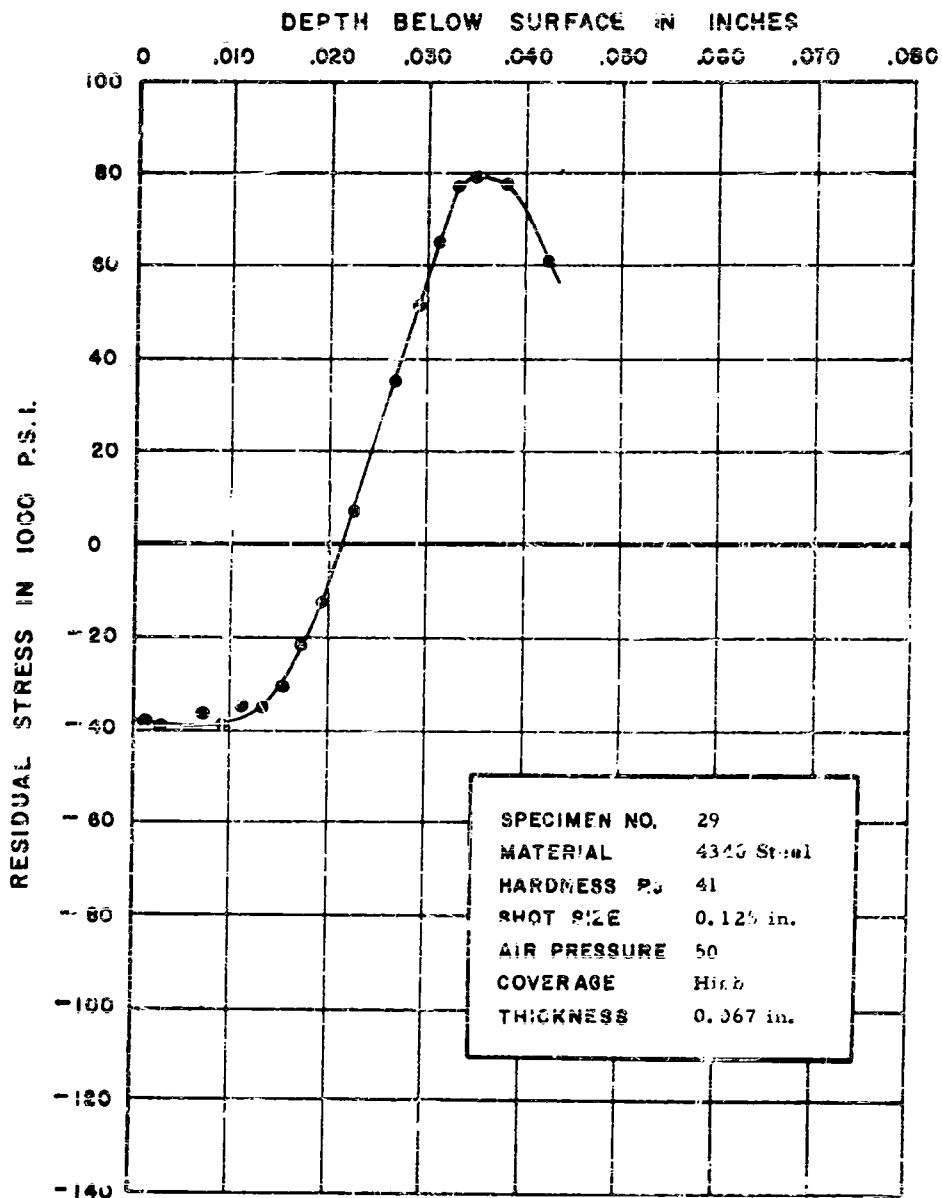
FIGURE 69. RESIDUAL STRESS DISTRIBUTION
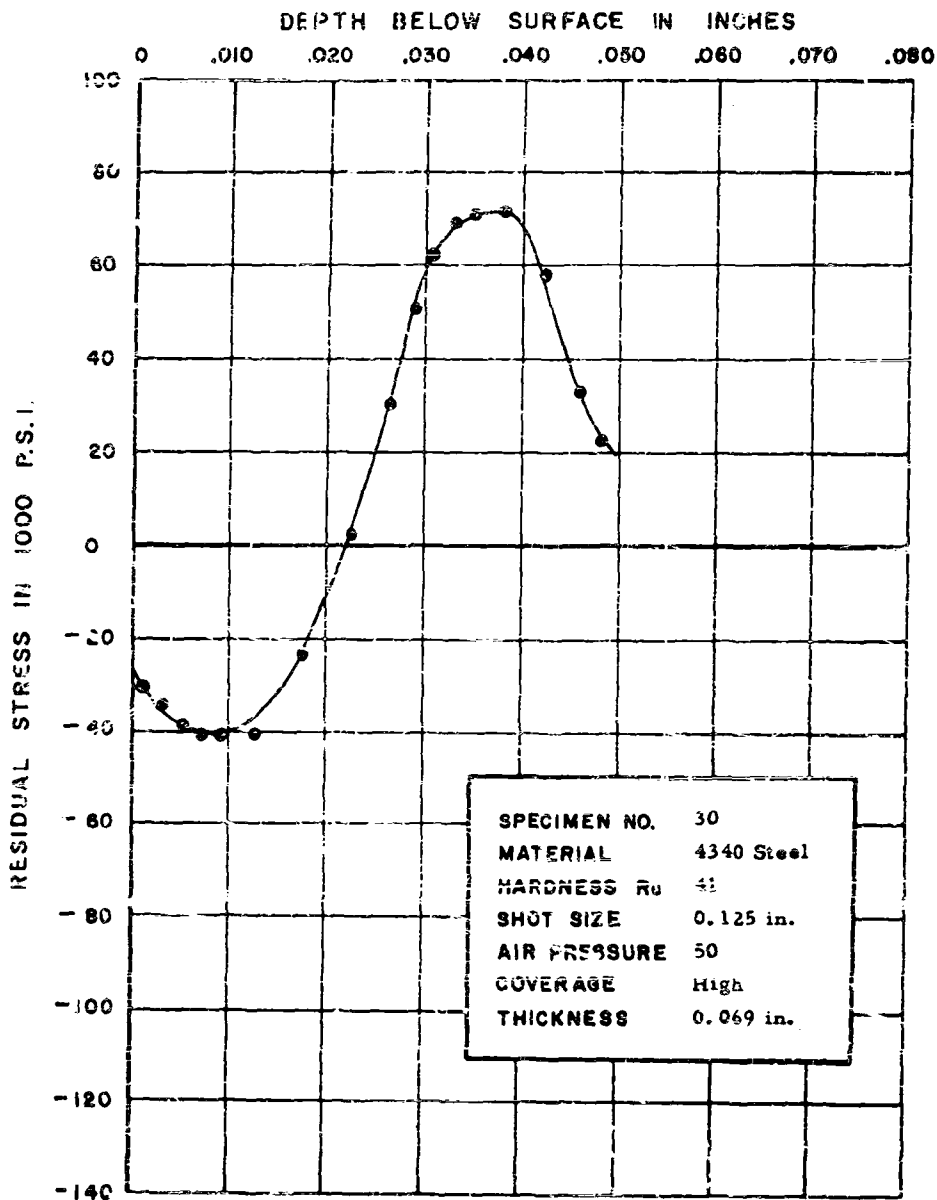
FIGURE 70. RESIDUAL STRESS DISTRIBUTION
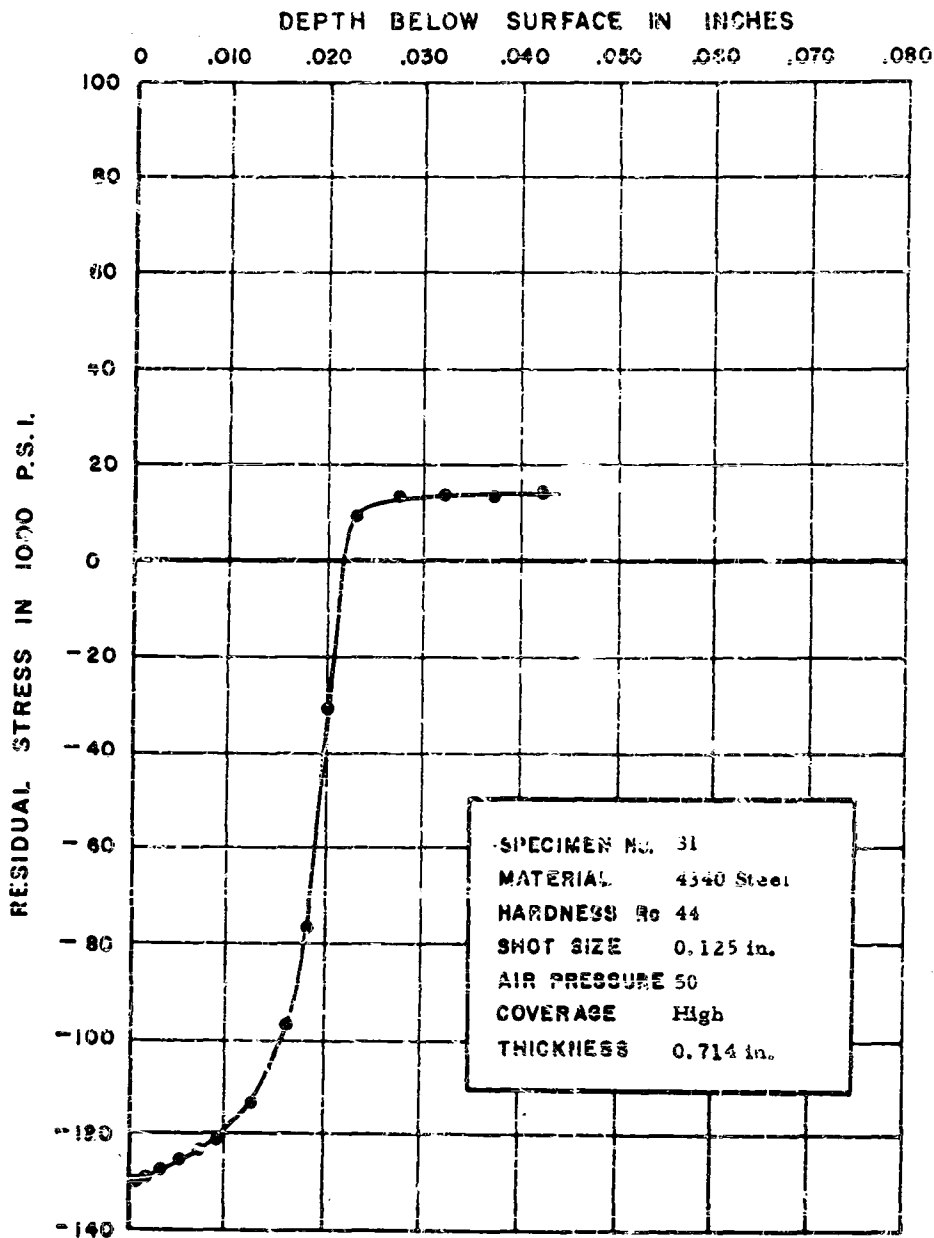
FIGURE 71. RESIDUAL STRESS DISTRIBUTION
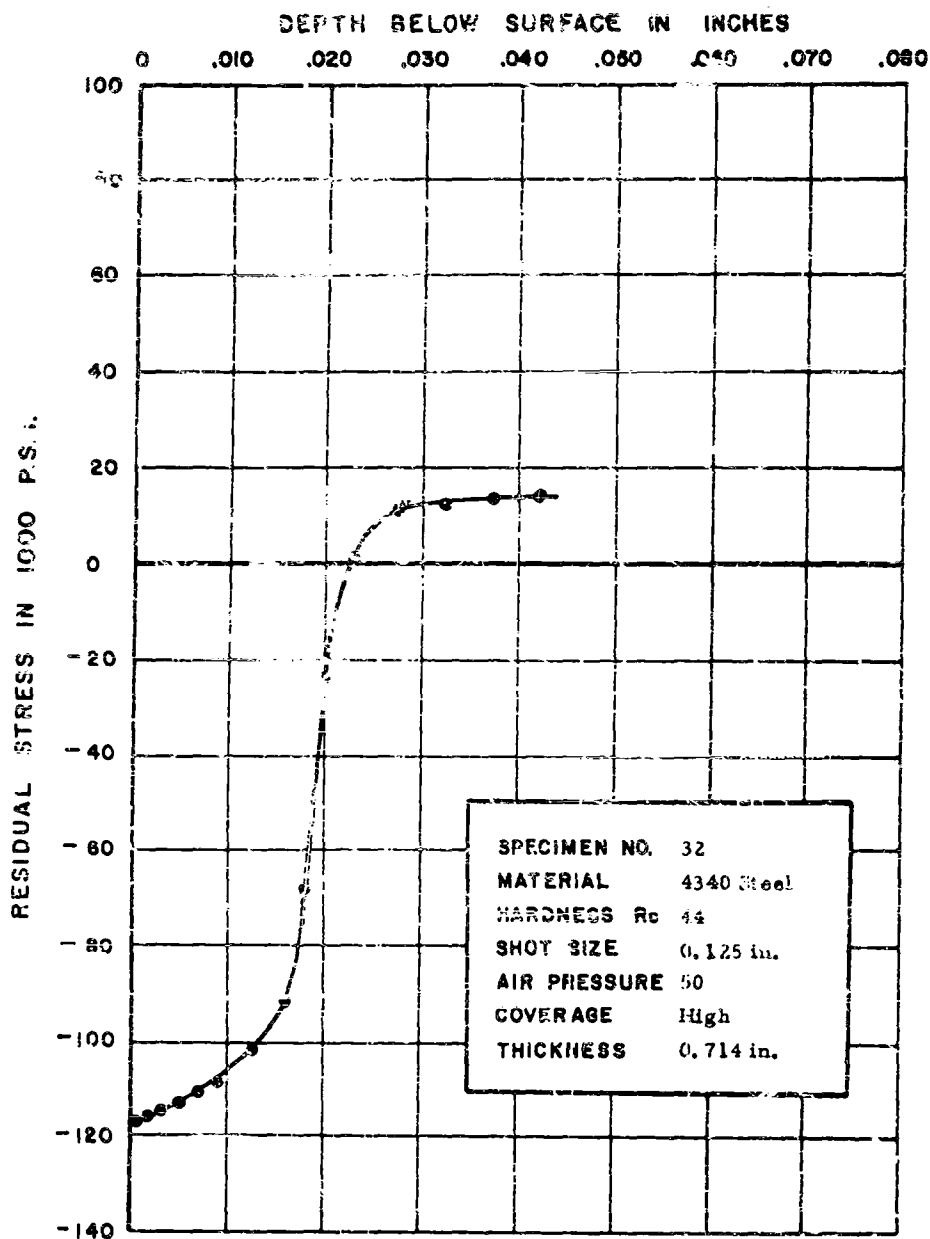
FIGURE 72. RESIDUAL STRESS DISTRIBUTION

The figure shows residual stress distribution with:
- X-axis: DEPTH BELOW SURFACE IN INCHES (0 to .080)
- Y-axis: RESIDUAL STRESS IN 1000 P.S.i. (-140 to 100)

SPECIMEN NO. 32
MATERIAL 4340 Steel
HARDNESS Rc 44
SHOT SIZE 0.125 in.
AIR PRESSURE 50
COVERAGE High
THICKNESS 0.714 in.

DEPTH BELOW SURFACE IN INCHES
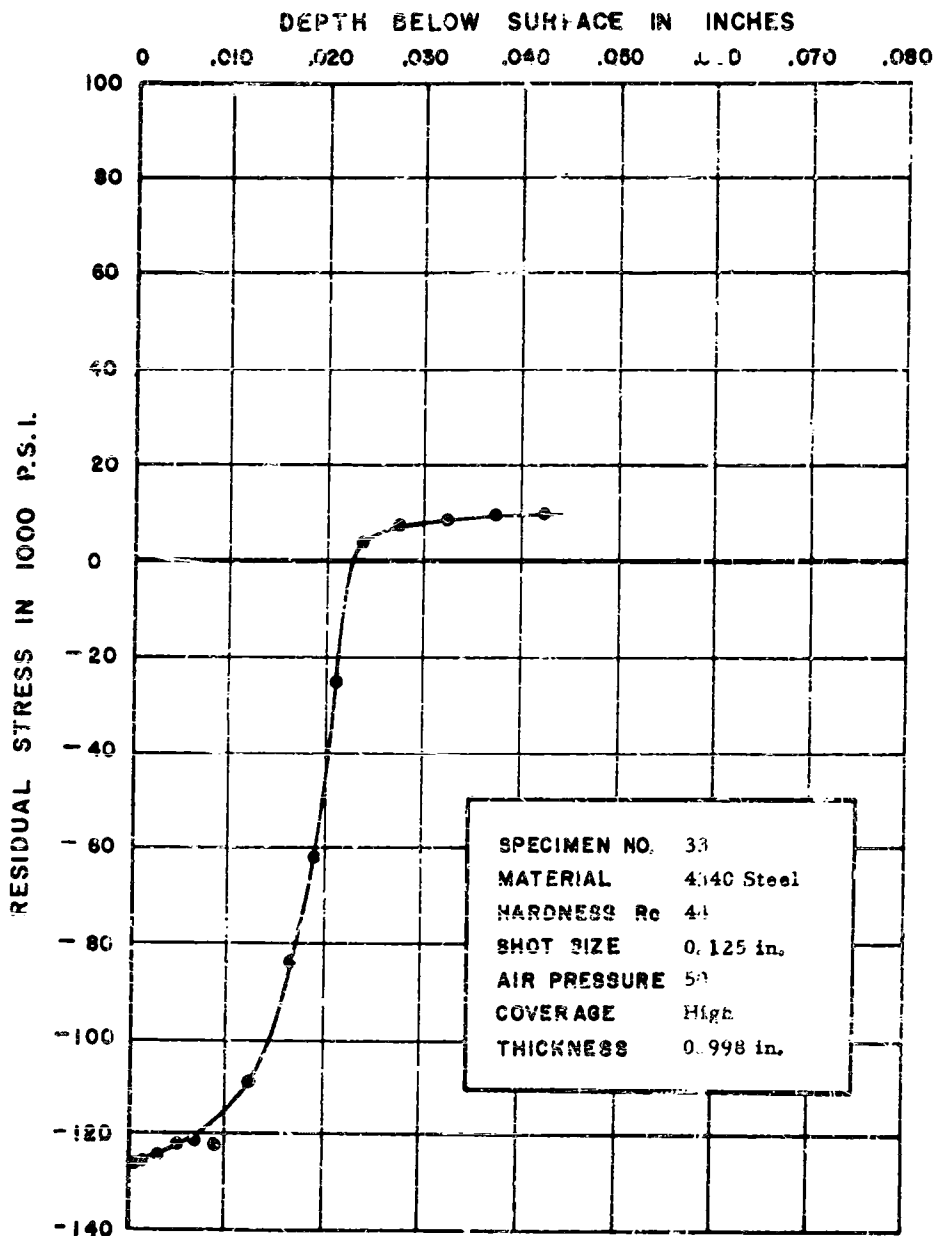
FIGURE 73. RESIDUAL STRESS DISTRIBUTION

SPECIMEN NO. 33
MATERIAL 4140 Steel
HARDNESS Rc 44
SHOT SIZE 0.125 in.
AIR PRESSURE 50
COVERAGE High
THICKNESS 0.998 in.
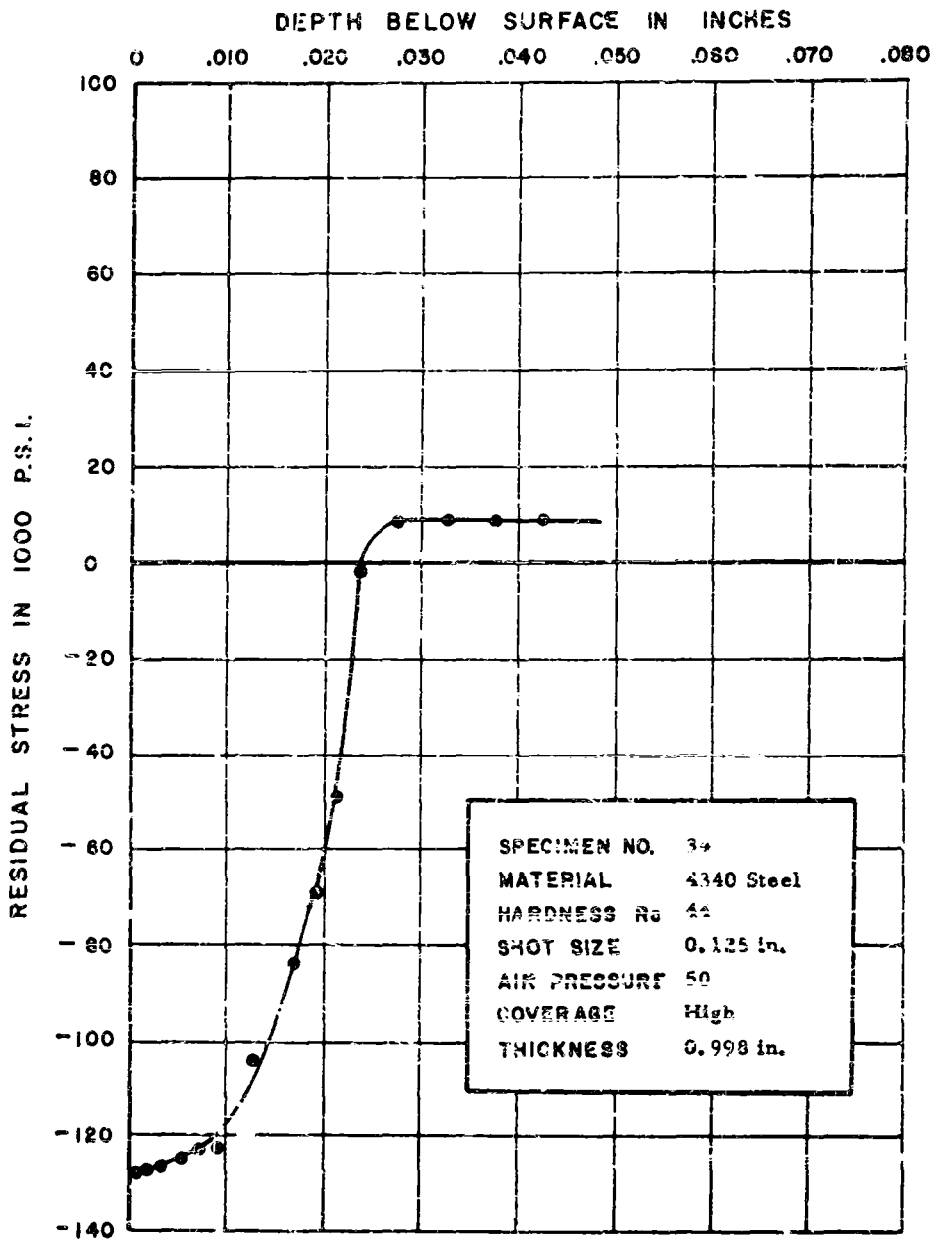
FIGURE 74. RESIDUAL STRESS DISTRIBUTION

APPENDIX III

RESIDUAL STRESS DATA

The following table contains the detailed data from which the residual stress distributions presented in Appendix II were calculated. Table 2 outlines the test conditions for the various specimens. A sample calculation was presented in WADC TR 55-56, Part 1.

TABLE 6
RESIDUAL STRESS DATA

Step	Specimen No. 1 $t_o = 0.4992$		Specimen No. 2 $t_o = .4984$		Specimen No. 3 $t_o = .4971$	
	dH	dt	dH	dt	dH	dt
1	0	0	0	0	0	0
2	.05	.0002	.04	.0002	.04	.0002
3	.07	.0003	.04	.0003	.04	.0003
4	.06	.0004	.03	.0005	.12	.0005
5	.16	.0007	.13	.0008	.13	.0006
6	.18	.0010	.15	.0010	.25	.0014
7	.27	.0016	.24	.0016	.37	.0021
8	.48	.0026	.43	.0024	.52	.0027
9	.60	.0034	.54	.0033	.66	.0035
10	.71	.0047	.73	.0049	.71	.0039
11	.71	.0062	.73	.0062	.81	.0043
12	.71	.0077	.73	.0072	.97	.0055
13	.73	.0098	.78	.0091	1.05	.0059
14	.70	.0118	.73	.0115	1.27	.0085
15	.67	.0131	.72	.0135	1.34	.0131
16	.68	.0178	.73	.0190	1.41	.0165
17	.68	.0222			1.41	.0184
18					1.37	.0224
19					1.27	.0293

Step	Specimen No. 4 $t_o = .4964$		Specimen No. 5 $t_o = .4970$		Specimen No. 6 $t_o = .4978$	
	dH	dt	dH	dt	dH	dt
1	0	0	0	0	0	0
2	.03	.0001	.01	0	.01	.0001
3	.05	.0002	.02	.0001	.03	.0001
4	.07	.0009	.07	.0004	.04	.0004
5	.07	.0006	.09	.0005	.10	.0006
6	.28	.0012	.19	.0011	.20	.0012
7	.44	.0021	.29	.0015	.30	.0017
8	.57	.0026	.40	.0021	.41	.0021
9	.76	.0036	.49	.0026	.48	.0026
10	.80	.0042	.59	.0031	.60	.0032
11	.98	.0047	.67	.0036	.72	.0038
12	1.10	.0054	.81	.0044	.89	.0047
13	1.15	.0061	1.40	.0077	1.32	.0072
14	1.40	.0087	1.70	.0105	1.64	.0097
15	1.43	.0131	1.69	.0147	1.69	.0150
16	1.40	.0159	1.68	.0182	1.66	.0188
17	1.40	.0181	1.68	.0182	1.66	.0188
18	1.37	.0222	1.60	.0231	1.63	.0234
19	1.38	.0261	1.63	.0271	1.58	.0284

TABLE 6 (CONTINUED)
RESIDUAL STRESS DATA

Step	Specimen No. 7 $t_o = .4954$		Specimen No. 8 $t_o = .4988$		Specimen No. 9 $t_o = .4983$	
	dH	dt	dH	dt	dH	dt
1	0	0	0	·0	0	0
2	.04	.0001	.04	.0001	-.09	.0001
3	.05	.0003	.09	.0004	-.06	.0003
4	.11	.0005	.13	.0005	+.05	.0005
5	.20	.0010	.27	.0013	-.05	.0008
6	.25	.0015	.33	.0019	+.05	.0014
7	.37	.0021	.42	.0024	+.21	.0021
8	.52	.0031	.69	.0039	+.31	.0027
9	.80	.0043	.90	.0048	+.54	.0040
10	1.09	.0055	1.17	.0056	+.74	.0050
11	1.34	.0068	1.54	.0077	+.94	.0060
12	1.49	.0078	1.80	.0093	+1.42	.0083
13	1.58	.0086	2.05	.0106	+1.83	.0101
14	2.03	.0117	2.20	.0127	+2.12	.0120
15	2.44	.0154	2.45	.0175	+3.22	.0173
16	2.51	.0144	2.44	.0205	+3.74	.0209
17	2.48	.0220	2.44	.0239	+3.96	.0237
18	2.60	.0236	2.42	.0240	+4.04	.0262
19	2.50	.0285	2.46	.0283	+4.03	.0310
20					+4.00	.0345
21					+4.03	.0371

Step	Specimen No. 10 $t_o = .4994$		Specimen No. 11 $t_o = .1292$		Specimen No. 12 $t_o = .1291$	
	dH	dt	dH	dt	dH	dt
1	0	0	0	0	0	0
2	-.08	.0001	.46	.0002	.54	.0002
3	-.03	.0003	1.72	.0007	2.09	.0007
4	+.07	.0005	2.40	.0010	2.82	.0010
5	0	.0007	4.63	.0019	5.39	.0019
6	+.07	.0015	6.82	.0027	7.89	.0029
7	+.24	.0022	10.47	.0044	11.41	.0042
8	+.34	.0028	11.64	.0059	12.62	.0053
9	+.57	.0090	12.18	.0078	13.43	.0068
10	+.75	.0049	12.59	.0101	14.22	.0098
11	+.89	.0059	12.89	.0132	14.59	.0129
12	+1.29	.0077	13.00	.0192	14.75	.0176
13	+1.57	.0092	13.06	.0239	14.76	.0220
14	+1.79	.0106	13.07	.0288	14.81	.0267
15	+2.87	.0150	13.12	.0338	14.82	.0324
16	+3.54	.0187	13.18	.0391	14.96	.0379
17	+3.97	.0217	13.21	.0439	15.03	.0419
18	+4.10	.0239	13.32	.0488	15.14	.0463
19	+4.27	.0294	13.37	.0535	15.22	.0516
20	+4.27	.0330				
21	+4.27	.0356				

TABLE 6 (CONTINUED)
RESIDUAL STRESS DATA

Step	Specimen No. 13 $t_o = .1292$		Specimen No. 14 $t_o = .1290$		Specimen No. 15 $t_o = .1292$	
	dH	dt	dH	dt	dH	dt
1	0	0	0	0	0	0
2	.48	.0002	.50	.0002	.22	.0002
3	.84	.0003	.83	.0003	.70	.0003
4	1.79	.0007	1.72	.0007	1.58	.0007
5	2.46	.0010	2.29	.0010	2.50	.0010
6	4.36	.0018	4.12	.0017	4.61	.0019
7	6.67	.0026	6.25	.0025	6.81	.0026
8	11.51	.0042	9.99	.0041	10.67	.0038
9	14.66	.0054	14.50	.0055	13.99	.0049
10	19.34	.0070	19.17	.0071	21.67	.0074
11	23.73	.0098	23.73	.0100	27.33	.0096
12	24.30	.0125	24.26	.0135	31.61	.0145
13	24.49	.0155	24.49	.0186	32.05	.0193
14	24.55	.0214	24.58	.0232	32.26	.0246
15	24.58	.0264	24.71	.0291	32.43	.0295
16	24.66	.0314	24.91	.0341	32.66	.0350
17	24.73	.0369	25.13	.0394	32.96	.0420
18	24.78	.0410	25.36	.0443	33.27	.0472
19	24.91	.0465	25.65	.0487	33.77	.0525
20	25.00	.0515	26.00	.0541	34.20	.0581
21					34.55	.0628

Step	Specimen No. 16 $t_o = .1291$		Specimen No. 17 $t_o = .1292$		Specimen No. 18 $t_o = .1291$	
	dH	dt	dH	dt	dH	dt
1	0	0	0	0	0	0
2	.29	.0001	.34	.0001	.45	.0002
3	.68	.0003	.78	.0003	.93	.0003
4	1.53	.0006	1.52	.0006	1.72	.0006
5	2.29	.0010	2.30	.0010	2.70	.0010
6	4.19	.0017	4.21	.0017	4.59	.0018
7	6.79	.0026	6.71	.0026	6.26	.0024
8	11.39	.0040	10.56	.0039	9.62	.0036
9	15.84	.0054	13.33	.0049	14.46	.0051
10	23.72	.0079	21.89	.0074	21.44	.0075
11	28.60	.0099	28.89	.0097	26.58	.0094
12	31.85	.0144	39.40	.0145	37.59	.0140
13	32.30	.0200	41.30	.0195	40.19	.0204
14	32.47	.0245	41.45	.0246	40.33	.0251
15	32.68	.0304	41.63	.0302	40.49	.0309
16	32.86	.0353	41.79	.0358	40.53	.0362
17	33.06	.0407	41.99	.0419	40.66	.0422
18	33.35	.0463	42.25	.0475	40.81	.0481
19	33.85	.0510	42.61	.0521	41.12	.0531
20	34.23	.0564	42.98	.0579	41.31	.0582
21	34.45	.0608	43.12	.0622	41.30	.0626

TABLE 6 (CONTINUED)

RESIDUAL STRESS DATA

Step	Specimen No. 19 $t_o = .1290$ dH	dt	Specimen No. 20 $t_o = .1289$ dH	dt	Specimen No. 21 $t_o = .0686$ dH	dt
1	0	0	0	0	0	0
2	.5	.0001	.6	.0001	-.4	.00014
3	.9	.0003	1.7	.0003	1.8	.00038
4	1.3	.0005	1.9	.0005	5.4	.00090
5	2.3	.0008	2.9	.0009	8.1	.00119
6	2.8	.0012	3.8	.0013	18.0	.00215
7	4.8	.0020	5.6	.0020	27.9	.0032
8	7.0	.0029	7.7	.0028	39.9	.0049
9	9.2	.0039	9.7	.0037	43.2	.0062
10	13.5	.0052	13.7	.0050	46.3	.0087
11	20.7	.0073	19.9	.0069	49.2	.0136
12	28.5	.0094	29.6	.0093	51.8	.0189
13	49.8	.0146	45.9	.0136	55.6	.0235
14	41.4	.0196	66.0	.0179	58.6	.0280
15	87.1	.0247	87.4	.0237	64.3	.0336
16	96.5	.0292	99.3	.0285	74.5	.0398
17	99.4	.0328	105.3	.0327		
18		.0394		.0373		
19	99.5	.0452	105.3	.0420		
20	100.0	.0509	105.4	.0476		

Step	Specimen No. 22 $t_o = .0670$ dH	dt	Specimen No. 23 $t_o = .0658$ dH	dt	Specimen No. 24 $t_o = .0667$ dH	dt
1	0	0	0	0	0	0
2	-.3	.0002	1.4	.0001	1.2	.0001
3	1.5	.0004	3.2	.0003	3.0	.0004
4	6.5	.0009	6.4	.0008	6.2	.0008
5	10.2	.0012	10.1	.0011	9.9	.0011
6	22.5	.0024	18.1	.0020	19.7	.0022
7	32.5	.0033	30.0	.0030	29.9	.0031
8	45.3	.0049	52.5	.0048	49.9	.0046
9	50.2	.0064	69.9	.0061	63.9	.0061
10	54.3	.0092	102.4	.0089	92.3	.0080
11	57.8	.0136	115.4	.0137	110.3	.0106
12	61.9	.0190	118.7	.0192	115.7	.0149
13	68.2	.0239	123.1	.0237	118.2	.0195
14	75.2	.0294	127.9	.0282	123.1	.0245
15	86.1	.0347	136.6	.0338	129.0	.0299
16	107.9	.0413	152.0	.0397	135.6	.0348
17					151.9	.0402

TABLE 6 (CONTINUED)

RESIDUAL STRESS DATA

Step	Specimen No. 25 $t_o = .0676$ dH	dt	Specimen No. 26 $t_o = .0659$ dH	dt	Specimen No. 27 $t_o = .0666$ dH	dt
1	0	0	0	0	0	0
2	.1	.0001	0	.0001	0	.0001
3	.2	.0002	.1	.0002	.2	.0002
4	.4	.0006	.4	.0006	.3	.0006
5	.8	.0010	.8	.0010	.4	.0009
6	1.7	.0020	1.9	.0019	1.5	.0020
7	2.3	.0029	3.1	.0029	2.8	.0030
8	4.0	.0043	5.5	.0046	4.6	.0045
9	6.1	.0061	7.7	.0062	7.0	.0064
10	10.7	.0091	13.1	.0093	11.3	.0095
11	13.1	.0115	15.1	.0113	14.4	.0118
12	15.0	.0174	17.4	.0174	17.4	.0181
13	15.1	.0228	17.5	.0226	17.5	.0229
14	15.9	.0238	18.1	.0272	18.0	.0284
15	16.4	.0354	19.0	.0332	18.7	.0345
16	18.0	.0415	20.5	.0383	20.7	.0407
17	20.1	.0464	22.9	.0437	23.0	.0454

Step	Specimen No. 28 $t_o = .0687$ dH	dt	Specimen No. 29 $t_o = .0672$ dH	dt	Specimen No. 30 $t_o = .0687$ dH	dt
1	0	0	0	0	0	0
2	0	.0001	.1	.0001	0	.0001
3	.2	.0002	.1	.0003	.1	.0003
4	.5	.0006	.2	.0005	.1	.0005
5	.7	.0009	.2	.0008	.3	.0008
6	1.7	.0020	.3	.0012	.3	.0012
7	2.7	.0029	.7	.0022	.6	.0020
8	4.9	.0046	1.1	.0031	.7	.0028
9	7.7	.0065	1.7	.0042	.9	.0040
10	11.7	.0094	2.2	.0053	1.8	.0053
11	14.7	.0118	3.3	.0072	2.9	.0075
12	18.0	.0182	4.8	.0096	4.2	.0096
13	18.0	.0235	10.3	.0149	8.1	.0143
14	18.8	.0287	16.8	.0199	13.7	.0187
15	19.1	.0344	24.7	.0253	19.7	.0237
16	21.0	.0398	32.1	.0303	24.9	.0279
17	23.0	.0452	36.3	.0348	29.5	.0329
18			38.6	.0400	31.9	.0379
19			40.6	.0449	33.1	.0437
20			44.3	.0503	35.5	.0494

TABLE 6 (CONTINUED)

RESIDUAL STRESS DATA

Step	Specimen No. 31 $t_o = .7141$		Specimen No. 32 $t_o = .7141$	
	dH	dt	dH	dt
1	0	0	0	0
2	.09	.0005	.09	.0004
3	.11	.0007	.11	.0006
4	.21	.0016	.20	.0017
5	.24	.0021	.25	.0022
6	.39	.0034	.37	.0036
7	.48	.0044	.46	.0047
8	.71	.0066	.65	.0056
9	.88	.0084	.84	.0086
10	1.31	.0121	1.20	.0126
11	1.54	.0148	1.47	.0159
12	1.94	.0221	1.76	.0220
13	1.94	.0283	1.78	.0284
14	1.93	.0239	1.76	.0352
15	1.94	.0407	1.75	.0411
16	1.93	.0471	1.75	.0471

Step	Specimen No. 33 $t_o = .9975$		Specimen No. 34 $t_o = .9980$	
	dH	dt	dH	dt
1	0	0	0	0
2	.01	.0002	.05	.0005
3	.03	.0005	.06	.0005
4	.07	.0014	.08	.0013
5	.10	.0019	.12	.0017
6	.15	.0032	.18	.0029
7	.22	.0044	.26	.0042
8	.32	.0067	.36	.0062
9	.43	.0086	.46	.0088
10	.60	.0118	.59	.0109
11	.73	.0153	.73	.0144
12	.92	.0210	.96	.0209
13	.97	.0265	.99	.0271
14	.93	.0330	97	.0329
15	.94	.0399	1.00	.0394
16	.93	.0461	.99	.0457

UNCLASSIFIED

AD